

# UNIVERSITÀ DEGLI STUDI DI NAPOLI

“FEDERICO II”



Scuola Politecnica e delle Scienze di Base

Dottorato di ricerca in Biologia Applicata

XXVII Ciclo

Tesi di Dottorato

Sterols mediate deadly messages in marine diatoms

Coordinatore

Ch.mo Prof.  
Ezio Ricca

Handwritten signature of Ezio Ricca in black ink.

Candidato

Dott.ssa  
Carmela Gallo

Tutors

Dott.  
Angelo Fontana  
Dott.ssa  
Giuliana D'Ippolito

<b>1. INTRODUCTION</b> .....	<b>4</b>
1.1 DIATOMS: GENERAL CHARACTERISTICS.....	4
1.2 CELL CYCLE AND CELL WALL BIOGENESIS.....	8
1.3 ECOLOGICAL IMPORTANCE .....	9
1.4. ECOLOGICAL FUNCTION OF MICROALGAL SECONDARY METABOLITES .....	12
1.5. DIATOMS AS SOURCE OF FUTURE FUEL .....	15
1.6. MODEL ORGANISM: <i>SKELETONEMA MARINOI</i> .....	16
1.7. MODEL ORGANISM: <i>CYCLOTELLA CRYPTICA</i> .....	17
1.8. AIM OF THESIS .....	19
<b>2. ISOLATION AND CHARACTERIZATION OF BIOACTIVE COMPOUNDS</b> .....	<b>20</b>
2. 1. INTRODUCTION.....	20
2. 2. RESULTS AND DISCUSSION .....	21
2. 2. 1. <i>Skeletonema marinoi</i> growth curve .....	21
2. 2. 2. <i>Effects of Skeletonema marinoi</i> cell extracts on its growth .....	23
2. 2. 3. <i>Isolation and characterization of bioactive compounds</i> .....	27
2. 3. 4. <i>Determination of EC<sub>50</sub></i> .....	37
<b>3. BIOCHEMICAL INVESTIGATION OF <i>S. MARINOI</i> CELL DEATH PATHWAY</b> .....	<b>42</b>
3. 1. INTRODUCTION.....	42
3. 2. RESULTS AND DISCUSSION .....	45
3.2.1. <i>NO and hROS production</i> .....	45
3.2.2. <i>In situ PCD detection</i> .....	49
<b>4. QUALITATIVE AND QUANTITATIVE ANALYSIS OF STEROL SULFATES IN DIATOMS</b> .....	<b>54</b>
4. 1. INTRODUCTION.....	54
4. 2. RESULTS AND DISCUSSION .....	54
4.2.1. <i>Sterol sulfates quantification along <i>S. marinoi</i> growth curve</i> .....	54
4.2.2. <i>Sterol sulfates analysis in other diatoms</i> .....	59
4. 2. 4. <i>Isolation and analysis of sterols from <i>S. marinoi</i> and <i>C. cryptica</i></i> .....	63
<b>5. STEROL BIOSYNTHESIS IN DIATOMS</b> .....	<b>66</b>
5. 1. INTRODUCTION.....	66
5. 2. RESULTS AND DISCUSSION .....	72
5.2.1. <i>Heterotrophic growth of <i>C. cryptica</i></i> .....	72

5.3.2. Characterization of sterols biosynthetic pathway .....	75
<b>6. INHIBITION OF STEROLS SULFOTRANSFERASE.....</b>	<b>84</b>
6. 1. INTRODUCTION.....	84
6. 2. RESULTS AND DISCUSSION .....	86
6.2.1. Preliminary sulfotransferase inhibitors assay.....	86
6.2.2. Effect of quercetin on <i>S. marinoi</i> .....	91
6.2.3. Effect of quercetin on <i>C. cryptica</i> .....	95
<b>7. CONCLUSIONS .....</b>	<b>99</b>
7.1. FURTHER DEVELOPMENTS.....	106
<b>8. EXPERIMENTAL SECTION .....</b>	<b>109</b>
8.1.1 Microalgae cultures .....	109
8.1.2. <i>C. cryptica</i> cultures for biosynthesis experiment.....	110
8.1.3. <i>S. marinoi</i> and <i>C. cryptica</i> cultures for experiment with sulfotransferase inhibitor .....	111
8.2. Extraction and fractionation of <i>S. marinoi</i> biomass.....	111
8.3. Purification and characterization of sterol sulfates .....	113
8.4.1. Biological assay .....	115
8.4.2. Chlorophyll a fluorescence measurement .....	115
8.4.3. Cells vitality measurement .....	115
8. 4. 4. Sulfotransferase inhibitor assay.....	116
8.5. hROS detection.....	116
8.6. NO measurements .....	117
8.7. Annexin V-FITC assay.....	118
8.8. TUNEL assay.....	118
8.9. Extraction procedure for quantitative analysis of sterol sulfates .....	119
8.10. Extraction procedure for lipid analysis.....	120
8.11. Isolation and analysis of sterols from <i>S. marinoi</i> and <i>C. cryptica</i> .....	121
8.12. Sterol sulfates quantitation.....	123
8.13. Estimation of glucose consumption in <i>C. cryptica</i> heterotrophic cultures .....	125
8.14. Fatty acid methyl esters analysis.....	126
8. 15. Estimate of quercetin incorporation.....	127
8. 16. RNA extraction and cDNA preparation for sulfotransferase analysis .....	127
8. 17. Real time PCR.....	127
8.18. Protein assay for biochemical analysis.....	128
8.19. Carbohydrates assay for biochemical analysis .....	128
<b>REFERENCES .....</b>	<b>130</b>

# 1. Introduction

## 1.1 Diatoms: General characteristics

Diatoms are member of the algal class *Bacillariophyceae* (division *Heterokontophyta*) and are one of the largest and ecologically most significant groups of organisms on Earth, with about 16,000 species found in both fresh and salt water (Norton et al., 1996). The oldest diatoms date back to the Lower Jurassic, but findings are very rare until the Late Cretaceous. An important characteristic of these organisms (10- 200  $\mu\text{M}$ ) is the ability to generate a silica cell wall, finely structured, known as frustule (Figure 1.1). The biosilica wall of a diatom cell is constructed in a petri-dish like fashion being composed of a top half (epitheca) that overlaps the slightly smaller bottom half (hypotheca). Their name *diatom* is indeed derived from the Greek *diatomos*, meaning “cut in half”, as reference to their distinctive two-part envelope made of silica. The bases of the two parts (epivalve and hypovalve) are joined by the elements called epicingulum and ipocingulum (girdle bands) which all together form the belt (Figure 1.1). The cytoplasm results fully protected, so that any exchange of material with the environment must be through appropriate pores or cracks. The frustule may have several silicate or chitinous appendices, which are species-specific and tightly regulated genetically (Round et al., 1990) and used for the taxonomic classification.

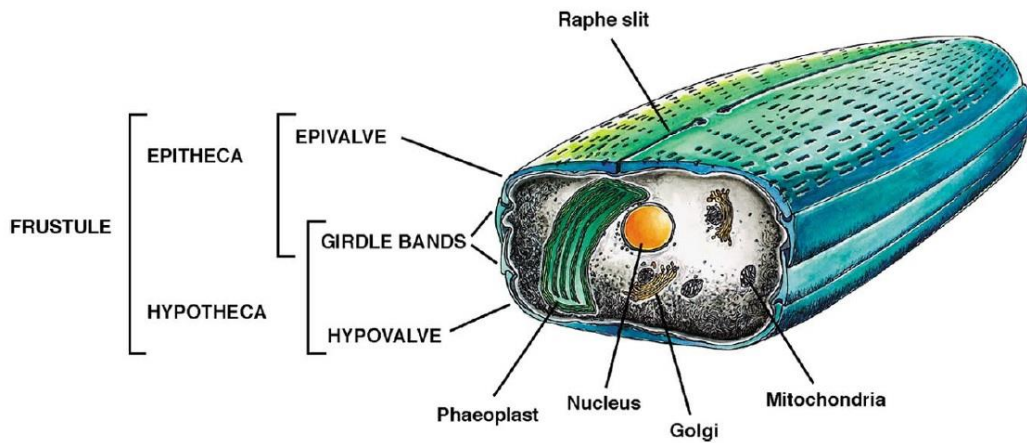


**Figure 1.1.** Schematic diagram of a diatom.

Diatoms are divided into centric or pennate according to the shape of the frustule. The centric diatoms have a radial symmetry, while the pennate have an elongated shape with bilateral symmetry compared to the plane of the valves (Figure 1.2). Among the pennates there is a further subdivision according to the presence or absence of raphe, a polysaccharide structure probably used for the movement of the cell on solid surfaces (*Van Den Hoek et al., 1997*). In fact, the species that are provided of raphe are often benthic, while the planktonic species, both centric and pennate, have only a relic vestige of this structure (*araphidinae*). Like other eukaryotic organisms capable of carrying out photosynthesis, diatoms are equipped with plastids inside of which there are complexes of proteins and pigments important for the capture of light. Diatoms are golden-brown color due to the presence of the accessory carotenoid pigment fucoxanthin that masks the green of chlorophyll *a* and *c*. Fucoxanthin and chlorophyll are held together within the antenna complex in order to capture the light from the Fcp proteins (fucoxanthin chlorophyll *a/c*-binding proteins). Fcp proteins are proteins homologous to Cab (Chlorophyll *a/b*-binding protein) of green algae and higher plants and, in analogy with the latter; their synthesis is activated by light (*Leblanc et al., 1999; Siat, 2007*). A

distinctive feature of diatoms is the presence of four membranes around their plastids that is likely due to different evolutionary origins.

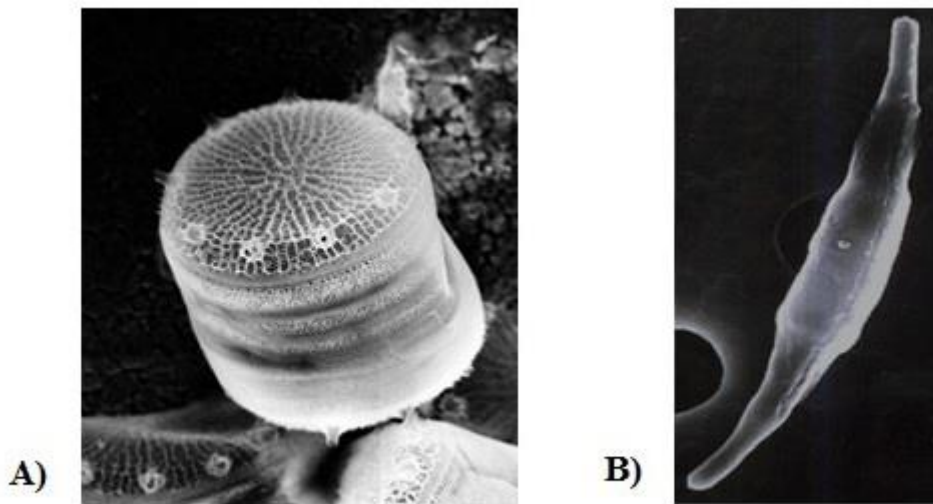


**Figure 1.2.**A) Pictures of the centric diatom *Thalassiosira pseudonana* and B) the pennate diatom *Phaeodactylum tricornutum*.

Phylogenetic analyzes have clearly indicated that the chloroplasts of most algae and higher plants are derived from a process of primary endosymbiosis occurred at least 1.5 billion of years ago from a photosynthetic bacterium (very similar to current cyanobacteria) and eukaryotic unicellular heterotroph. Instead diatom chloroplasts might be the result of a second event of endosymbiosis occurred about 1 billion years later in which an eukaryotic alga, probably a red alga, was incorporated into a second eukaryotic heterotrophic cell (*Bhattacharya, 1995*) (Figure 1.3).

Phylogenetic studies indicate that diatoms diverge early from the lineage that gave rise to green algae and higher plants. According to this, the recent genome sequencing of two species of diatoms has shown that these organisms have unique characteristics. The

most striking is definitely that half of their genes encode proteins that are related to those of animals instead of plants (Armbrust et al., 2004; Bowler et al., 2008).

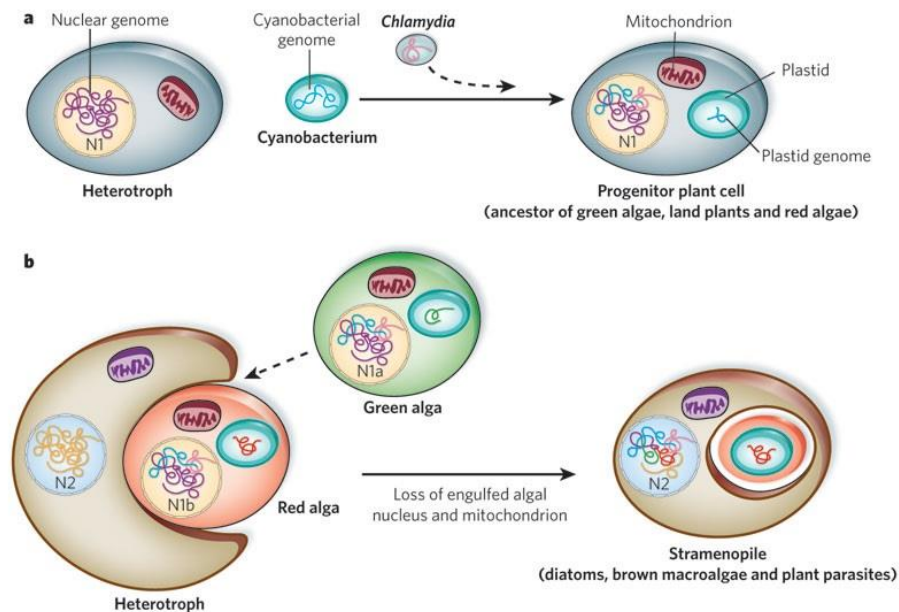


**Figure 1.3.** Representation of the origin of diatom plastids through sequential primary (a) and secondary (b) endosymbioses and their potential effects on genome evolution. a) During primary endosymbiosis, a large proportion of the engulfed cyanobacterial genome is transferred to the host nucleus (N1), with few of the original genes retained within the plastid genome. The potential for invasion of the host by a chlamydial parasite is indicated with a dashed arrow, and the ensuing transfer of chlamydial genes to the host nucleus is indicated in pink. The progenitor plant cell subsequently diverged into red and green algae and land plants, readily distinguished by their plastid genomes. b) During secondary endosymbiosis, a different heterotroph engulfs a eukaryotic red alga. Potential engulfment of a green algal cell as well is indicated with a dashed arrow. The algal mitochondrion and nucleus are lost, and crucial algal nuclear and plastid genes (indicated in blue, purple and pink) are transferred to the heterotrophic host nucleus, N2 (Armbrust, Nature 2009).

## 1.2 Cell Cycle and cell wall biogenesis

Vegetative cells of diatoms are diploid. In a normal cycle of asexual division two daughter cells originates from a mother cell. Each valve of the parental cell becomes the epitheca of the daughter cell (*Pickett-Heaps et al., 1990*) and each daughter cell will generate a new hypotheca (Figure 1.4). Before the division, the cell elongates, pushing the epitheca away by the hypotheca, and the nucleus divides through an "open" mitosis. After the protoplast was divided by the invagination of the plasma membrane, each daughter cell generates a new hypotheca. This structure, which covers one half of the cell, is commonly generated through the production of polarized vesicles known as silica deposition vesicle (SDV). The construction of the hypotheca provides that the pattern of silica is wrapped by an organic matrix which prevents the dissolution. Once the entire structure is generated, the organic structure is poured out, after which the two daughter cells can be separated. The design of the wall is reproduced from one generation to another, implying the presence of a strong genetic control.

This form of division results in a size reduction of the daughter cell that received the smaller frustule from the parent and therefore the average cell size of a diatom population decreases, until the cells are about one-third their maximum size. This is considered the threshold value. The regeneration of the size takes place through sexual reproduction, followed by the formation of auxospores. The resulting male and female gametes unite to create a diploid auxospore that is larger than the parents. Then, the new cell goes against processes of asexual division until an appropriate signal does not induce again gametogenesis. Sexual reproduction involves several mechanisms, described in detail by *Mann (1993)*. Centric diatoms in the sexual division are always oogama with flagellated male gametes. Among the pennate diatoms there is much more variety and we can find cases of anisogamia, isogamia and automixis. Sexual

reproduction can be sometimes induced when cells are exposed to unfavorable growth conditions. It has been reported that changes in the conditions of light, temperature, nutrient availability and salt concentration can induce a change in the mode of reproduction by asexual to sexual (Armbrust & Chisholm, 1990).

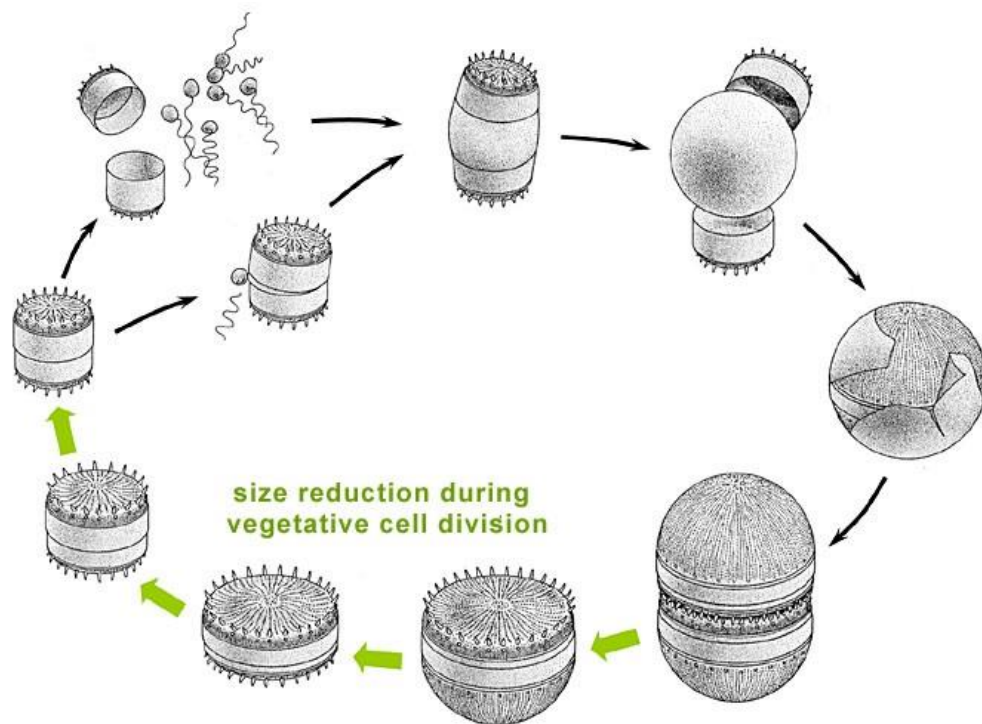


**Figure 1.4** Life cycle of diatoms. The illustration is modified from the original used by Round et al. (1990, fig. 55).

### 1.3 Ecological Importance

The marine phytoplankton represents the major contributor of marine carbon fixation. These organisms can fix approximately the same amount of carbon, a few grams per square meter per day, as a terrestrial forest (Smetacek, 2001).

Diatoms are the most important group of eukaryotic phytoplankton and are responsible for about 20% of marine primary productivity (Falwoski et al., 1998; Mann, 1999)

(Figure 1.5). For this reason they are always regarded as the most representative organisms of phytoplankton and predominant components at the base of the food chain of aquatic ecosystems. Their abundance is generally highest at the beginning of spring and in the autumn, when light intensity and day length are optimal for their photosynthesis. In some regions of the oceans, the annual production of fixed carbon can be up to  $2 \text{ kg m}^{-2}$  equivalent to a cereal or corn crop (Field et al., 1998).

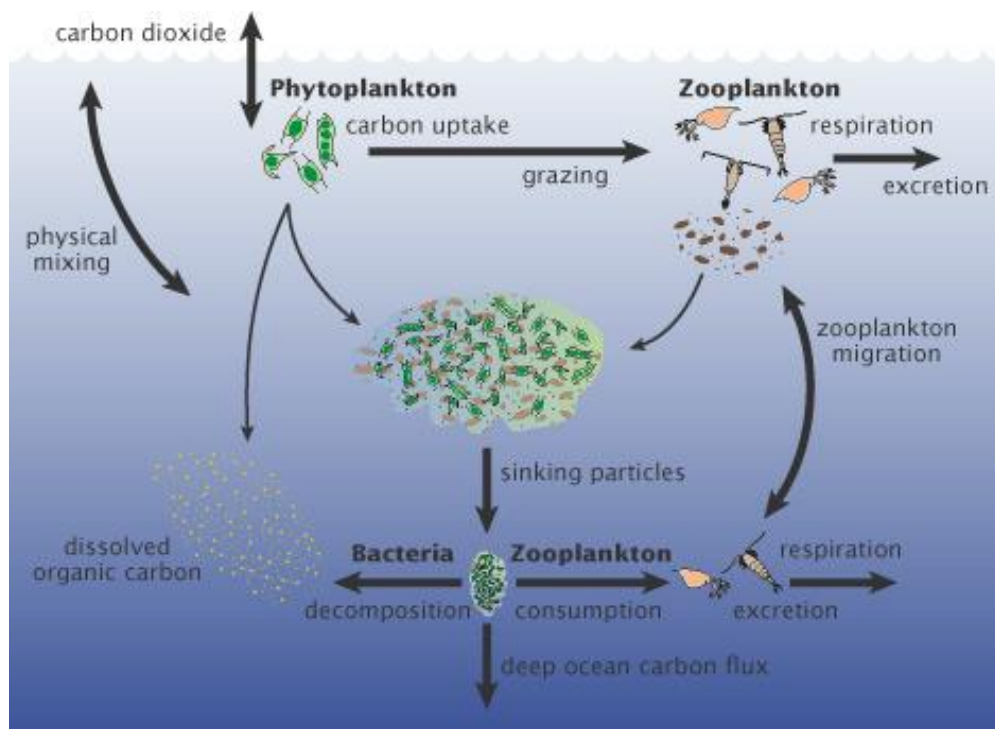


**Figure 1.5.** The carbon cycle in the ocean. Phytoplankton is responsible for most of the transfer of carbon dioxide from the atmosphere to the ocean. Carbon dioxide is consumed during photosynthesis, and the carbon is incorporated in the phytoplankton. Most of the carbon is returned to near-surface waters when phytoplankton is eaten or decomposes, but some falls into the ocean depths. (Illustration adapted from A New Wave of Ocean Science, U.S. JGOFS.)

The quick exponential growth of phytoplankton from hundreds to hundreds of thousands of cells per milliliter is named algal bloom (flowering) (Figure 1.6). Sometimes these events involve toxic phytoplankton such as dinoflagellates of the

genera *Alexandrium* and *Karenia* or diatoms of the genus *Pseudo-nitzschia*. These phenomena then are referred to as “harmful algal blooms”. Of the over 5000 known species of marine phytoplankton, about 300 species can under certain circumstances proliferate in exponential numbers and about 2% of these species can produce potent toxins, which can negatively affect the local ecosystem as well as fishing and aquaculture activities (Landsberg, 2002).

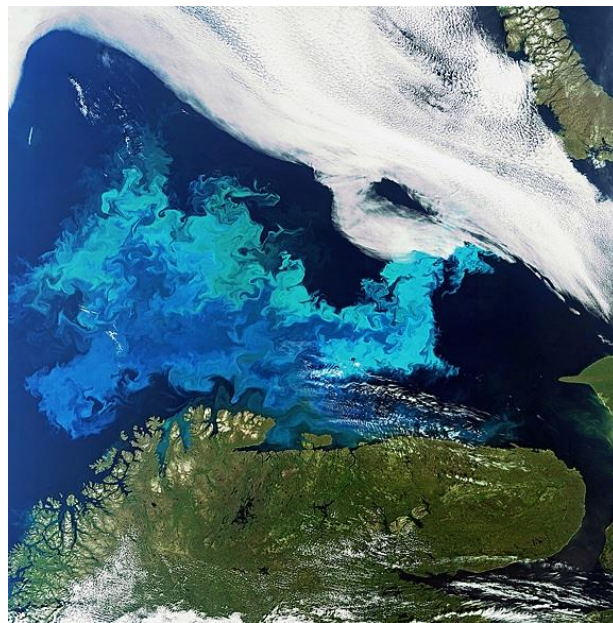


**Figure 1.6.** Algal Bloom in the Barents Sea as seen from space.

For their frustule structure, diatoms greatly influence the marine cycle of silicon. The following "rain" of frustules at the end of the bloom forms the organic silica deposits on the ocean floor. Huge fossil deposits of diatomite or diatomaceous earth (silica residues of frustules of dead diatoms) illustrate the success of this class of algae in the course of thousands of years.

#### 1. 4. Ecological function of microalgal secondary metabolites

Many microalgae produce a variety of different, often unique, secondary metabolites which are released into the environment (Hay, 1996). They are not directly involved in building up the machinery of life and constitute a very small fraction of the total biomass of an organism.

In marine ecosystems, chemical ecology interactions are for the most limited to invertebrate species, such as sponges, mollusks, echinoderms and polychaetes, particularly in benthic tropical ecosystems, where species diversity and resource competition are expected to be high (Hay & Fenical, 1996). On the contrary, most studies on phytoplankton growth and distribution patterns have been focused on physical factors. Nevertheless, secondary metabolites may also play an important role in determining development, dynamics and fate of algal blooms (Landsberg, 2002; Paffenhöfer et al., 2005). Domoic acid is produced in higher quantities by several diatoms of the genus *Pseudo-nitzschia* during the stationary growth phase and under silica and phosphor limitation, but production ceases under nitrogen limitation (Pan et al., 1998). Stress induced by nutrient limitation may not only limit growth rate but also trigger mechanisms that lead to growth decline and even cell death (Janora et al., 2006). Moreover, biotic interactions also appear to be an important role in regulating phytoplankton growth in a number of systems. It is now understood that nutrient limitation and other abiotic stress stimuli, such as light limitation, can initiate intracellular signaling pathways that cause cells to undergo programmed cell death (PCD) in both eukaryotic and prokaryotic phytoplankton (Berges & Falkowski, 1998; Bidle & Falkowski, 2004; Berman et al., 2004), but the chemically-mediated interactions, both inter- and intra-specific, within phytoplankton communities are poorly

understood due to the lack of information on the chemical nature and biosynthetic pathways of the involved allelochemicals.

In such situations, like at the end of a bloom, species producing allelochemicals have an enhanced advantage in the competitive balance. Pratt (1966) observed that the phytoplankton community in the Narragansett Bay was alternatively dominated by blooms of the diatom *Skeletonema costatum* and the dinoflagellate *Olisthodiscus luteus*. In vitro and in situ experiments showed that *O. luteus* achieved dominance by producing a tannin-like substance that had an inhibitory effect on *S. costatum* at high concentrations, but stimulated the growth of this diatom at lower concentrations. Pratt suggested that this may explain the alternating dominance of these two species. Another example is the occurrence of the monospecific bloom of the domoic acid-producing diatom *Pseudo-nitzschia pungens* in Cardigan Bay simultaneously with another diatom *Rhizosolenia alata* in Hillsborough River estuary (Subba Rao et al., 1995). The authors reported that the growth of *R. alata* and *P. pungens* were simultaneously suppressed (*R. alata* by domoic acid, and *P. pungens* by *R. alata* cell-free extracts) and hypothesized that allelopathy may therefore play a role in algal succession.

A second line of research has been highlighting the role of secondary metabolites as information-conveying molecules (infochemicals) in cell-to-cell signaling (Vos et al., 2006). There is clear evidence in terrestrial ecosystems that when attacked by grazers plants can produce secondary metabolites that attract the carnivores of these grazers (Agrawal, 2000). Several authors have suggested that similar interactions may also occur in aquatic ecosystems (Wolfe, 2000). Steinke et al. (2002) suggest that the volatile dimethylsulfide that is released during grazing by microzooplankton can be exploited by mesozooplankton copepods to efficiently graze on. It has been also shown that secondary metabolites produced by phytoplankton can also have adverse effects on the zooplankton grazers. The negative impact of toxins on their predators provides a

strategy for an indirect process of chemical defense. For example when diatom populations are subjected to grazing by copepods they may release aldehydes that can reduce the reproductive capacity of the copepod population, potentially providing an anti-grazing strategy (*Ianora et al, 2004*). Miralto et al. (1999) were the first to identify 2- trans-4-cis-7-cis-decatrienal, 2-trans-4-trans-7-cis-decatrienal, and 2-trans-4-trans-decadienal as diatom compounds responsible for inhibitory effects on copepod embryogenesis. Then a new class of oxygenated fatty acid metabolites, previously intensely studied in mammals and higher plants, was reported from marine microalgae (*d'Ippolito et al., 2005; Fontana et al., 2007*). The term used for this class of compounds is oxylipins. Gerwick defined “oxylipin” as an encompassing term for oxidized compounds formed from fatty acids by a reaction involving at least one step of mono- or di-oxygenase dependent oxidation (*Gerwick et al., 1991*). Marine diatoms produce a number of oxylipins including hydroxy acids, epoxyalcohols, -oxo-acids and the above mentioned polyunsaturated aldehydes, mainly derived from eicosapentaenoic acid (EPA) and chloroplastic C16-fatty acids (*Pohnert, 2002; d'Ippolito et al., 2003; Cutignano et al., 2006; Fontana et al., 2007a*). The first direct proof of a mechanism involving lipoxygenases was obtained with the characterization of the intermediate 9-hydroperoxy-hexadeca-6Z,10E,12Z-trienoic acid in *Thalassiosira rotula* (*d'Ippolito et al., 2006*). Within the eco-physiological role in marine environments, oxylipins seem to have more than one function. In addition to antimetabolic activities and the consequent block of embryogenesis and induction of teratogenic effects in copepods, it was demonstrated that their synthesis in *Pseudonitzschia arenysensis* (formerly *P. delicatissima*) can vary during the algal growth in a manner dependent on cell number, suggesting therefore that these compounds may also play a role of chemical signal at the end of bloom (*d'Ippolito et al., 2009*). Vardi also reported that diatoms can utilize secondary metabolites as part of a sophisticated surveillance system to monitor

environmental stress conditions or chemical defense (*Vardi, 2008*). Nevertheless, despite these studies, which metabolites are involved in intraspecific cellular communication and what signaling pathways induce cell death and affect marine blooms is far to be understood.

### **1. 5. Diatoms as source of future fuel**

Large scale production of microalgal biomass and organic compounds has been a topic of industrial interest for decades (*Becker, 1994; Lee, 2001*). For example considerable research efforts have been invested into biomass per se, polymers, food supplements, enzymes, toxins, coloring substances (pigments) and lipids (*Pulz & Gross, 2004; Harun et al., 2010*). Microalgae have also been harnessed for the treatment of wastewater and as a means to obtain “green energy” products (*Pulz & Gross, 2004; Harun et al., 2010*). Due to increasing energy price and environmental issues, there is a high demand for renewable, carbon neutral, transport fuel, which is environmentally and commercially sustainable. Production of microalgae for biofuels has been emerging as a potential alternative to other biological sources of fuels since algae generally have high oil content and rapid biomass production. In fact, these phototrophic organisms can grow very quickly (approximately 1-3 doubling per day) and can accumulate between 30 and 60% of their dry mass as lipids, with this broad range being due to species and growth condition-dependent variability. Intriguingly, lipid content can even reach up to 90% of dry mass when cells are subject to physiologically stressful conditions, such as nutrient starvation or photo-oxidative stress (*Scheehan et al., 1998; Spolaore et al., 2006; Chisti, 2007; Schenk et al., 2008; Hu et al., 2008; Khozin-Goldberg et al., 2011*). Diatoms can also be cultivated in non-potable water and on non-arable land and therefore have small demands in comparison with terrestrial crops (*Chisti, 2007*). These characteristics make

these microalgae suitable for large-scale bio-fuel cultivation. In 1998, the Aquatic Species Program recommended a list of 50 microalgal strains (Aquatic species program close-out report; [www.nrel.gov/docs/legosti/fy98/24190.pdf](http://www.nrel.gov/docs/legosti/fy98/24190.pdf)), selected from a pool of over 3000 candidates, which held the most promise as biofuel-production organisms. Sixty percent of the selected strains were diatoms, which were chosen based on criteria such as high growth rates and lipid yields, tolerance of harsh environmental conditions, and performance in large-scale cultures. Diatoms are found in marine, freshwater and soil habitats, but also specific extreme or variable environments of salinity, temperature (ice or hot springs) and pH. Furthermore, these prokaryotes exhibit trophic flexibility. The majority of species are autotrophic, but mixotrophy and obligate heterotrophy occur. *Cyclotella cryptica*, a candidate biofuels production strain, is capable of growth on glucose only in the dark, likely due to its glucose transport mechanism being induced in the absence of light (Hellenbust, 1971).

#### **1.6. Model Organism: *Skeletonema marinoi***

The diatom *Skeletonema marinoi* (Figure 1.7) is common in the Adriatic Sea where, in winter, is responsible for the yearly maximum of phytoplankton biomass. This cosmopolitan diatom forms dense coastal and oceanic blooms and can contribute to a large part of diet of higher trophic organisms. These blooms affect negatively copepod reproduction. The effect has been suggested to the production of short chain aldehydes which interfere with the normal development of the eggs (Ianora et al., 2004, cited as *Skeletonema costatum*). The physiology and carbon fixation pathways of *S. marinoi* have been studied (Puskaric & Mortain-Bertrand, 2003) and it also has become a model species in ecological and environmental studies (Mortainbertrand et al., 1988; Ianora et al., 2004; Yamasaki et al., 2007). This species can exist as solitary cells or form chains

of more than 20 individuals. The reasons why *S. marinoi* and some other species of diatoms form chain-like colonies are not clear, but other organisms (bacteria and *Phaeocystis* sp.) can start to grow in filaments or colonies after sensing cues from grazers (Long et al., 2007). Each cell is 2–12  $\mu\text{m}$  and contains one or two large chloroplasts.

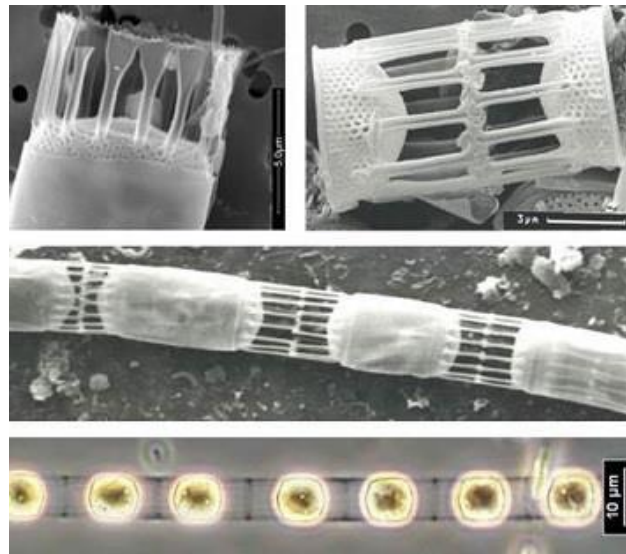


**Figure 1.7.** Images of *Skeletonema marinoi* (Sarno & Zingone, 2005).

### **1.7. Model Organism: *Cyclotella cryptica***

*Cyclotella cryptica* is a planktonic species first isolated from brackish water. It is typically found in harbors and in parts of the Great Lakes where there are abnormally high chloride concentrations. It has been known to account for up to 18.5% of diatom abundance in the Oswego Harbor of Lake Ontario. It occurs at maximum abundance around 20°C (Herth & Zugenmaier, 1977; Liu & Hellebust, 1976; Makarewicz, 1987; Mills et al., 1993; Stoermer & Ladewski, 1976; Stoermer & Yang, 1969). *C. cryptica* can exhibit different morphologies depending on salinity and its diameter can range from 5–25  $\mu\text{m}$  depending on environmental conditions. Other examples of the

phenotypic plasticity of *C. cryptica* lend themselves well to the algal biofuel and biomass industries as the photomicrographs in this feature illustrate (Figure 1.8). The first is its ability to produce high concentrations of oil as the cells senesce and the second is its ability for heterotrophic growth (*Lewin & Ralph, 1960*). This species is typically characterized as photoautotrophic, meaning it uses inorganic carbon sources and light in photosynthesis. However, this species is also capable of heterotrophic growth in benthic environments by utilizing glucose. It has also been the target of genetic manipulation *Dunahay et al. (1996)* to help increase lipid accumulation and increase the efficiency of oil production in these versatile marine diatoms.

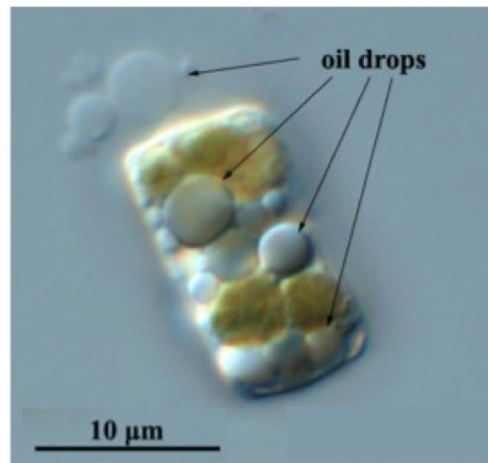


**Figure 1.8.**Image of *Cyclotella cryptica* Reimann, Lewin & Guillard. This image highlights the high oil content (oil drops) of this diatom.

## 1.8. Aim of thesis

The marine diatoms are unicellular algae that play an important ecological role in the global primary production (*Falkowski et al., 1998*). These unicellular protists are able to survive and proliferate in a wide range of environmental conditions, by adapting their metabolism through mechanisms largely unknown. Understanding these processes is of great ecological interest and can have wide application in different biotechnological sectors. In the last years, the research group of Institute of Biomolecular Chemistry (ICB-CNR, Pozzuoli, Naples) where I have carried out my PhD studies, has been investigating chemistry and biochemistry of diatoms with the aim of clarifying the basic process linked to defense and adaptation induced by biotic triggers.

In this frame, this work of doctoral thesis was focused on lipid metabolism of diatoms. The first part of the work aimed at identifying secondary metabolites with regulatory role in the physiological pathway of cell death of *Skeletonema marinoi* that was chosen as ecologically-relevant model species. In the second part of the work we wanted to evaluate the biochemical inhibition of the physiological processes of cell death as tool to control the growth of *Cyclotella cryptica* in view of use this species for the biological production of biofuels and bioproducts. Since *C. cryptica* is also capable of heterotrophic growth, this species was also designed to study the biosynthetic pathways in diatoms.

For this purpose the thesis work faced the following issues:

- Isolation and characterization of bioactive compounds
- Biochemical investigation of *S. marinoi* cell death pathway
- Qualitative and quantitative analysis of sterol sulfates in diatoms
- Sterol biosynthesis in diatoms
- Inhibition of sterols sulfotransferase

## 2. Isolation and characterization of bioactive compounds

### 2. 1. Introduction

Diatoms are responsible for sudden and massive growths, known as “bloom”, in the oceans and seas of the planet. The phenomenon is the basis of the marine food chain, and contributes to the capture of approximately 40% of global carbon dioxide, although these organisms constitute less than 1% of the Earth's biomass (*Field et al, 1998*). Maintaining a steady state with such a high ratio of primary productivity / biomass implies that, on average, these organisms grow, die and are replaced almost every week (*Valiela, 1995*). Programmed cell death (PCD) is a form of autocatalytic cell suicide leading to apoptotic-like morphological changes and, ultimately, cellular dissolution. This deadly pathway has been extensively reported in multicellular organisms, and recently it has also been demonstrated to occur in different species of phytoplankton, refuting the long-held misconception among biological oceanographers whereby that phytoplankton are immortal unless they become prey of herbivorous zooplankton (*Bidle & Falkowsky, 2004*). However, the physiological factors and biochemical pathways involved in cell death and their role in determining the end of the bloom are little known. It has been reported that diatoms produce antimetabolic metabolites in response to physical damage during copepod grazing (*Pohnert, 2000*) and high level of oxygenated fatty acid derivatives (“oxylipins”) have been correlated to culture progress (*d’Ippolito et al., 2005*), but there is no evidence of metabolites that can be synthesized and secreted to play as death signals or trigger bloom/culture termination.

In this study the diatom *Skeletonema marinoi* was analyzed in relation to the ability to produce compounds that may act as intraspecific inhibitory or cytotoxic signals. The chemical approach to identify active molecules employs bioassay-guided fractionation of organic extracts. The bioassay-guided method has the advantage of deselecting

inactive fractions in favor of active constituents, but the analytical protocol is limited by a number of critical issues including degradation of the products and formation of artifacts during the chromatographic steps.

## **2. 2. Results and discussion**

### *2. 2. 1. Skeletonema marinoi growth curve*

In a first experimental set, *S. marinoi* cultures (in 10L- carboy, Figure 2.1) have been sampled in mid-exponential (constant maximal growth rate), early stationary (as soon as the growth rate decreases) and declining phases of growth (after a substantial decrease in cell concentration) to investigate the production of physiological cytotoxic compounds. These phases have been chosen since they represent critical steps in the evolution of an algal culture, being characterized by different dominant cell processes (growth, senescence and mortality) that are supposed to reflect changes in cell metabolism.

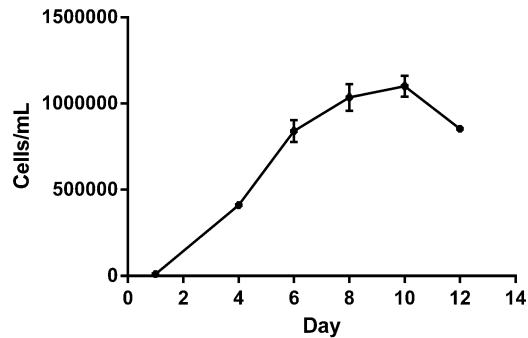


**Figure 2.1.** *S. marinoi* cultures in 10-L carboy and the relative growth curve.

In a second set of experiments, *S. marinoi* from 40 L culture was harvested in the first point of declining phase. The large culture of the diatom was carried out in an inclined photobioreactor that uses a combined system of micro and macro insufflations in order to limit the adhesion of cells on surfaces without damaging them.

Using daily addition of nutrients and buffering at pH 7.5 by 50 mM MOPS, we obtained growth curves of the duration of 7 days (Figure 2.2) with  $1.0 \pm 0.2 \text{ g L}^{-1}$  of biomass ( $1.0 \pm 0.2 \text{ g L}^{-1}$ ). Diatom cultures were also grown under  $\text{CO}_2$  bubbling. As showed in the Figure 2.2 5%  $\text{CO}_2$  in air induced an increase of cell growth during stationary phase maintaining the same duration of the growth curve (7 days). Accordingly, biomass increased from  $1.0 \pm 0.2 \text{ g L}^{-1}$  to  $1.6 \pm 0.1 \text{ g L}^{-1}$  of culture, which was the best yield for *S. marinoi* in the photobioreactor.

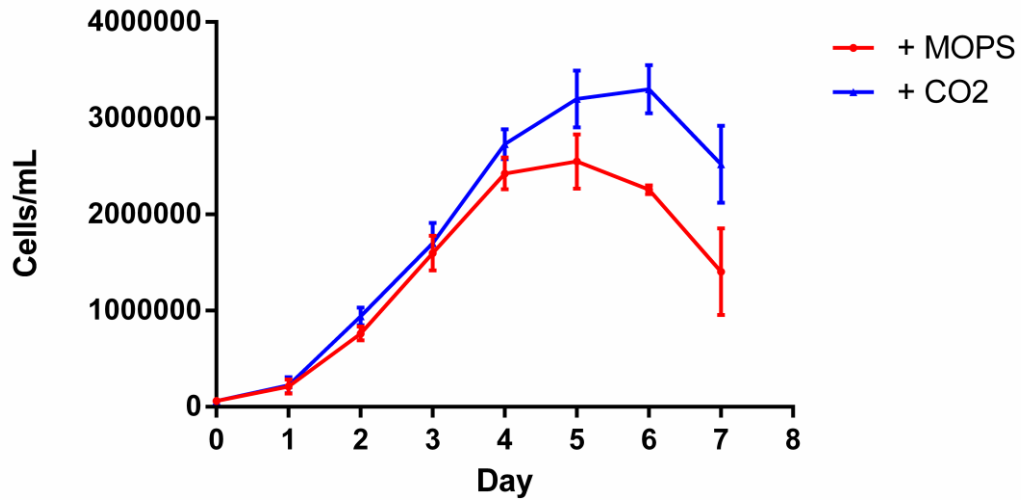


**Figure 2.2.** Growth curves (Cells/mL) of *S. marinoi* in 40-L photobioreactor, by using MOPS or CO<sub>2</sub> to buffer the pH.

### 2. 2. 2. Effects of *Skeletonema marinoi* cell extracts on its growth

Samples of cultures (1L) were collected from the 3 phases of microalgal growth (exponential, stationary, and declining). After harvesting by gentle centrifugation, cell pellets were extracted in boiling methanol (Jüttner, 2001; Cutignano et al., 2006) as described in the section 8.2 and the resulting material was tested in duplicate on exponentially growing cultures of *S. marinoi* in 24-well plates in f/2 medium (Figure 2.3).

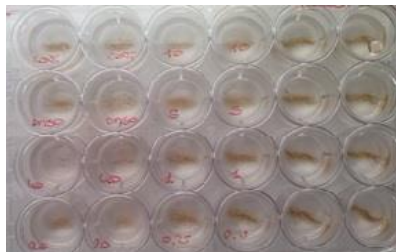


**Figure 2.3.** 24-well plates inoculated with *S. marinoi* exponentially growing cultures. Biological assay were performed as described in section 8.4.1.

In order to assess the products close to physiological levels, the organic extracts in 10  $\mu\text{L}$  methanol were tested at 60, 40 and 20  $\mu\text{g mL}^{-1}$ . As shown in Figure 2.4 only the extracts obtained from the declining phase had a strong negative effect on the growth of *S. marinoi*, with complete inhibition at 40  $\mu\text{g mL}^{-1}$  in 24 h. The cells appeared broken and morphologically altered (Figure 2.5), with a massive presence of debris after 48 hours of incubation.

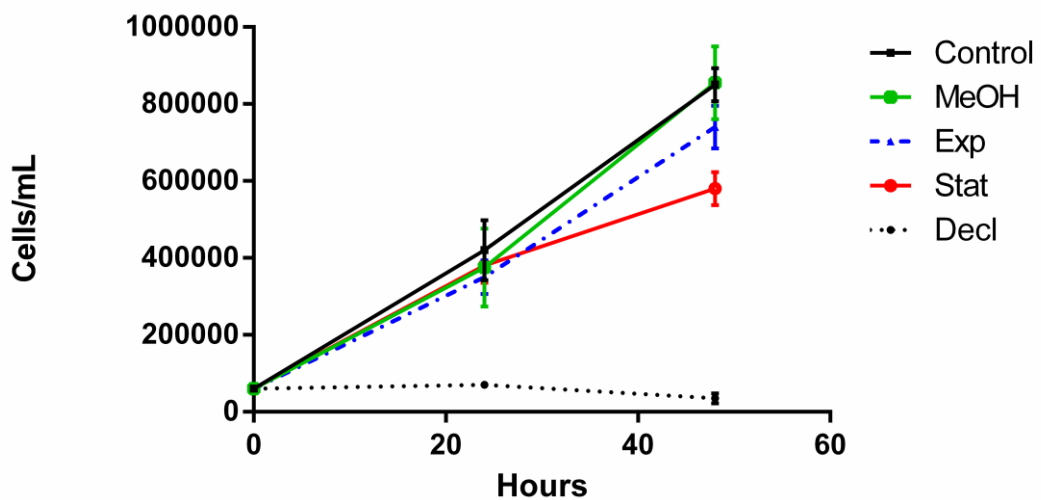


**Figure 2.4.** Effect of organic extracts obtained from different stages of microalgal growth on *S. marinoi* cells: exponential (Exp), stationary (Stat) and declining (Decl) phase, compared to standard growth (Control) and cells incubated with only 10  $\mu\text{L}$  of methanol to exclude that the observed activity was due to the solvent in which the samples were diluted or to a non-optimal physiological state of cells used for the assays. All extracts were tested at a concentration of 40  $\mu\text{g mL}^{-1}$  in 24-well plates.



**Figure 2.5.** Cellular morphology of *S. marinoi* at 0 (a), 24 (b) and 48 (c) hours by the addition of bioactive extracts from declining growth phase (magnification of 40 x). It is evident a progressive destruction of cellular integrity until massive presence of debris at 48 h (c).

To corroborate these results, the active extract was also tested at  $40 \mu\text{g mL}^{-1}$  with increasing cell numbers ( $6 \cdot 10^4$ ,  $5.5 \cdot 10^5$ , and  $8 \cdot 10^5$  cells  $\text{mL}^{-1}$ ) and the effect was monitored up to 5 days. As reported in Figure 2.6, the cytotoxic response showed linear dependence on cell number and incubation time. According to these results,  $6 \cdot 10^4$  cells  $\text{mL}^{-1}$  and 48 hours of incubation time were established as standard conditions to evaluate compound activity.

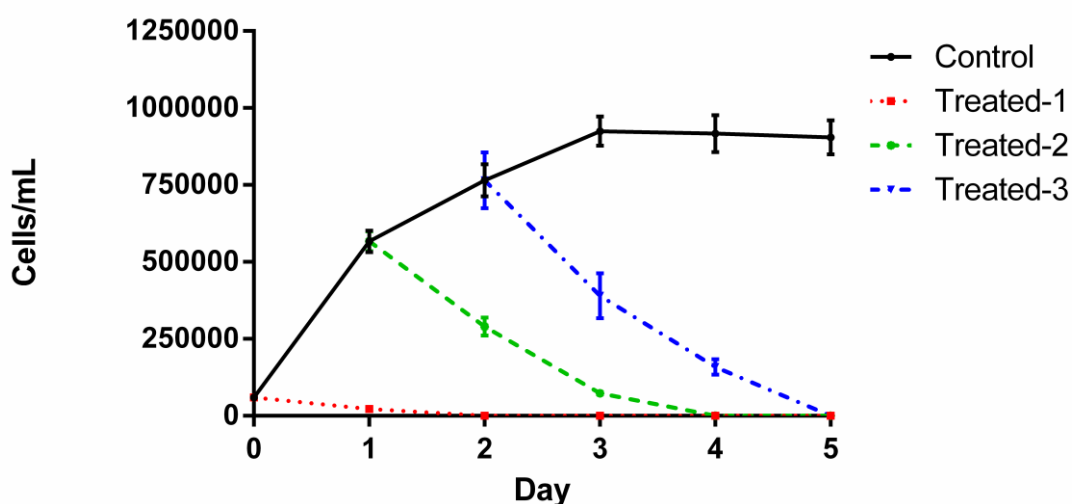


**Figure 2.6.** Effect of organic extracts obtained from declining stage of microalgal growth on *S. marinoi* cells at concentration of  $40 \mu\text{g mL}^{-1}$ . The extract was tested at increasing cells concentrations from  $6 \cdot 10^4$  (Treated-1),  $5.5 \cdot 10^5$  (Treated-2) to  $8 \cdot 10^5$  (Treated-3) cells  $\text{mL}^{-1}$  and monitored until 5 days of incubations. The control curve (Control) is the standard growth curve obtained in 24-wells in 5 days.

The active extract obtained from declining phase was also tested at scalar concentrations of 60, 40 and 20  $\mu\text{g mL}^{-1}$  (Figure 2.7). The cell death effect was apparently dose-dependent since a reduced toxicity has been observed at lower concentration of the extract, although the effect is still significant. There was a mortality rate of 100% in 24 hours at concentration of 60  $\mu\text{g mL}^{-1}$ . About the same mortality rate was reached in 48 hours at concentration of 40  $\mu\text{g mL}^{-1}$ . At concentration 20  $\mu\text{g mL}^{-1}$  there was a mortality rate of about 90% in 48 hours. Extracts collected in other growth phases were not active or did not induce specific variation of morphology of the tested cells (n=3).

In the extracts from declining growth phase should therefore be present an organic compound that, independently from the availability of nutrients and other external factors, induces cell death. The investigation of the presence of cytotoxic compounds proceeded only in these extracts by a bioassay-guided fractionation. This means a step-by-step separation of the components of active extract by assessing the biological activity, followed by next round of separation and assaying (Weller, 2012).

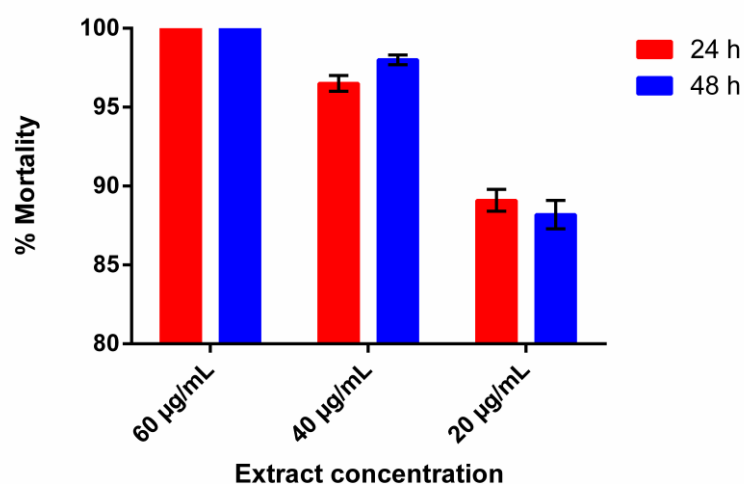


**Figure 2.7.**Effect of the organic extracts from the declining growth phase assayed at different concentrations: 60, 40, 20  $\mu\text{g mL}^{-1}$  of *S. marinoi* culture. Data are expressed as percentage of mortality after 24 and 48 hours of incubation with the extracts. Biological response increased as increased quantities of extract are administered.

### 2. 2. 3. Isolation and characterization of bioactive compounds

The entire procedure of bioassay-guided fractionation is reported in Figure 2.8.

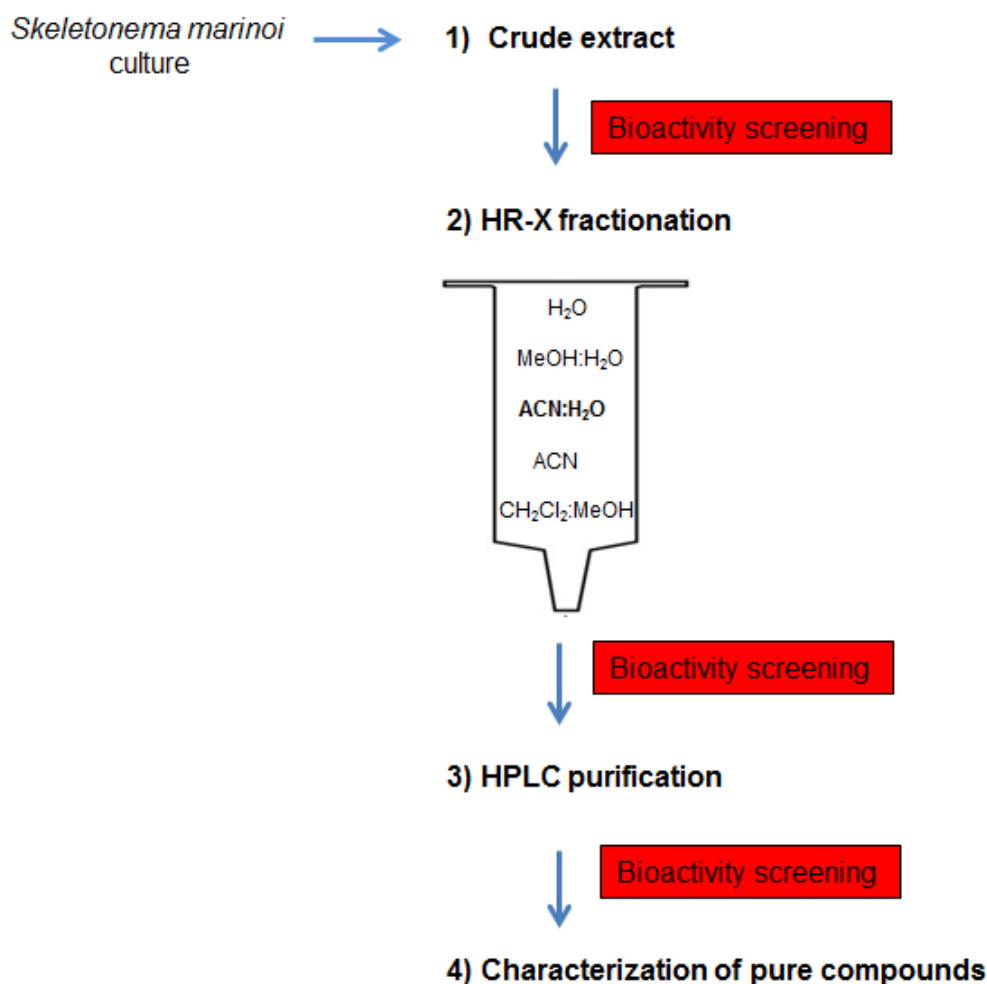


**Figure 2.8.** Schematization of the entire process of bioassay-guided fractionation from the extract of the organic pellets of *S. marinoi*. By 20 L of *S. marinoi* culture we obtained  $1.84 \pm 0.54$  g of bioactive extract from declining growth phase. After fractionating this extract on HR-X resin, only the fraction eluted with acetonitrile: water ( $56.1 \pm 11.2$  mg) was active. We obtained an HPLC bioactive fraction containing a mixture of 3 sterol sulfates ( $1.8 \pm 0.35$  mg). These sterols were purified in the last HPLC step and characterized.

As a first step of purification, it has been investigated a new method for fractionation of organic extracts based on solid phase extraction on polystyrene–divinyl benzene columns (CHROMABOND® HR-X). This chromatographic support allows separation

of organic compounds on the basis of their polarity and molecular weight. Fractionation of algal extracts gave six fractions eluted with decreasing polarity solvents, from water to dichloromethane (Table 8.1). As shown in Figure 2.9, the HR-X column selectively enriched different classes of compounds in the various fractions. In particular, salts were eluted with water in fraction 1 along with the sugars that were also present in fraction 2 together with pigments. Fraction 3 was characterized by compounds of intermediate polarity, including sulfoquinovosyldiacylglycerols (SQDGs) and phospholipids (PLs), while fraction 4 mostly contained pigments, monogalactosyl diacylglycerols (MGDGs) and minor levels of free fatty acids. Fraction 5 showed most of the neutral lipids, such as sterols and triglycerides, together with part of digalactosyl diacylglycerols (DGDGs).

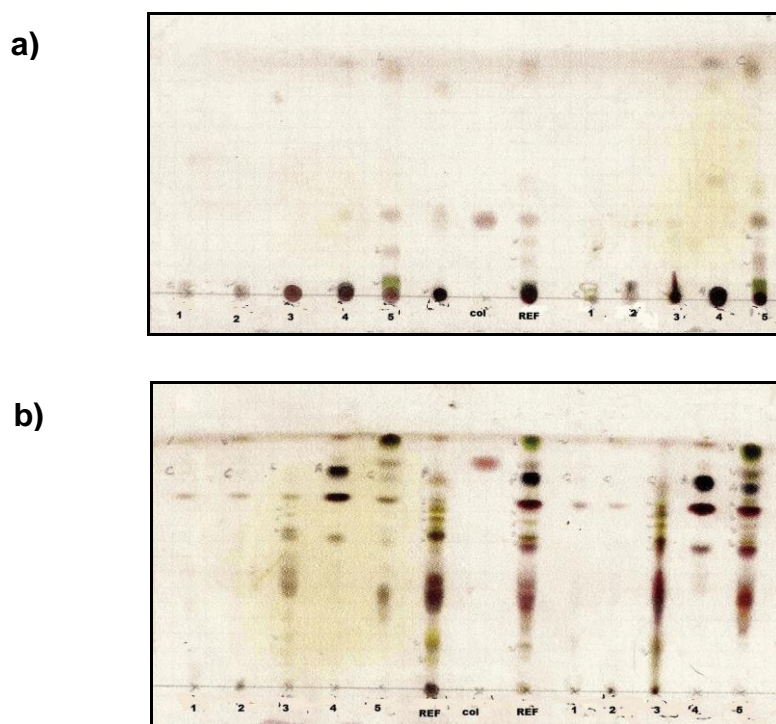


**Figure 2.9.** TLC analysis of HR-X fractions of two *S. marinoi* active extracts (**REF**); a) TLC eluted in EP:EE (1:1; v/v); b) TLC eluted in CHCl<sub>3</sub>: CH<sub>3</sub>OH: H<sub>2</sub>O (65:25:4; v/v/v). Spots were detected by Ce(SO<sub>4</sub>)<sub>2</sub> e cholesterol (**col**) was used as reference.

These fractions were tested in 24-wells assay on *S. marinoi* cells. The activity was found to be conserved in the fraction eluted with CH<sub>3</sub>CN:H<sub>2</sub>O at concentration of 20 µg mL<sup>-1</sup>. The bioactive mixture was then fractionated by HPLC on a reversed phase semipreparative column (Table 8.2). Fractions were collected every two minutes and, after removal of the organic solvents, these samples were tested again on *S. marinoi* as described above. Activity was found at 10 µg mL<sup>-1</sup> (48 h) only in the material eluted between 10-12 minutes (Figure 2.10). NMR and MS analysis revealed that this fraction contained a mixture of sterol sulfates and sulfoquinovosyldiacylglycerols (SQDGs).

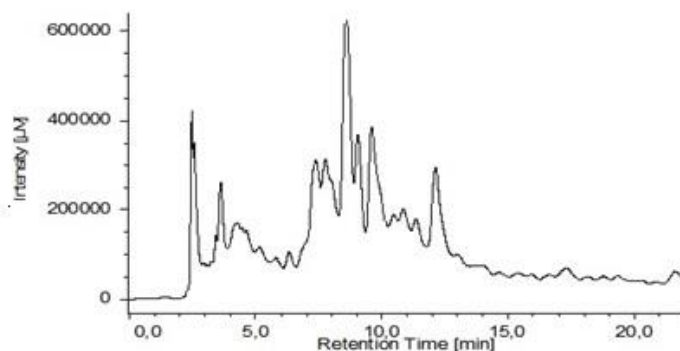


**Figure 2.10.** HPLC profile of bioactive HR-X fraction. UV profile was monitored in the wavelength range from 200 to 600 nm and the fractions were collected every two minutes. Bioactive fraction is at 10-12 minutes.

As shown in Figure 2.11 reporting NMR spectra of crude organic extract, HR-X and HPLC bioactive fractions, the protocol of purification enriched the active components and activity increased along the various purification steps (Table 2.1).

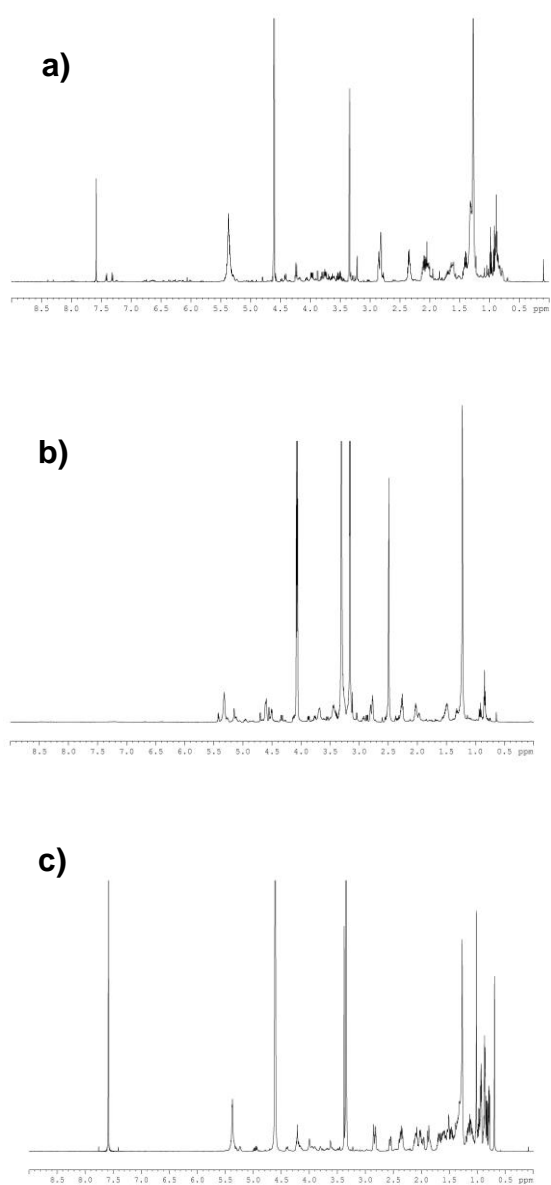


**Figure 2.11.** NMR spectra (600 Hz) of bioactive fractions: *S. marinoi* organic extract from declining growth phase (a); active HR-X fraction eluted in CH<sub>3</sub>CN:H<sub>2</sub>O (b); HPLC active fraction from semipreparative purification (RT 10-12 min of HPLC profile) (c).

**Table 2.1** EC<sub>50</sub> (48 h) of the active fractions obtained in the different steps of purification

	EC <sub>50</sub> (µg/mL)	±SD
<b>Extract</b>	21,5	2,58
<b>HR-X fraction</b>	10	1,37
<b>I purification</b>	5	0,1

To complete the characterization of the bioactive products, the purification protocol was repeated by starting from larger amount of material. The first step of fractionation was carried out by radial chromatography on Chromatrotron as illustrated in section 8.3. Product elution was achieved by an increasing gradient of MeOH in CHCl<sub>3</sub> and the compounds of interest (fraction 2) were recovered in CHCl<sub>3</sub>/CH<sub>3</sub>OH 85:15 (v/v) (Figure 2.12).

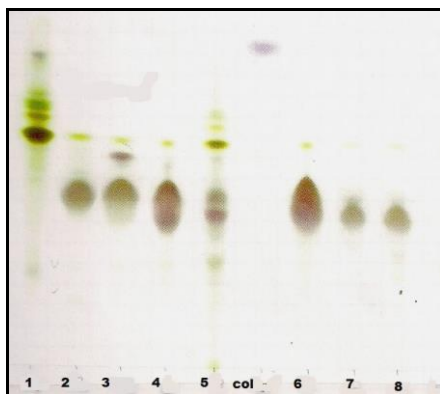


**Figure 2.12.** TLC analysis of Chromatrotron fractions eluted in CHCl<sub>3</sub>: CH<sub>3</sub>OH: H<sub>2</sub>O (65:25:4; v/v/v). Spots were detected by Ce(SO<sub>4</sub>)<sub>2</sub> e cholesterol (col) was used as reference. Fraction 2 was enriched in sterol sulfates.

The bioactive fraction was then purified by HPLC equipped with an Evaporative Light Scattering Detector (ELSD) on a reversed phase analytical column under the same elution conditions used before (Table 8.3). In this last step of purification by HPLC the

mean compound **2** (Figure 2.14) has a cytotoxic activity at concentration  $5 \mu\text{g mL}^{-1}$  of culture (48 h). This compound corresponds to one of three peaks showed in the ELSD profile at RT 12 minutes in the Figure 2.13 and was then analyzed by MS and NMR. The baseline and the other peaks showed in the chromatogram were assayed and were not active on *S. marinoi* cells. Compounds **1** and **3** (RT 12 and 16 min) were not tested for the small amount in the mixture that was not well measurable.

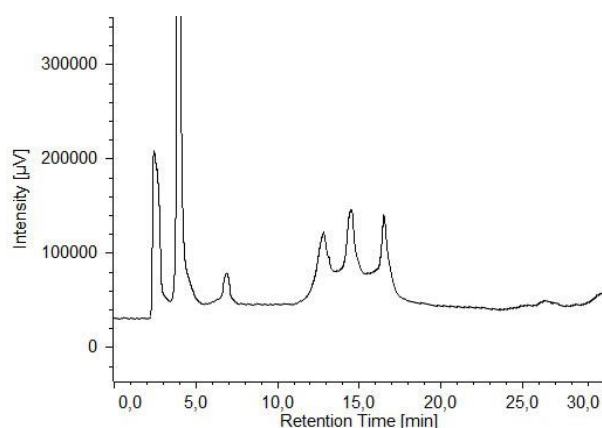


**Figure 2.13.**ELSD profile of bioactive fractions: the three peaks at RT 12 min coincide with the active fractions.

The active compounds are three sterol sulfates (StS) that were purified in the last HPLC step and characterized. Structures are reported in the Figure 2.14, reporting their ESI MS/MS fragmentation pattern.

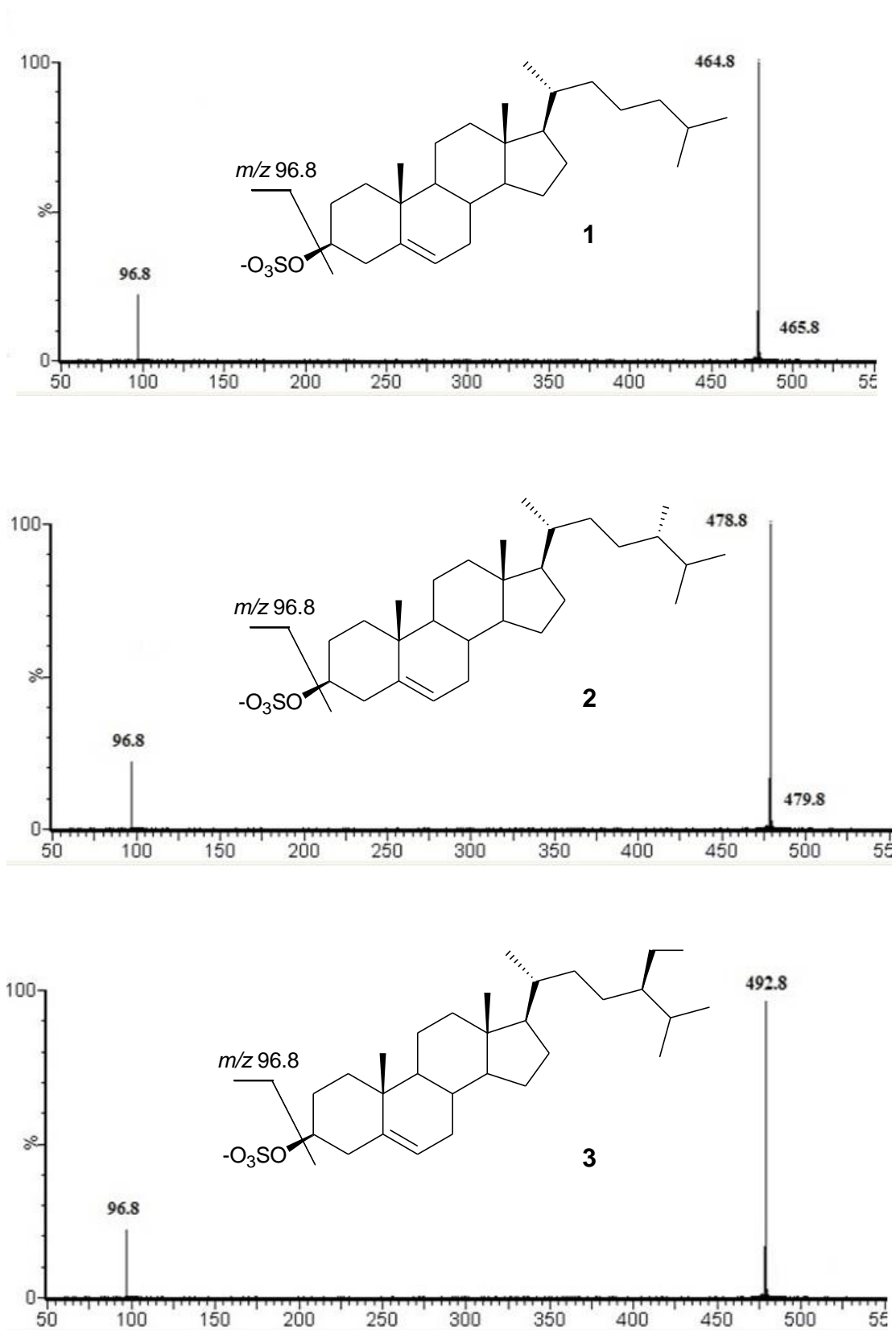


**Figure 2.14.** ESI MSMS spectra (with loss of  $\text{HSO}_4^-$  residue) and the chemical structure of the isolated sterols: 5-cholesten-3 $\beta$ -ol sulfate (1); 24-methylcholest-5-en-3 $\beta$  ol sulfate (2); 5-sitosten-3 $\beta$ -ol sulfate (3).

The main compound is the compound **2** (Figure 2.14), identified as dihydrobrassicasterol sulfate (24-methylcholest-5-en-3  $\beta$ -ol sulfate) (**StS-2**). The ion-negative mass spectrum of this compound exhibited a molecular ion species at  $m/z$  478.8, corresponding to  $[M-H]^-$  and a fragment ion peak in MS/MS analysis at  $m/z$  96.9, interpreted as loss of  $HSO_4^-$  residue. The structure was confirmed by  $^1H$ -NMR analysis (Figure 2.15) and  $^{13}C$ -NMR (Figure 2.16) data. In particular the  $^{13}C$  NMR spectrum measured in  $CD_3OD$  was consistent with the presence of 28 carbon atoms and J-Mod experiment showed the presence of six methyl groups, ten methylene, nine methine, one bonded with oxygen atom, and three quaternary carbons. The  $^1H$ -NMR confirmed the presence of six methyl groups, with signals at  $\delta$  0.75 (s), 0.83 (d), 0.84 (d), 0.91(d), 0.98 (d) and 1.06 (s) ppm. 2D-COSY experiment allowed establishing the connectivities of C-1 to C-8 and C-15 to C-21 within the steroidal framework. The proton spectrum included also an olefinic proton at  $\delta$  5.42 ppm and a complex signal at  $\delta$  4.24 ppm assigned to a  $3\beta$ -oxygenated methine and its downfield chemical shift was identical to that reported in the spectrum of the  $5\alpha$ -cholestan- $3\beta$ -yl sulfate reported in literature (Ricchio et al., 1985; D'Auria et al., 1987; D'Auria et al., 1989) confirming a sulfate group located there. We confirmed the stereochemistry ( $24\beta$ -alkyl sterol) by the resolution of the signal at 0.84 ppm in  $^1H$  NMR spectra (Nes et al., 1976) and by  $^{13}C$  signal of C-28 carbon signal and other side chain signals that are different in  $\alpha$  and  $\beta$ -epimer (Wright et al., 1978).

Compound **1** (**StS-1**) and **3** (**StS-3**) have the same nuclei and differed in the side chain, as confirmed by the  $^1H$  NMR spectra. In particular comparing the NMR data of compounds **1** with those of compound **2** we found the absence of the methyl group in position 24, whereas the compound **3** showed an ethyl group in the place of the methyl in the same position (Figure 2.15). To establish the absolute stereochemistry of carbon 3 ( $\delta$  79.81 ppm) we compared the multiplicity and the chemical signal of the proton in

this position to the spectrum of the commercial sodium cholesteryl sulfate (Sigma Aldrich) (Figure 2.16). According to these analysis, compounds **1** and **3** were characterized as 5-cholesten-3 $\beta$ -ol sulfate (m/z 464.8) and 5-sitosten-3 $\beta$ -ol sulfate (m/z 492.8), respectively.

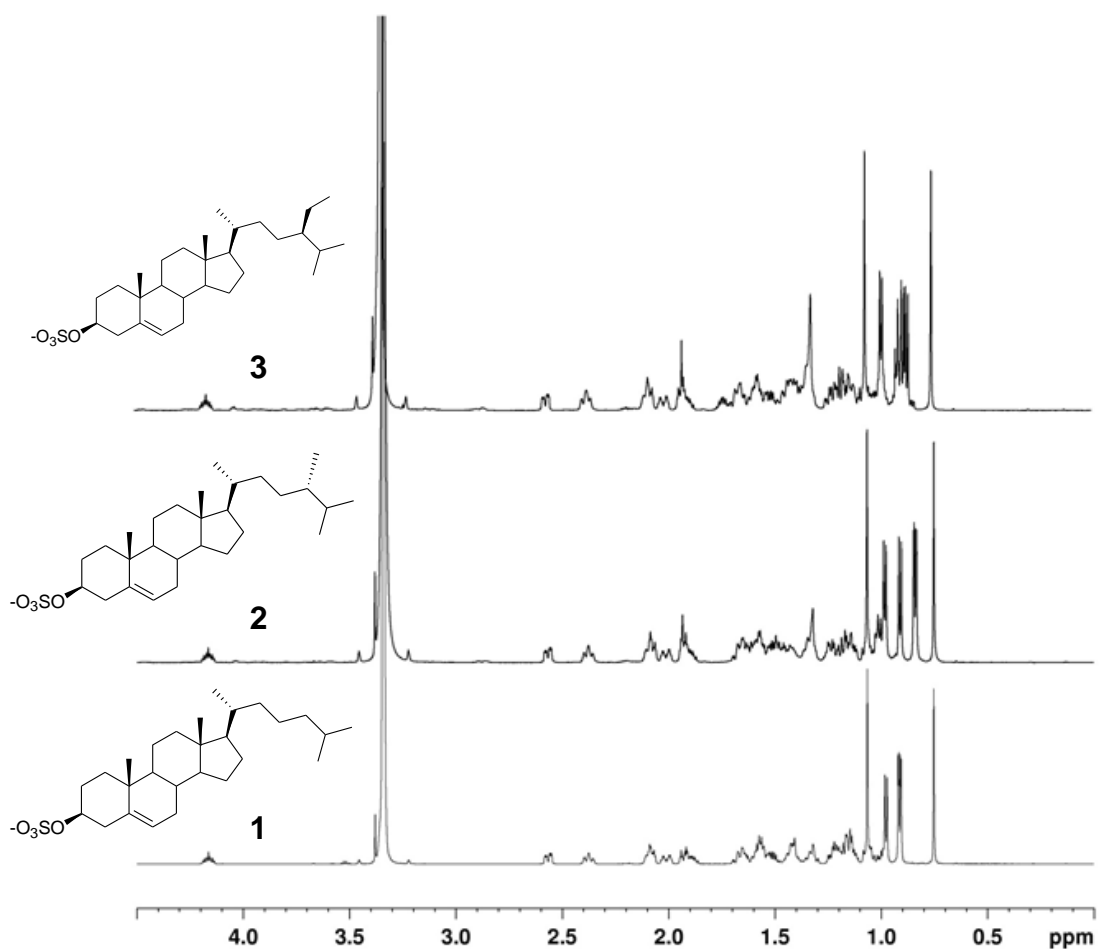


**Figure 2.15.** <sup>1</sup>H NMR spectra of three sterol sulfates characterized. In the region around 0.7 ppm there are the main differences in the multiplicity and chemical shifts of the proton signals corresponding to different alkyl group in the lateral chain of the three compounds.

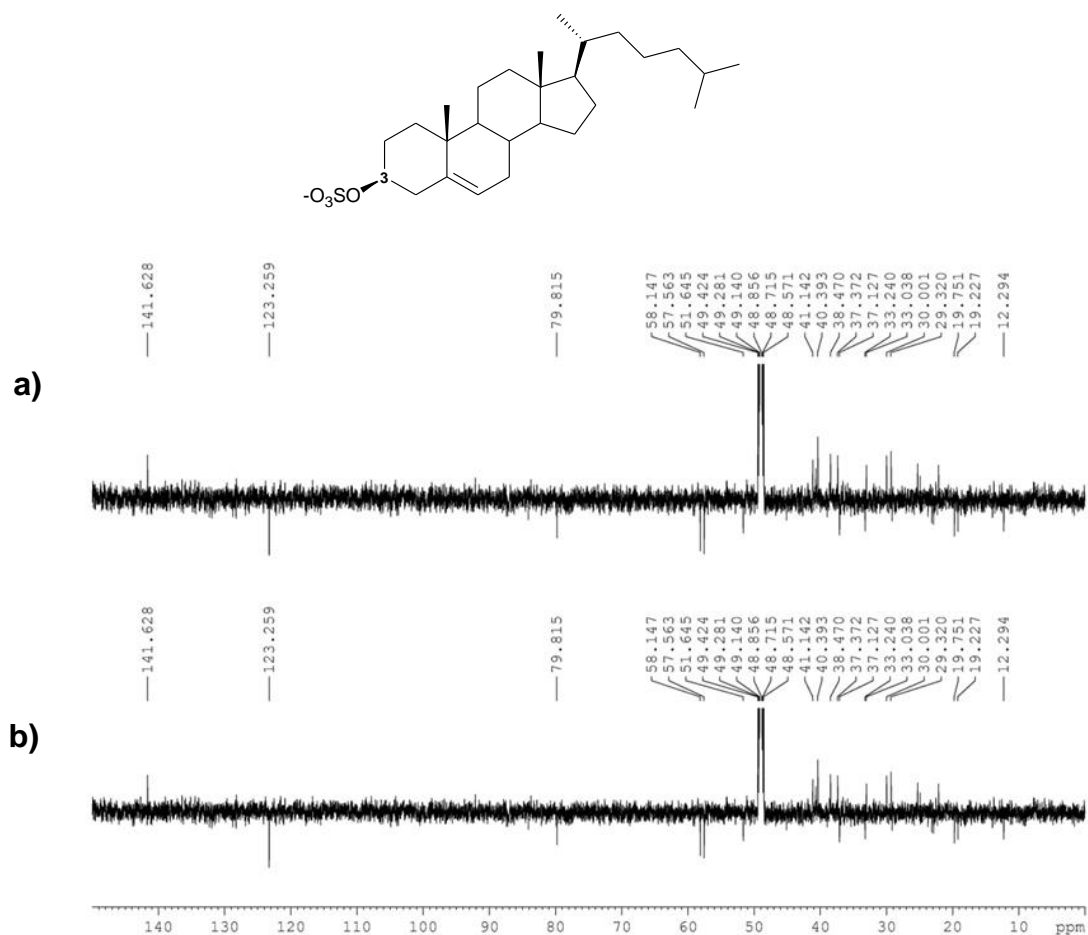


**Figure 2.16.J**-Mod experiment of 5-cholesten-3 $\beta$ -ol sulfate (from *S. marinoi* extract) (a) and of commercial 5-cholesten-3 $\beta$ -ol sulfate (b). The structure of StS-1 is exactly the same of that of commercial compound. The chemical shift of the signal of C-3 carbon (79.815 ppm) confirmed a sulfate group in this position.

To confirm the biological activity of the sulfated sterols, the commercial analog 5-cholesten-3 $\beta$ -ol sulfate (StS-1) was tested. The toxic dose of the natural compound was the same of the synthetic cholesterol sulfate, supporting that the biological activity of the active fractions was really due to this class of compounds and not to other trace compounds.

#### 2. 3. 4. Determination of $EC_{50}$

The  $EC_{50}$  values (concentration required to cause 50% mortality) were calculated using linear regression analysis of StS-1 concentration as natural logarithm data versus percentage mortality (Ma et al., 2004; Sebaugh, 2011; Liu et al.; 2012).

$EC_{50}$  was established by using increasing amounts of the pure compound to  $5 \cdot 10^4$  cell  $mL^{-1}$  cultures of *S. marinoi* and by measuring the responses for each dose until saturation- i.e. the point at which increasing the concentration of compound does not increase the magnitude of the response. The response at different concentrations of StS-1 was recorded between 0.5 to 100  $\mu g mL^{-1}$ . As assessment of cell viability, the chlorophyll *a* fluorescence and the vitality by the fluorescein diacetate assay were estimated. Chlorophyll *a* fluorescence can well match the chemically estimated chlorophyll *a* biomass (Veldhuis & Kraay, 2000) and has been considered as a measure of the total amount of intact cells. As demonstrated in Figure 2.17, significant excitation and emission peaks were observed that correspond to expected peaks for chlorophyll *a* fluorescence. An excitation peak was observed at 434 nm, while an emission peak at 684 nm was found. Subsequent fluorescent determinations used an excitation wavelength of 451/5 nm and an emission wavelength of 679/5 nm with diatom cells dilutions *in vivo*: 200  $\mu L$  of each culture (n=3) were directly pipetted in a black 96-wells plate, mixed and measured. The fluorescent response was found to be linear with cell number for all concentrations tested (Figure 2.18). This observation suggests that this method of determination could be used to assess cell growth. Calibration curve was repeated before each fluorescence assay.

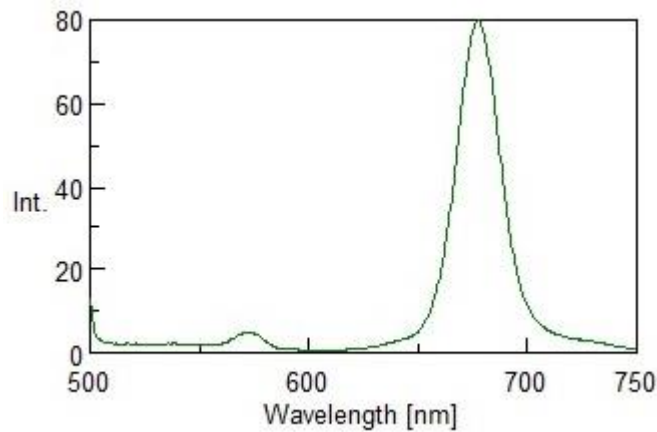


**Figure 2.17.** Chlorophyll *a* fluorescence emission spectrum in a *S. marinoi* culture by using an excitation wavelength of 434 nm. The emission peak at 684 nm was used for cellular density measurement.

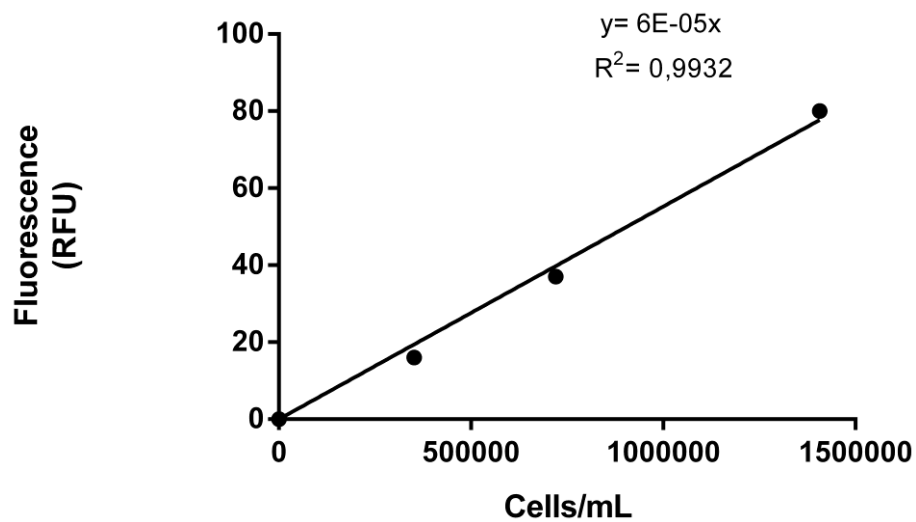


**Figure 2.18.** Correlation between cells number (Cells/mL) of *S. marinoi* cultures and fluorescence measurements of chlorophyll *a* (intensity measured as relative units of fluorescence; RFU).

Fluorescein diacetate has been used in many studies as an indicator of microalgal cell viability after exposure to cytotoxic conditions (Vasconcelos et al., 2000; Bentley-Mowat, 1982). This molecule is nonfluorescent but can move across biological membranes. When FDA enters viable cells, it is quickly hydrolysed by esterases with release of free fluorescein that can be measured by spectrophotometry (Figure 2.19).

Fluorescein does not cross intact plasma membranes therefore it is trapped inside live cells. Consequently, so long as the integrity of plasma membranes is not compromised, cells accumulate fluorescein and become brightly fluorescent whereas damaged cells remain nonfluorescent.

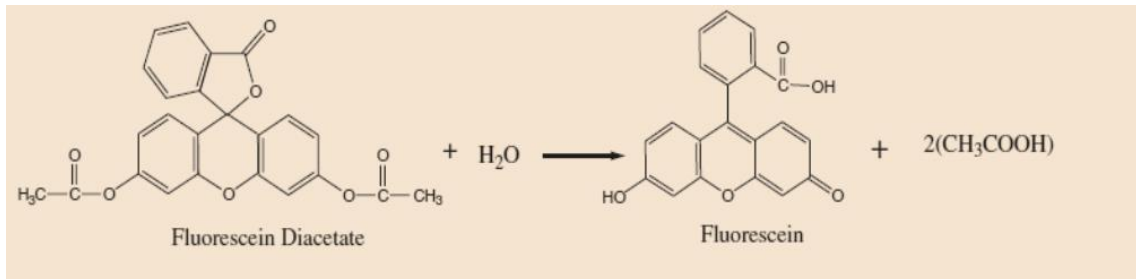


**Figure 2.19.** FDA formula and hydrolyzation by viable cells.

We monitored the chlorophyll a and FDA fluorescence after 24 and 48 hours of incubation with increasing amounts of StS-1 and, as shown in the Figure 2.20, the relative fluorescence of both probes decreases as the concentration of StS-1 increases.

The dose-response plot of Figure 2.21 shows that EC<sub>50</sub> of StS-1 was 2.22 mg L<sup>-1</sup> at 48 h (4.77 μM). The same experiment with higher cellular concentrations of *S. marinoi* (from 1·10<sup>5</sup> to 1·10<sup>6</sup> cell mL<sup>-1</sup>) revealed medium EC<sub>50</sub> of 3.27 ± 0.6 mg L<sup>-1</sup> (7.03 μM) at 48 h.

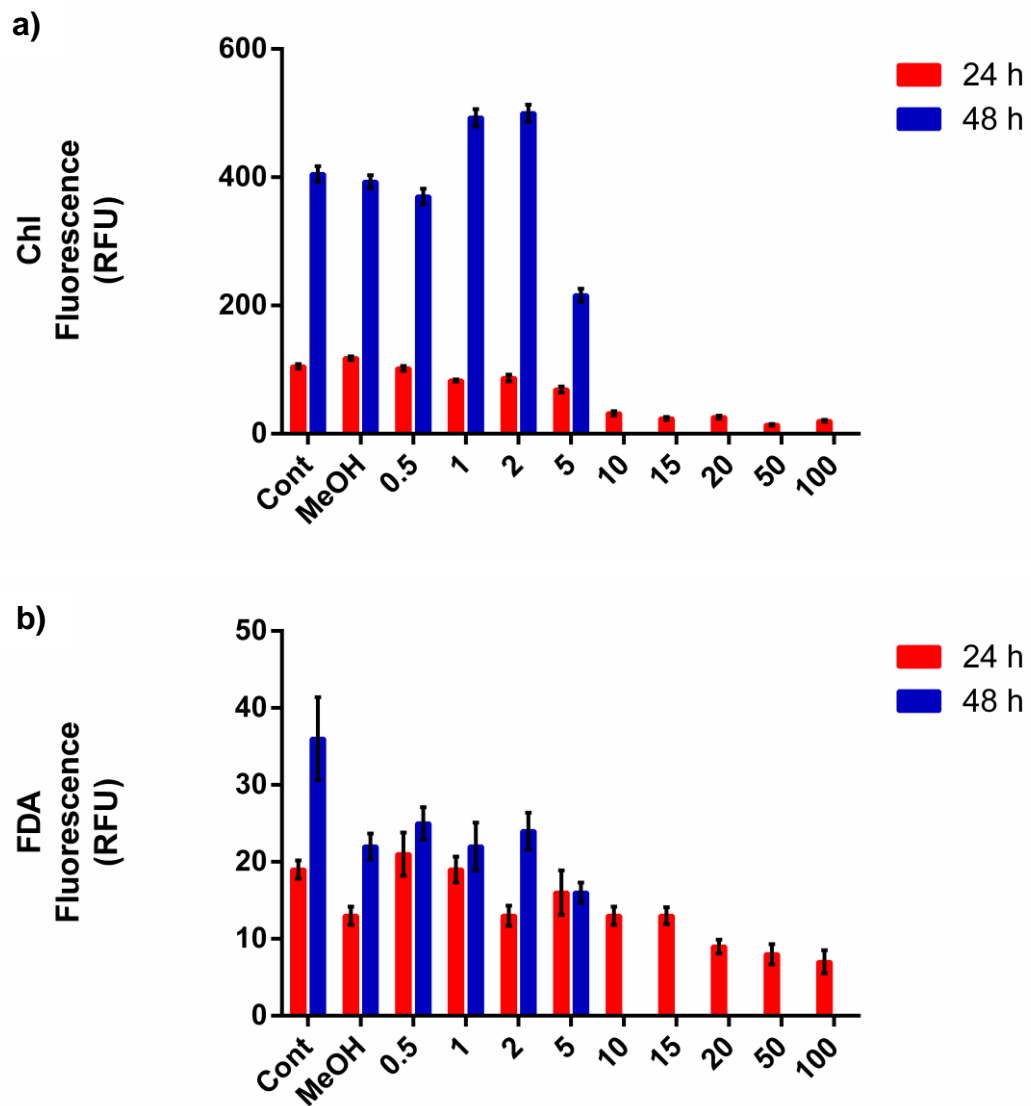


**Figure 2.20.** Quantitation in relative fluorescence units (RFU) in 24 and 48 hours of *chl a* fluorescence (a) and FDA fluorescence (b) in cells untreated (Cont and MeOH) and treated with StS-1 from 0.5 to 100  $\mu\text{g mL}^{-1}$ . There was linearity between StS-1 dose and response of both of probes until concentration of 5  $\mu\text{g mL}^{-1}$ , meaning a linear proportionality between cell death and the dose tested in the range 0.5-5  $\mu\text{g mL}^{-1}$ . In the range 10-100  $\mu\text{g mL}^{-1}$  didn't increase the magnitude of the effect.

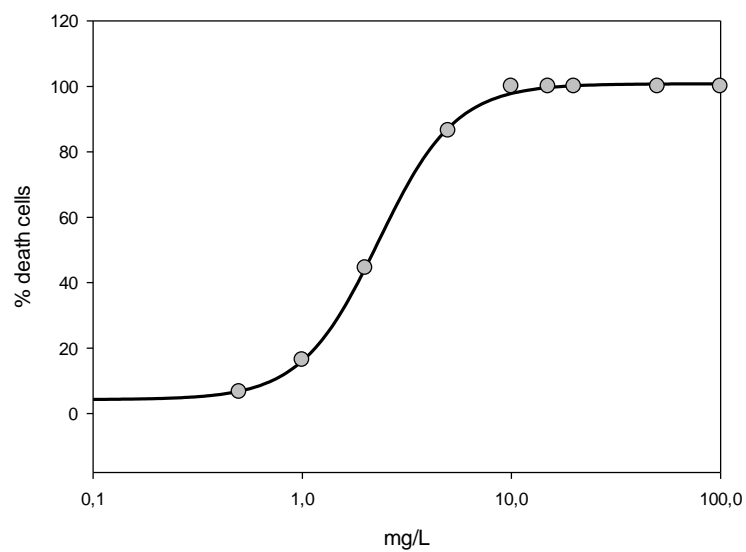


**Figure 2.21.** Dose- response analysis standard curve (SigmaPlot analysis) of *S. marinoi* cells treated with different concentrations of StS-1 (48 h). All responses were normalized to 100% of mortality according to the FDA fluorescence value and were plotted against compound concentration (on Log scale). By interpolation of the inflection point of the sigmoidal curve the  $EC_{50}$  value of  $2.22 \text{ mg L}^{-1}$  was calculated.

### 3. Biochemical investigation of *S. marinoi* cell death pathway

#### 3.1. Introduction

Autocatalytic cell death triggered by specific environmental stresses (cell age, nutrient deprivation, high light levels, oxidative stress) in prokaryotic and eukaryotic unicellular phytoplankton provides a mechanism to explain the high lysis rates independent of viral attack or grazing (*Franklin et al.*, 2006). This cellular self-destruction is analogous to programmed cell death (PCD) in multicellular organisms, a form of autocatalytic cell suicide in which an endogenous biochemical pathway leads to apoptotic-like morphological changes and, ultimately, cellular dissolution (Figure 3.1). PCD involves the expression and biochemical coordination of specialized cellular machinery, such as receptors, adaptors, signal kinases, proteases, and nuclear factors. A specific class of intracellular cysteinyl aspartate-specific proteases, termed caspases, is of particular interest due to their ubiquitous role in both the initiation and execution of PCD through the cleavage of various essential proteins in response to proapoptotic signals (*Thornberry and Lazebnik*, 1998.). The discovery of caspase homologues, paracaspases and metacaspases, in morphologically diverse organisms, including animals, higher plants, slime molds, unicellular protists, fungi, and bacteria (*Uren et al.*, 2000), suggests that they may represent an ancestral core of executioners that led to the emergence of the cell death machinery. Presumably, early ancestors of plants and animals had minimal apoptotic machinery, with the more complex PCD systems in animals emerging with metazoans. Their cellular roles, however, still remain an open question regarding unicellular protists and plants.

Autocatalytic cell death in diatoms was first documented in *Ditylum brightwellii* (*Brussaard et al.*, 1997) and *Thalassiosira weissflogii* (*Berges & Falkowski*, 1998) in response to nutrient limitation. Later, a threshold and dose-dependent response to

secondary metabolites (oxylipins) elicited from diatoms during stress and derived by enzymatic oxidation of fatty acids (*D'Ippolito et al., 2005; Fontana et al., 2007*), such as the aldehyde 2-trans, 4-trans-decadienal, was shown to induce morphological and biochemical features of apoptosis (*Casotti et al., 2005*). Subsequently, *Vardi et al. (2006)* demonstrated a stress surveillance and cell-cell communication system in *Phaeodactylum tricornutum* that employs secondary messengers (e.g., nitric oxide and calcium) to critically regulate PCD and cell fate. A novel calcium-regulated protein (ScDSP), with a transmembrane domain and a pair of EF-hand motifs, also was identified in the last years in the diatom *Skeletonema costatum* and shown to have strong up-regulation of gene expression in dying cells, suggestive of a role in the signal transduction of stress to the death machinery (*Chung et al., 2005*). Finally activation of autocatalytic PCD in the diatom *Thalassiosira pseudonana* was reported as a central death pathway in response to nutrient starvation (*Bidle & Bender, 2008*).

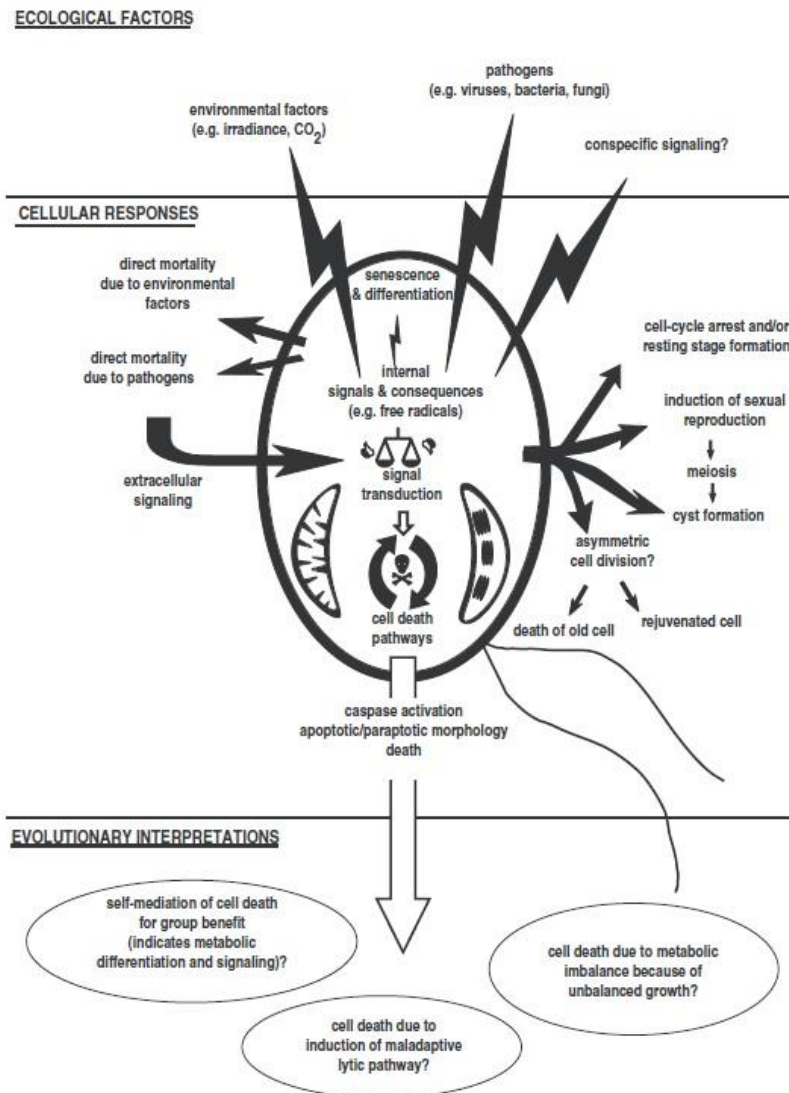


**Figure 3.1.** Summary of the causes, consequences and evolutionary implications of cell death processes in unicellular phytoplankton. Simple cause and effect relationships are probably complicated by metabolic heterogeneity amongst unicellular populations, the influence of undocumented life-history processes (sexual cycles, asymmetric division) and intercellular signaling (Franklin et al., 2006).

These studies have provided intriguing mechanistic insights into how diatoms couple environmental stress levels with cell death (Falciatore et al., 2000; Bratbak, et al., 1993). Nevertheless, we still have very little mechanistic insight into the biochemical execution of autocatalytic cell death in diatoms. Biological analyses were carried out to clarify whether the mechanism of cell death triggered by sterol sulfates was due to a type of apoptosis. Since the genome of *S. marinoi* is not known, we did not have access

to the molecular data related to the caspase pathway involved in cell death. However, apoptotic cells show also characteristic pattern of morphological changes, such as the externalization of phosphatidylserine (PTS) in the membrane and nuclear DNA fragmentation that can be used to target the cellular process. Thus were used these phenotypic modifications to study the cytotoxic effect of apoptotic process induced by cholesteryl sulfate (StS-1).

It has been assessed the production of reactive oxygen species (ROS) and nitric oxide (NO) induced by StS-1 in *S. marinoi*. ROS and NO are both well established as signaling molecules, mediating a wide range of cellular responses (Apel & Hirt, 2004; Laloi et al., 2004; Wilkins et al., 2011) including hormone signaling, cell cycle, stress and defense response, and PCD (Mittler et al., 2004; Kwak et al., 2006). Because NO requires H<sub>2</sub>O<sub>2</sub> to induce cell death (Delledonne et al., 2001; de Pinto et al., 2002), synergistic ROS and NO interactions has been also suggested as possible trigger of cell death in plants and microalgae. In marine diatoms, namely *Thalassiosira weissflogii* and *Phaeodactylum tricornutum*, aldehyde products have been demonstrated to induce calcium-dependent NO synthase-like activity in signal transduction of PCD regulatory pathway (Vardi, 2006). In the last years a novel gene, DSP-1 (ScDSP-1) (Chang et al., 2008), encoding a death-specific protein (DSP) was obtained from *Skeletonema costatum*. DSP expression was also associated with NO production pathway.

## **3. 2. Results and discussion**

### *3.2.1. NO and hROS production*

The effect of StS-1 on NO production in *S. marinoi* was measured by using the NO-sensitive dye 4-amino-5-methylamino- 2',7'- difluorescein diacetate (DAF-FM). This

compound is essentially nonfluorescent until it reacts with NO to form a fluorescent benzotriazole (Figure 3.2). DAF-FM diacetate is cell-permeant and passively diffuses across cellular membranes. Once inside cells, it is deacetylated by intracellular esterases to become DAF-FM. The fluorescence quantum yield of DAF-FM is  $\sim 0.005$ , but increases about 160-fold, to  $\sim 0.81$ , after reacting with nitric oxide.

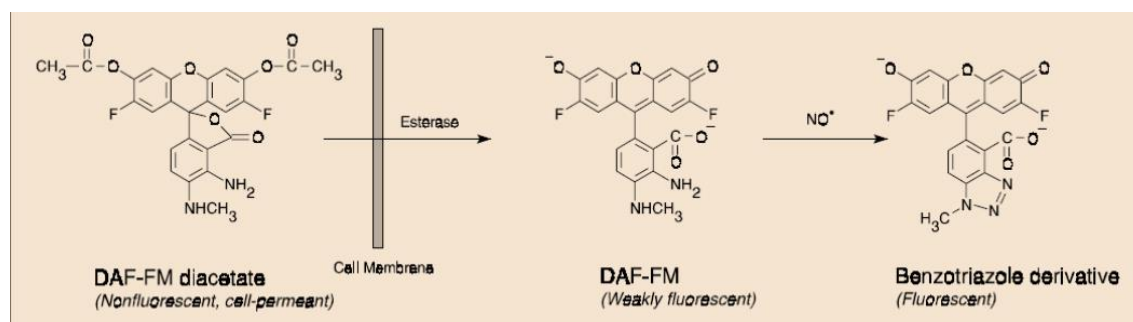


**Figure 3.2.** Reaction scheme for the detection of nitric oxide (NO) by DAF-FM and DAF-FM diacetate. This compound is essentially nonfluorescent until it reacts with NO to form a fluorescent benzotriazole derivative.

The increase in fluorescence was not immediate in the samples incubated with StS-1 compared to those incubated with the NO donors SNP and NONATE (Figure 3.3). Nevertheless, a significant increase was detected after 3 hours. At 4 hours, the fluorescence of samples incubated with lower concentration of StS-1 ( $50 \mu\text{g mL}^{-1}$ ) was comparable with that of the samples incubated with NONATE under the same experimental conditions, while the highest concentration mimicked the effect of SNP. StS-1 determined accumulation of green fluorescence corresponding to NO generation inside the cells (Figure 3.4), while control cells revealed only presence of fluorescence due to chlorophyll *a*.

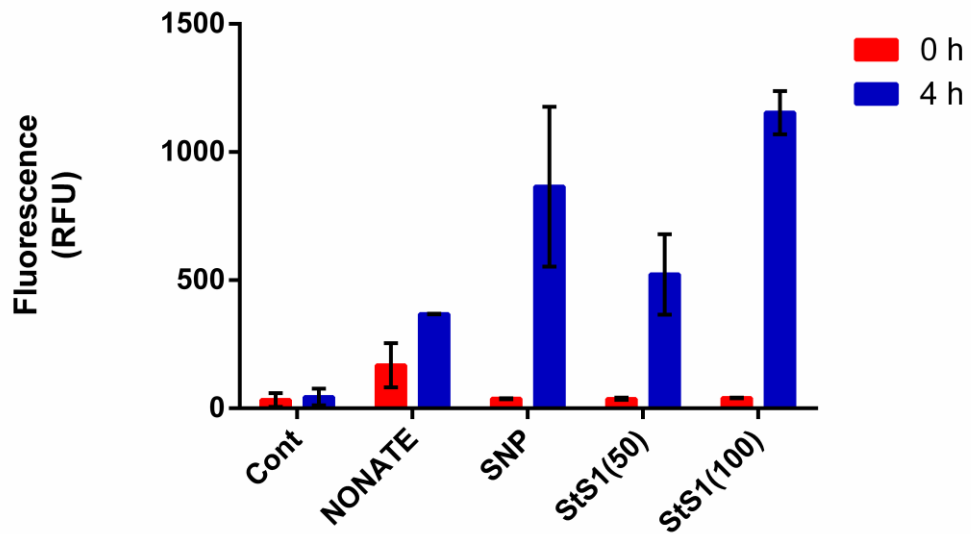


**Figure 3.3.** Estimated production in relative fluorescence units (RFU) in 4 hours of DAF-FM fluorescence in cells untreated (Cont), treated with StS-1 (50 and 100  $\mu\text{g mL}^{-1}$ ) and with NO donor diethylamine nitric oxide (DEANO) and sodium nitroprusside (SNP), as positive controls to verify the reliability of DAF-FM as a probe for NO detection in *S. marinoi* cells. After 4 hours of incubation with StS-1 the samples fluorescence was comparable with that of the samples incubated with NONATE and SNP.

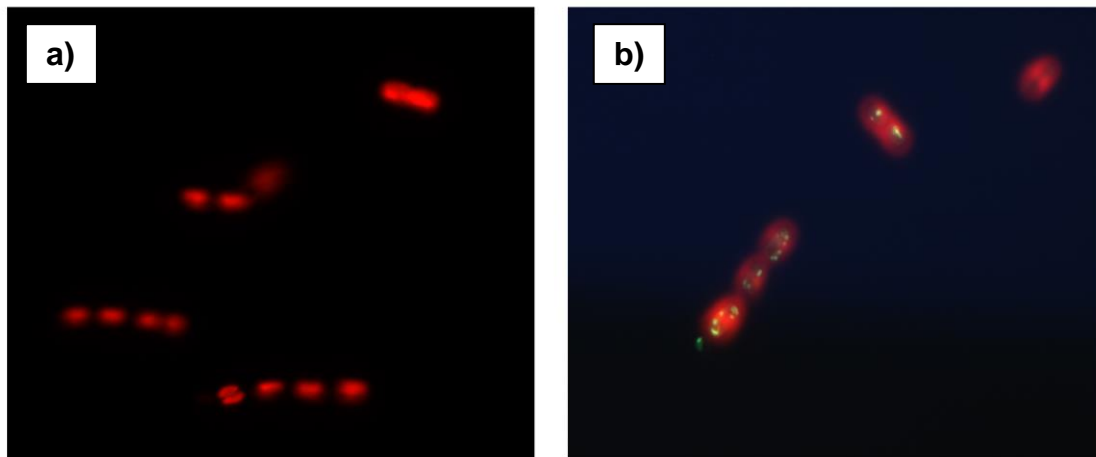


**Figure 3.4.** Photo by epifluorescence microscopy by using a 530/30 BP emission filter for red and green fluorescence emission (magnification of 40 x) after 4 hours of incubation: control cells (a); cells incubated with StS-1 (b), in which there is a clear green fluorescence due to formation of benzotriazole derivative of DAF-FM, index of NO production.

Reactive Oxygen Species (ROS) encompass a number of reactive molecules and free radicals. The production of oxygen radicals is the result of aerobic processes. These molecules, produced as byproducts during the mitochondrial electron transport or by oxidoreductase enzymes and metal catalyzed oxidation, have the potential to cause a number of deleterious events. Initially, it was thought that only phagocytic cells were responsible for ROS production as their part in host cell defense mechanisms. Recent work has instead demonstrated that ROS have a more general role in cell signaling, being part of many different cell processes, including apoptosis and gene expression (Hancock *et al.*, 2001). Occurrence of *hROS* (highly reactive oxygen species) has been previously detected in aged cells of *S. marinoi* by hydroxyphenyl fluorescein (HPF) (Fontana *et al.*, 2007), a fluorescein derivative that is nonfluorescent until it reacts with the hydroxyl radical or peroxyxynitrite anion (Figure 3.5).

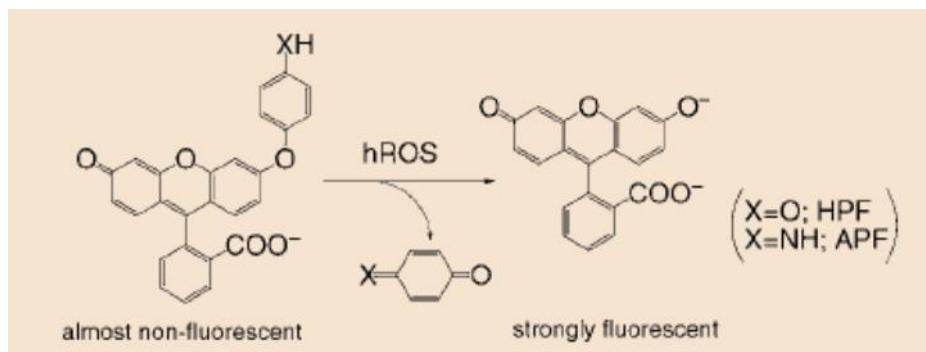


**Figure 3.5.** Scheme of O-dearylation reaction of HPF with hROS. HPF revealed an intense green fluorescence when reacts with hROS and is converted in its O-dearylated derivative.

As shown in Figure 3.6, incubation of *S. marinoi* with StS-1 triggered synthesis of *hROS* as detected by HPF. After 4 hours the intensity of fluorescence of the samples treated with the sulfated lipid was clearly higher than that of the positive control ( $H_2O_2$ ). The concentration of  $H_2O_2$  chosen for the experiment was 200  $\mu M$  because with higher concentrations the culture medium was colored bright green after only an hour (the

same effect was obtained with the chosen concentration of H<sub>2</sub>O<sub>2</sub> after 4 hours and in the wells inoculated with StS-1 after about 20 hours).

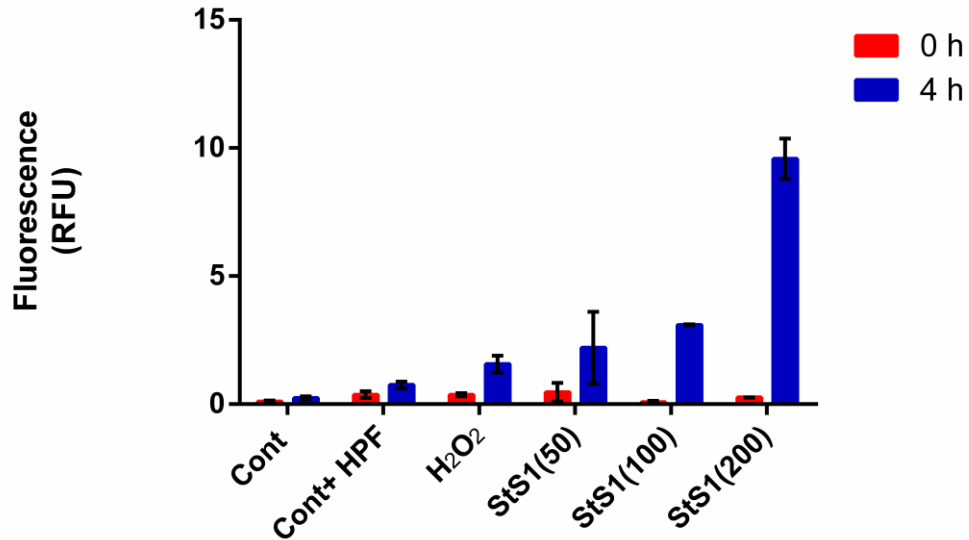


**Figure 3.6.** Quantitation in relative fluorescence units (RFU) in 4 hours of HPF fluorescence in cells untreated (Cont and Cont + HPF), treated with StS-1 (50, 100, 200  $\mu\text{g mL}^{-1}$ ) and with H<sub>2</sub>O<sub>2</sub> (200  $\mu\text{M}$ ) chosen as positive control. The estimated fluorescence intensity revealed a hROS production by cells treated with StS-1 that is higher to that of the positive control also at the lowest tested concentration.

### 3.2.2. *In situ* PCD detection

Cells undergoing apoptosis display a characteristic pattern of morphological changes like phosphatidylserine (PTS) externalization and nuclear disintegration. Thus was assessed the effect of StS-1 on apoptosis by incubation of *S. marinoi* cells with Annexin V-FITC and TUNEL.

Staining with Annexin V-FITC was used for *in vivo* testing phosphatidylserine (PTS) externalization (Bidle & Bendert, 2008), a diagnostic marker of PCD (Figure 3.7).

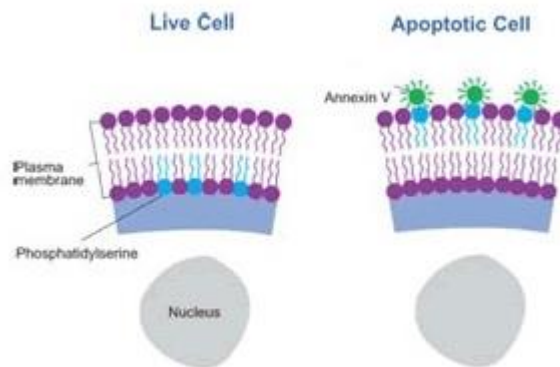


**Figure 3.7.** Mechanism of detecting apoptotic cell by Annexin V-FITC. After binding to the phospholipid surface, annexin V assembles into a trimeric cluster. This trimer consists of three annexin molecules which are bound to each other via non-covalent protein-protein interactions. The formation of annexin trimers results in the formation of a two-dimensional crystal lattice on the phospholipid membrane. This clustering of annexin on the membrane greatly increases the intensity of annexin when labeled with a fluorescent probe (FITC).

The collapse of the nucleus is associated with the activation of endonuclease, which cleaves the nuclear DNA into oligonucleosome length DNA fragments (*Orrenius et al., 2003*). Therefore, the occurrence of DNA fragmentation indicates that the self-destruction mechanism in diatoms is similar to the apoptosis –like pathway in metazoans (*Vardi et al., 1999; Segovia et al., 2003; Casotti et al., 2005*). Free 3'OH ends of DNA, generated by activation of endonuclease activity in dying cells, were fluorescently labeled with a conventional in situ terminal transferase- mediated dUTP nick end-labeling (TUNEL) assay (*Gavrieli et al., 1992*) by using an In Situ Cell Death Detection Kit Fluorescein. This is based on the detection of single- and double-stranded DNA breaks that occur at the early stages of apoptosis. Apoptotic cells are fixed and permeabilized. Subsequently, the cells are incubated with the TUNEL reaction mixture that contains TdT (enzyme terminal deoxynucleotidyl transferase) and fluorescein-dUTP (2'-Deoxyuridine, 5'-Triphosphate). During this incubation period, TdT catalyzes the addition of fluorescein-dUTP at free 3'-OH groups in single- and double-stranded

DNA. After washing, the label incorporated at the damaged sites of the DNA is visualized by flow cytometry and/or fluorescence microscopy.

Given the absence of literature about diatoms (Casotti et al., 2005; Vardi et al., 1999; Chung, 2005), it was first necessary to develop the experimental method suitable for cell labeling. In particular, we established the optimal number of cells, the conditions of fixation and permeabilization, time of incubation and concentration of StS-1.

Assuming that the increased fluorescence intensity could be attributed to excessive incubation time with StS-1, which may have already caused a massive DNA fragmentation, cultures were inoculated with different concentrations of compound (2.5, 5 and 10  $\mu\text{g mL}^{-1}$  of StS-1) and the assay was performed at different times of incubation. In triplicates, cultures of *S. marinoi* were inoculated in 20 mL of f/2 with 2.5 e 5  $\mu\text{g mL}^{-1}$  of StS-1. The cells were recovered after 3, 6, 12, and 24 h of incubation and used for the detection of phosphatidylserine externalization and for TUNEL. For the TUNEL assay, the best time for the success of the experiment was found to be 12 h with a concentration of 2.5  $\mu\text{g mL}^{-1}$  of StS-1. At the same concentration, for the Annexin assay the best sampling is found to be 2 h.

As shown in Figure 3.8, *S. marinoi* cells incubated for 2 h with 5  $\mu\text{M}$  StS-1 were clearly tagged by the intense green fluorescence in agreement with the PTS externalization across the membrane. Untreated cells did not reveal any fluorescence due to PTS neither inside nor outside the diatom cells.

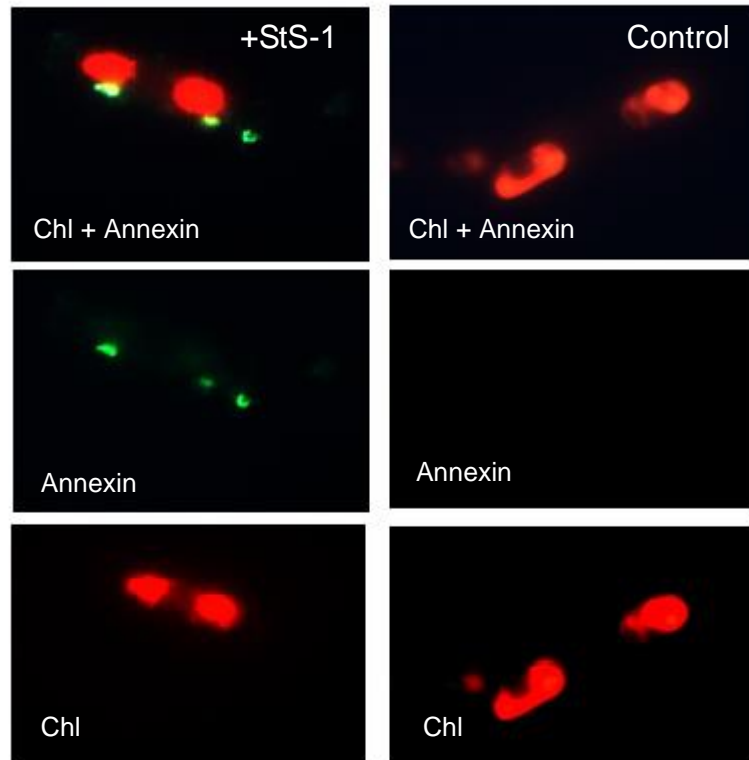


**Figure 3.8.** Observation by epifluorescence microscopy (magnification of 100 x) of cells treated with 5  $\mu$ M StS-1 and untreated cells (Control) after Annexin V-FITC assay. Images were taken by using 515/565 band filter for only green fluorescence, a LP615 band filters for only red fluorescence emission and 525/50 band filter for both green and red fluorescence emission. Both cell samples showed red fluorescence due to chlorophyll, but only +StS-1 cells showed the green fluorescence outside the nucleus, in agreement with the PTS externalization across the membrane.

TUNEL results with *S. marinoi* after addition of 5  $\mu$ M StS-1 is reported in figure 3.9. Diatom cells were considered positive (and therefore apoptotic) when both red fluorescence from the chloroplast (due to chl) and green fluorescence from the nucleus were visible after 12 h. It is evident by comparing the images of the cells treated with negative control on the right column (control samples from cultures without StS-1 addition) the presence of a green fluorescence in the nucleus in agreement with the DNA fragmentation.

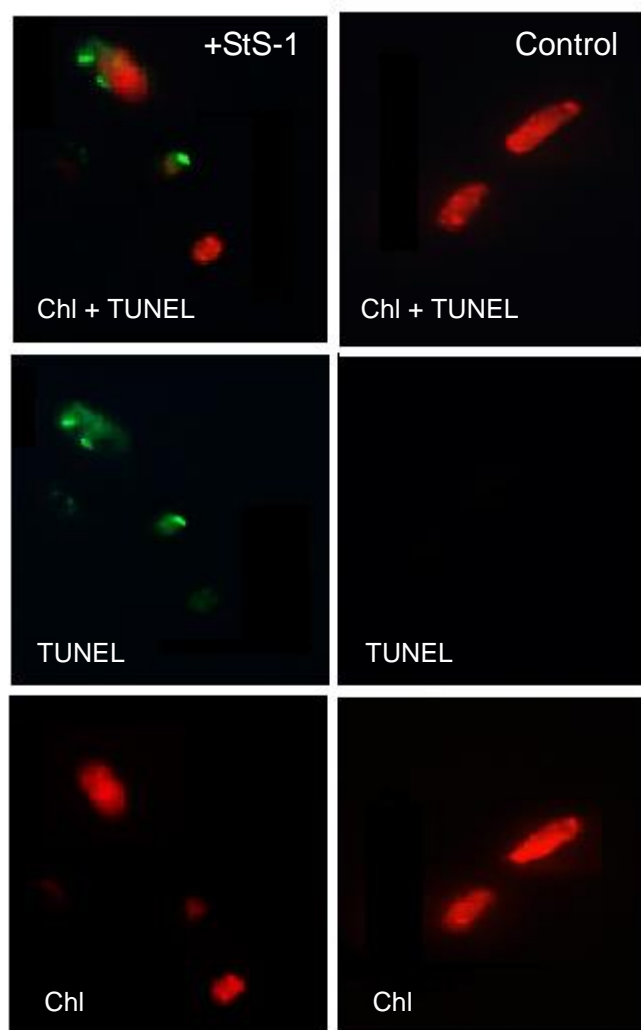


**Figure 3.9.** Fluorescence micrographs (magnification of 100 x) of control cells (Control) and cells treated with 5  $\mu$ M StS-1 after TUNEL assay. Images were taken by using 515/565 band filter for only green fluorescence, a LP615 band filters for only red fluorescence emission and 525/50 band filter for both green and red fluorescence emission. Both cell samples showed red fluorescence due to chlorophyll, but only +StS-1 cells showed the green fluorescence inside the cells, in agreement with labeled 3'OH free-ends of fragmented DNA.

## **4. Qualitative and quantitative analysis of sterol sulfates in diatoms**

### **4. 1. Introduction**

Sterol sulfates have been reported from many marine organisms, including sponges (*Gunasekera, et al., 1994, Patil et al., 1996*), echinoderms (*Goodfellow & Goao, 1983, Shubina et al., 1998*), ophiuroids (*McKee et al., 1994*) and mammals (*Langlais et al., 1981*). These compounds have been described as HIV inhibitors (*Lerch & Faulkner, 2001; McKee et al., 1994*), cytotoxic agents (*D'Auria et al., 1987; D'Auria et al., 1998*) and enzyme inhibitors (*Makarieva et al., 1986; Zvyagintseva et al., 1986*). There are a few reports of sterol sulfates also in diatoms (*Kates et al., 1977; Kazufumi & Masami, 2002*) but to the best of our knowledge their physiological role has been never investigated in this line of microalgae. The purpose of this part of the thesis work was to develop a method of quantitation for sterol sulfates in order to investigate the physiological production in *S. marinoi* and the correlation with the cytotoxic dose. We have also investigated the distribution of species of diatom sterols compared to the sterol sulfates and their presence in other diatom species.

### **4. 2. Results and discussion**

#### *4.2.1. Sterol sulfates quantification along S. marinoi growth curve*

Cholesterol can be assessed by enzymatic, colorimetric or chromatographic methods (*Burke et al., 1974; Grizard et al., 1995*). All these methods suffer of severe technical limitations or do not allow discriminating between different molecular species. On the other hand, most methods for sulfated sterols require solvolysis and derivatization of the natural products (*Lalumière et al., 1976; Connor et al., 1998*). For this reason, a new method based on quantification by LC-MS has been developed. As shown in Figure 4.1,

good resolution of the three peaks corresponding to StS-1 ( $m/z$  465.1), StS-2 ( $m/z$  479.1) and StS-3 ( $m/z$  493.1) of *S. marinoi* was achieved by using a C8 reverse phase column and a linear gradient of methanol in water (Table 8.4). To the best of our knowledge, there is only another LC-MS application that has been proposed for the analysis of sterol sulfates in human plasma (Shackleton & Reid, 1989). The novel methodology proved to be direct and sensitive, allowing detection of sterol sulfates in 10-20  $\mu\text{g}$  of crude diatom extracts.

Furthermore, use of [25,26,26,26,27,27,27- $\text{D}_7$ ]-cholesterol sulfate as internal standard, allowed simple quantification of the natural products.

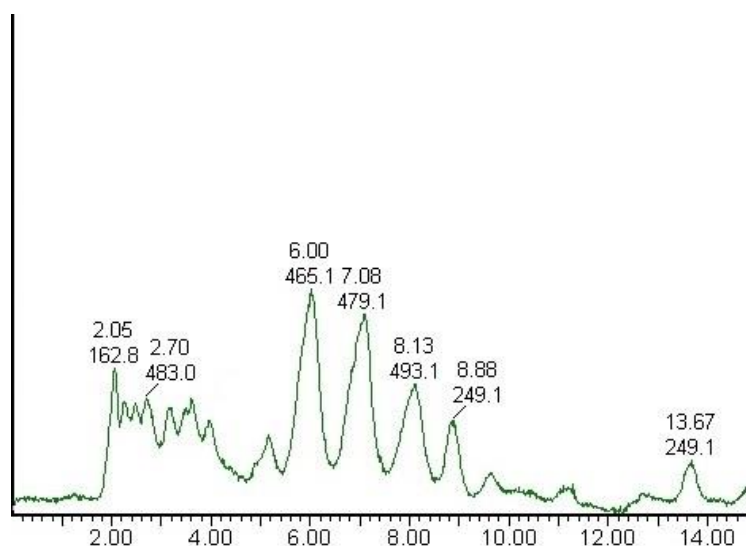


**Figure 4.1.** Total ion current (TIC) MS profile acquired in full scan MS of *S. marinoi* extract. Numbers above peaks indicate the molecular weight of the most intense ion. Three peaks correspond to three sterol sulfates: StS-1 ( $m/z$  465.1), StS-2 ( $m/z$  479.1) and StS-3 ( $m/z$  493.1).

In order to monitor level of sterols along growth curve of *S. marinoi*, diatom cell were harvested every day by gentle centrifugation of 0.3 L of culture. The resulting pellets were extracted by MeOH and analyzed by LC-MS as described in section 8.9. The last samples were collected on the 12<sup>th</sup> day, corresponding to the first point of declining

growth phase. The total amount of sterol sulfates *per* liter of culture increased along the growth curve of *S. marinoi*, ranging from  $13.9 \pm 0.05 \mu\text{g/L}$  of in the early exponential phase to  $807.11 \pm 0.95 \mu\text{g/L}$  in the last point of the curve during the beginning of the declining phase. As shown in Figure 4.2, concentration of the sterol sulfates increased dramatically concurrently with the cell number, thus suggesting an increase in cellular production of these compounds corresponding to a progress of the growth towards senescence.

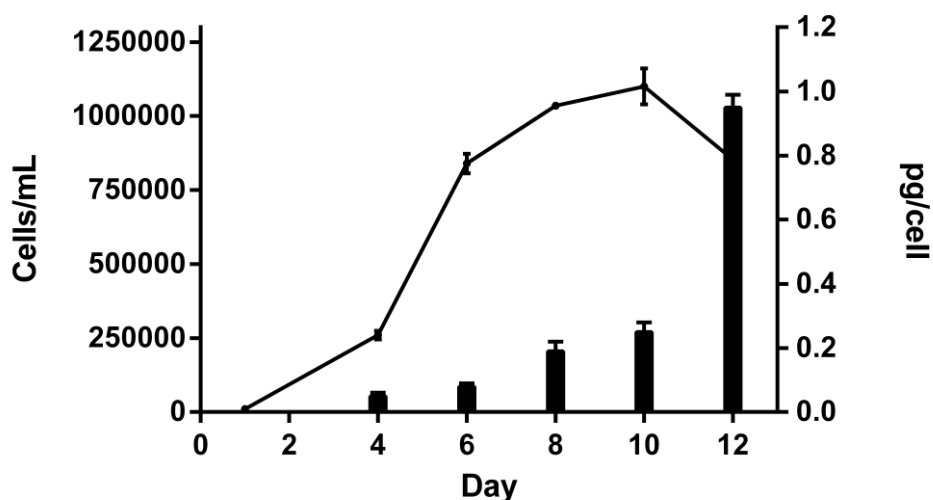


**Figure 4.1.** Sterol sulfates quantification along *S. marinoi* growth curve.

Moreover, the amount of sterol sulfates *per* mg of extract greatly increased from the beginning to the end of the growth curve (Figure 4.2), corroborating the major activity of the extract obtained from the point of declining growth phase in the first part of the work (Chapter 2).

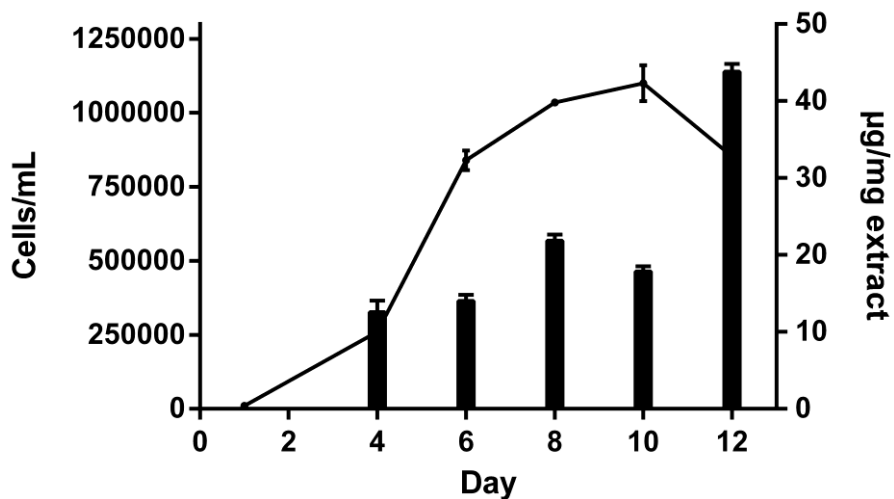


**Figure 4.2.** Sterol sulfates distribution along *S. marinoi* growth curve expressed as  $\mu\text{g mg}^{-1}$  organic extract. Recovery of the extraction procedure was calculated by recovery of internal deuterated standard.

LC-MS profile of the three sterol sulfates collected along 12 days of *S. marinoi* cultures revealed that StS-2 was the compound that mostly accounted for the great increase of sterol sulfates in the declining phase (Figure 4.3).

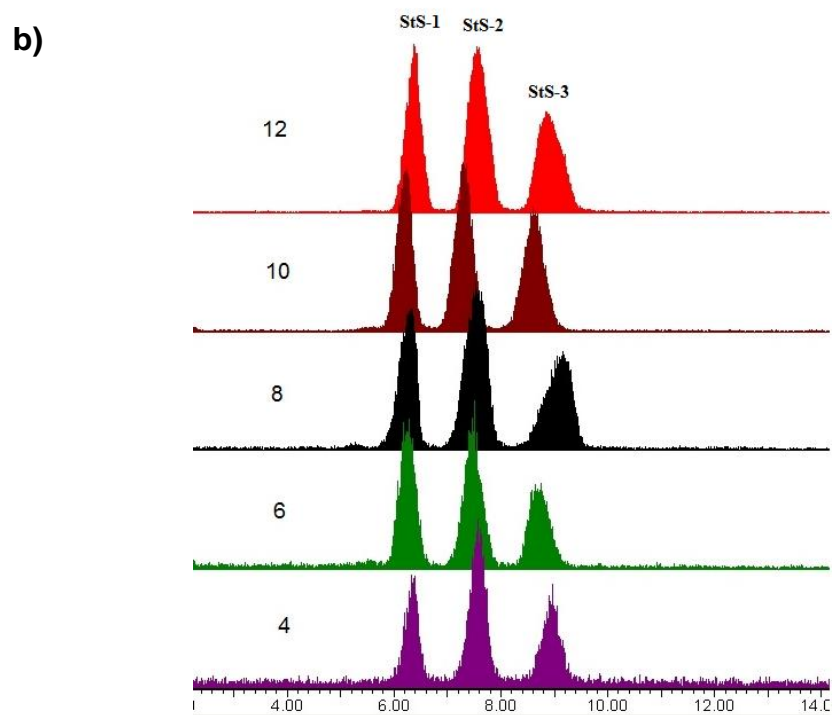
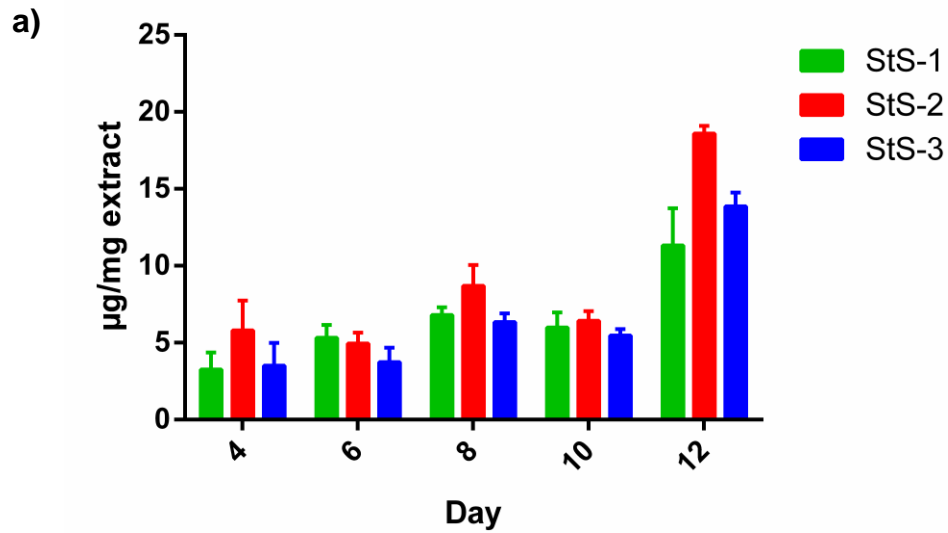


**Figure 4.3.**Relative composition of StSs in *S. marinoi* biomass (a). Data are expressed as  $\mu\text{g}$  of sterol sulfates isolated for mg of organic extract: StS-1 (MW 466), StS-2 (MW 480) and StS-3 (MW 494); LC-MS profile of three StSs in samples collected at different days along growth curve of *S. marinoi* (b).

These results support the hypothesis that cellular production of these compounds occurs under physiological conditions and the gradual increase along the growth curve suggests a physiological mechanism of preparation to senescence. It is worth noting that the estimated amount of sterol sulfates ( $0.8 \text{ mg L}^{-1}$ ) in *S. marinoi* during the declining phase is in the same range of the  $EC_{50}$  value ( $2.2 \text{ mg L}^{-1}$  at 48 h) that we established with standard StS-1 in the auto-allelopathic assays. These data confirmed the physiological induction of cell death triggered by sterol sulfates in the marine diatom *S. marinoi*.

#### 4.2.2. Sterol sulfates analysis in other diatoms

The LC-MS method developed for *S. marinoi* allowed determination of these compounds in other related species of marine diatoms. The first species to be analyzed were *Pseudonitzschia multistriata*, *Pseudonitzschia arhenysensis* and *Phaeodactylum tricorutum* (Figure 4.4). These diatoms have a recognized ecological role in many marine habitats and, unlike *S. marinoi*, are better characterized at molecular level.

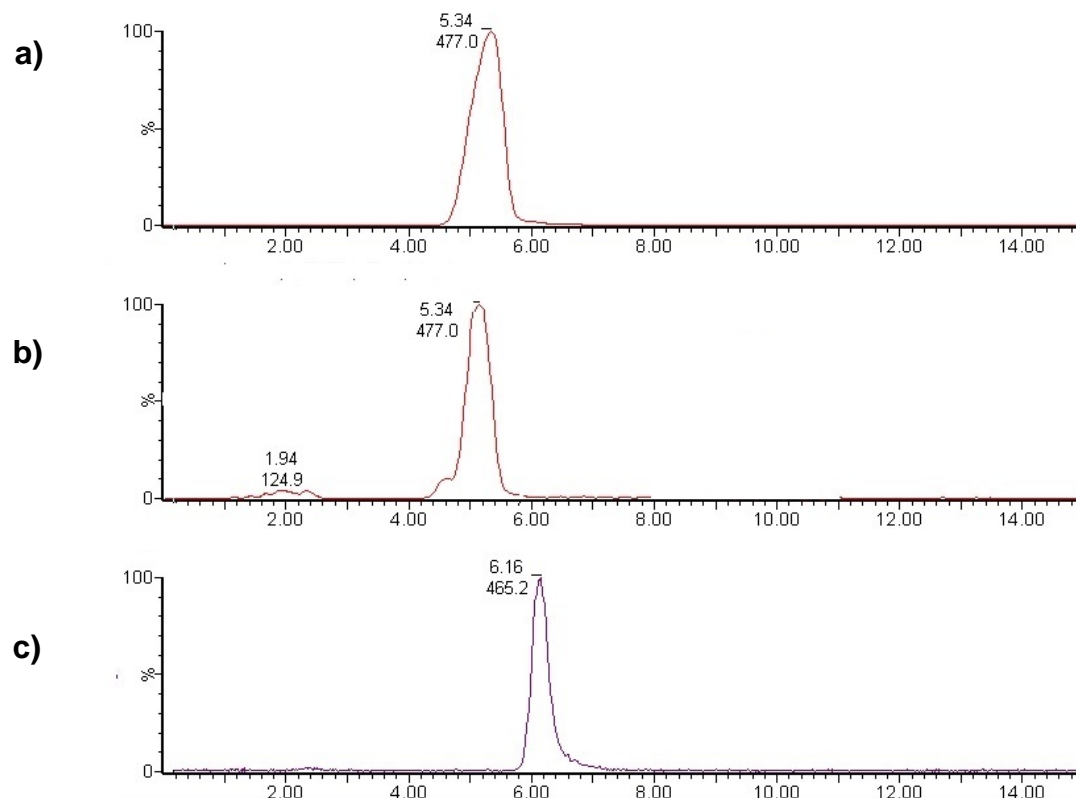


**Figure 4.4.** Extraction ion profile ( $m/z$  477.0 and 465.2) acquired in full scan MS of sterol sulfates in *P. tricornutum* (a), *P. arhenysensis* (b), *P. multistriata* (c) extracts.

*P. tricornutum* showed major presence of a sterol sulfate that was not present in *S. marinoi*. This product was characterized by a molecular ion at  $m/z$  477.1 (Figure 4.4, a) and was identified by purification and NMR study as 24-methylene cholesterol sulfate (StS-4) (Figure 4.5). This metabolite was also found in *P. arenysensis* (Figure 4.4, b), whereas the extracts of the sister species *P. multistriata* contained only StS-1 (Figure 4.4, c). On the other hand, StS-2 and StS-4 were predominant in *Cyclothella criptica* and *Thalassiosira weissflogii* (Figure 4.6).

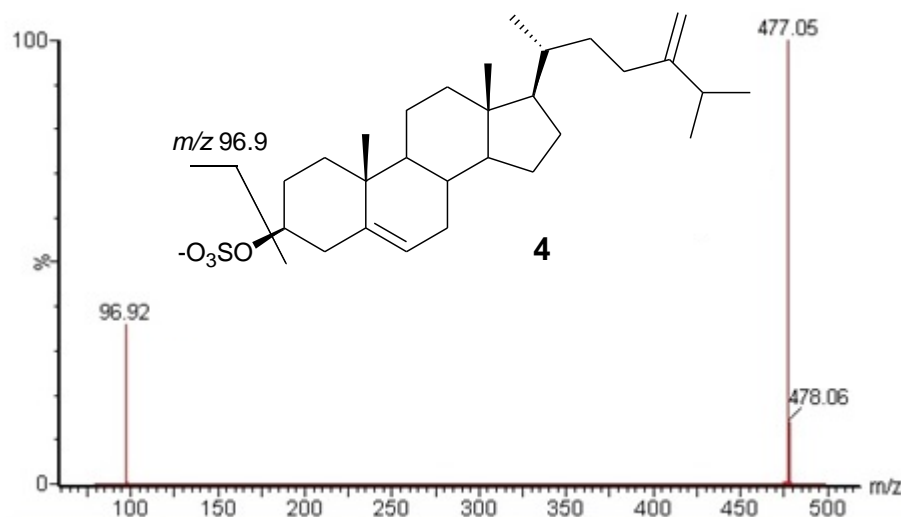


**Figure 4.5.**ESI MS/MS spectrum of 24-methylene cholesterol sulfate (**4**) with loss of  $\text{HSO}_4^-$  residue ( $m/z$  96.92).

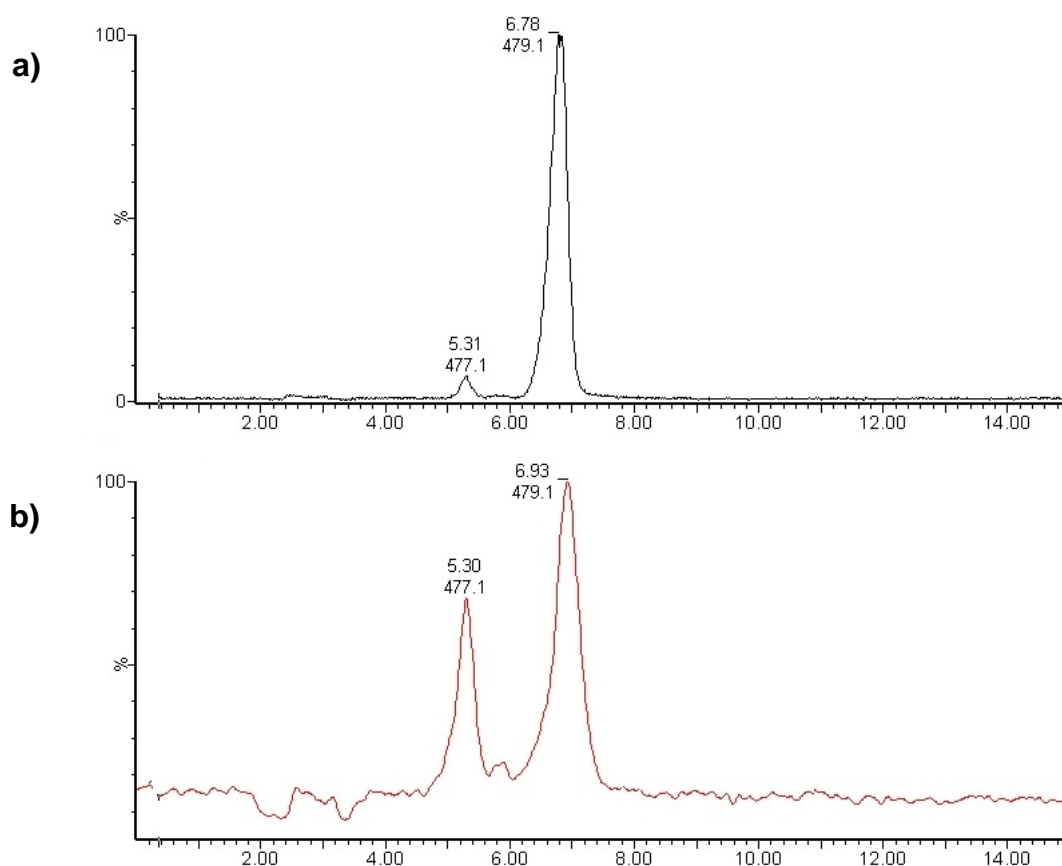


**Figure 4.6.**Extraction ion profile ( $m/z$  477.1, 479.1) of sterol sulfates acquired in full scan ESI MS of *C. cryptica* (a) and *T. weissflogii* (b) extracts. StS-4 ( $m/z$  477.0) and StS-2 ( $m/z$  479.1) are the predominant compound in these species.

It would be interesting to investigate therefore the biosynthetic pathway of sterol and the subsequent step of sulfonation to understanding the biochemical mechanism underlying the different distribution of these molecules.

The LC-MS analysis of sterol sulfates in diatoms suggests a species specific distribution of these molecules with the lineage. To verify the occurrence of sterol sulfates variation along the growth curve in other species, samples were collected along the growth curve of *C. cryptica*. The results showed a gradual and significant increase of the level of sterol sulfates from  $15.0 \pm 3.4 \mu\text{g L}^{-1}$  in the exponential phase to  $100.3 \pm 5.6 \mu\text{g L}^{-1}$  in the declining phase. Because the lower density of *C. cryptica* cultures, the total amount of sterol sulfates for liter of culture was lower than in *S. marinoi* cultures even if the amount of sterol sulfates per cell (Figure 4.7) was very close in the two diatoms ( $0.65 \pm 0.01 \text{ pg cell}^{-1}$  in *C. cryptica* and  $0.95 \pm 0.04 \text{ pg cell}^{-1}$  in *S. marinoi*).

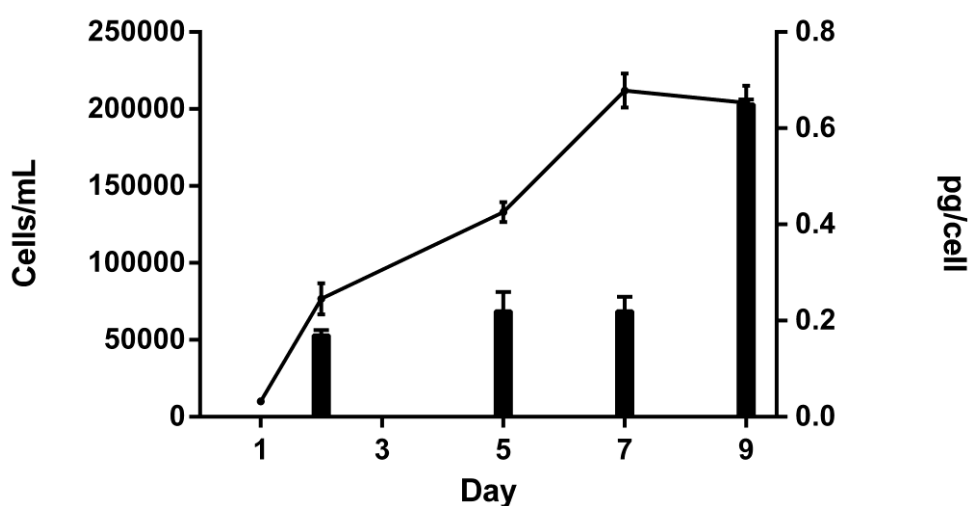


**Figure 4.7.** Sterol sulfates quantification expressed as  $\text{pg cell}^{-1}$  along *C. cryptica* growth curve.

#### 4. 2. 4. Isolation and analysis of sterols from *S. marinoi* and *C. cryptica*

The pool of sterols in these species was analyzed in order to assess if differences in the sterol sulfates pattern were also reflected by a different distribution of sterols in marine diatoms and to check if there was a distribution similar to that observed with the corresponding sulfated derivatives.

After enrichment by HR-X SPE, *S. marinoi* and *C. cryptica* extracts (that eluted with  $\text{CH}_2\text{Cl}_2:\text{CH}_3\text{OH}$ , see section 2.2.2.) were purified by sequential chromatographic steps to give a pure fraction of sterol mixture from both species. In Figure 4.8 is reported the TLC analysis of the first chromatographic step on silica column.

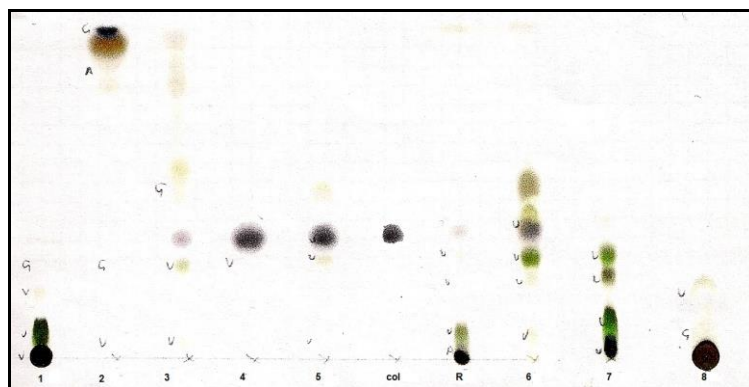


**Figure 4.8.** TLC analysis of a *S. marinoi* HR-fraction (R) purification eluted in petroleum ether: ethylic ether (1:1; v/v). Spots were detected by  $\text{Ce}(\text{SO}_4)_2$  e cholesterol (col) was used as reference. Fraction 4 contains pure sterol mixture.

Sterols were then analyzed by GC-MS on acetyl derivatives obtained by reaction with acetic anhydride in dry pyridine overnight at room temperature. The complete course of the derivatization was monitored by TLC in petroleum ether: ethylic ether (6:4; v/v) (Figure 4.9).

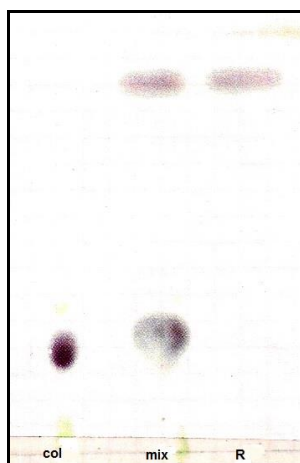


**Figure 4.9.** TLC analysis of acetylation reaction; cholesterol (col) was used as reference. Mix of starting mixture and final product (mix) was analyzed with the only final product (R) that revealed as one spot up the TLC. Spots were detected by  $Ce(SO_4)_2$ .

GC-MS profile revealed a sterol mixture composed of cholesterol (**1**), dihydrobrassicasterol (**2**), 24-methylene cholesterol (**3**) and  $\beta$ -sitosterol (**4**) in *S. marinoi* (Figure 4.10a), whereas only dihydrobrassicasterol (**2**) and 24-methylene cholesterol (**3**) in *C. criptica* (Figure 4.10b). Every compound was unambiguously identified by mass spectra, diagnostic fragments and retention times compared to those reported in literature (Wyllie & Djerassi, 1968; Wyllie & Amos, 1977).

Relative abundance of each species was estimated by area integration of the single peak in the two species. In *S. marinoi* the main component was dihydrobrassicasterol with a relative abundance percentage of 49.8 %, while cholesterol and 24-methylene cholesterol were respectively the 31.3 and 11.7 % of the mixture.  $\beta$ -sitosterol was the minor constituent with only 7.2 %. In *C. criptica* dihydrobrassicasterol accounted for the most abundant species with a percentage of 61.3 % versus 38.2 % of 24-methylene cholesterol. These analyses proved a close correlation between the qualitative and quantitative composition of free and sulfated sterols in the two diatom species (after identification of 24- methylene cholesterol in the extract of *S. marinoi*, re-analysis of the

sulfated pool revealed the presence of 24- methylene cholesterol sulfate). This result indicated that sulfonation was most likely not responsible for modulation of the pool of sulfated sterols along the growth curve, thus suggesting that regulation of the levels of this class of compounds could be dependent on biosynthesis of the terpene skeleton.

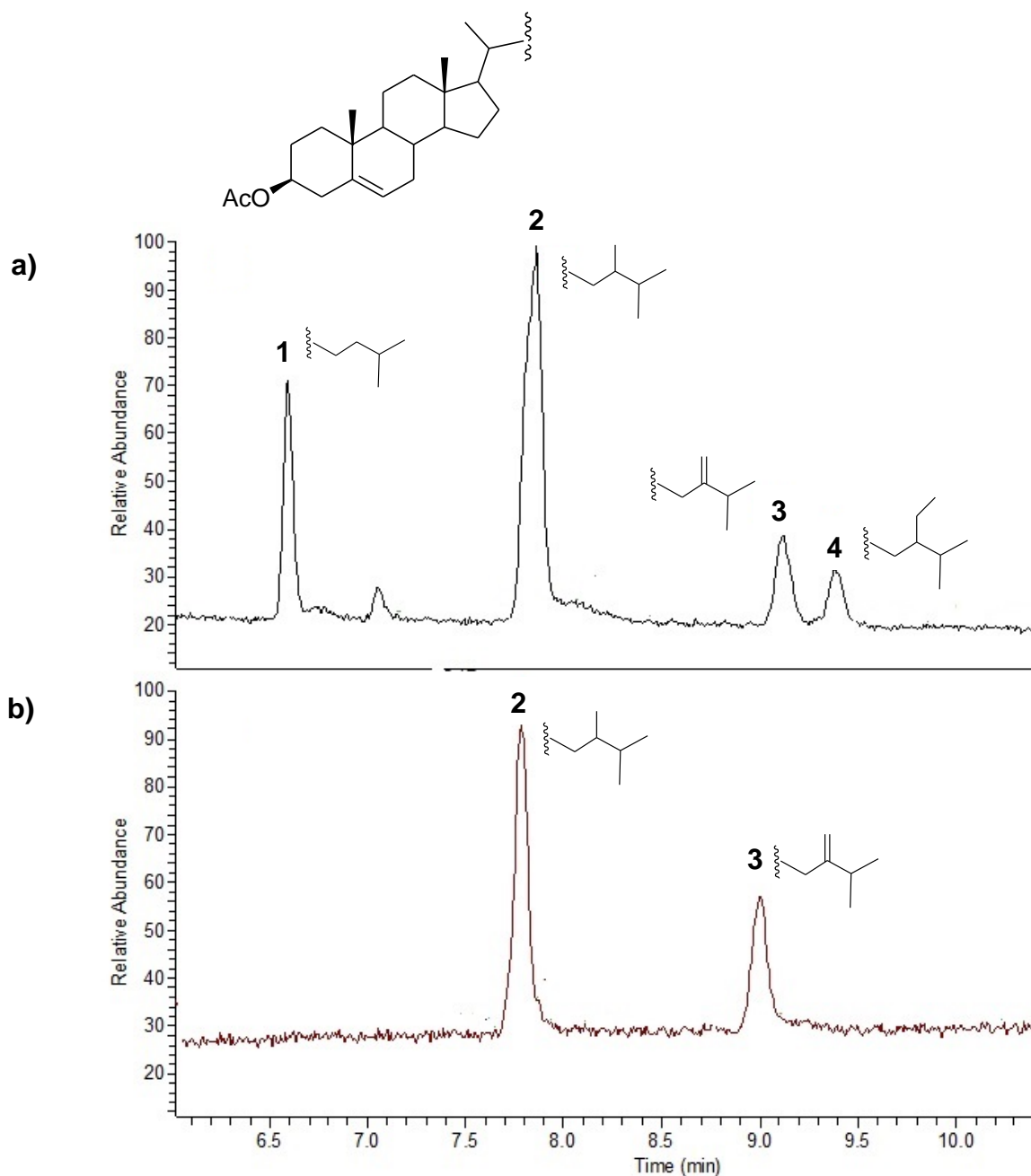


**Figure 4.10.** GC Chromatograms of acetylated derivatives of *S. marinoi* (a) and *C. cryptica* (b) sterols with respective chain side structures. In *S. marinoi* we found 4 different sterols: cholesterol (1), dihydrobrassicasterol (2), 24-methylene cholesterol (3) and  $\beta$ - sitosterol (4), while in *C. cryptica* we reported only dihydrobrassicasterol (2) and 24-methylene cholesterol (3).

## 5. Sterol biosynthesis in diatoms

### 5. 1. Introduction

In eukaryotes, sterols are important components of the plasma membrane, play relevant roles in cellular defense and signaling, and are precursors of several hormones and bioactive secondary metabolites (*Adolph et al.*, 2004; *Benveniste*, 2004; *Dufourc*, 2008; *Vinci et al.*, 2008; *Galea & Brown*, 2009; *Tomazic et al.*, 2011). The ability to synthesize sterols is a common feature of eukaryotes, with rare exceptions represented by some insects, nematodes and oomycete plant pathogens, such as *Phytophthora* spp. (*Desmond & Gribaldo*, 2009; *Gaulin et al.*, 2010). Therefore, being deeply rooted in the early history of eukaryotic life, the sterol biosynthesis pathway can be considered as a prime example of metabolic evolutionary conservation. It is believed that the Last Eukaryotic Common Ancestor (LECA) already possessed some of the metabolic enzymes of the present sterol pathway (*Desmond & Gribaldo*, 2009). The presumed presence of a primitive form of this pathway in the LECA is reflected by the conservation of many aspects of the pathway in all sterol-producing organisms. Despite the diversity in the end products of the sterol biosynthesis pathway, many upstream reactions and intermediates are ubiquitously conserved in the different taxonomical groups (Figure 5.1). A recent acquisition is the existence of two distinct pathways for the synthesis of sterols and other terpenoids in nature. In plants and other photosynthetic organisms, the two pathways co-occur but are responsible for synthesis of different products. Thus sterols and terpenes are generally produced by the cytosolic mevalonate (MVA) pathway, whereas carotenoids derive from the plastidic methylerythritol phosphate (MEP) pathway (*Cvejic & Rohmer*, 2000). This differentiation is less clear in green algae and some red algae, where sterol synthesis has been suggested to depend on MEP pathway (*Massé et al.*, 2004; *Lohr et al.*, 2012).

The MVA pathway has been well studied since the 1950s. The first two steps involve condensation of three molecules of acetyl-coenzyme A (acetyl-CoA) to produce hydroxymethyl glutaryl-CoA (HMG-CoA) (*Amdur et al., 1957; Mizioro & Lane, 1977*) (Figure 5.1). HMG-CoA is then reduced to MVA, which is subsequently phosphorylated twice before decarboxylation to isopentenyl pyrophosphate (IPP) (*Agranoff et al., 1960*). IPP isomerase (IDI) converts IPP to dimethylallyl pyrophosphate (DMAPP) and produces the basic building blocks for the construction of sterols and other terpenes (*Dhe-Paganon et al., 1994*).

Unlike the MVA pathway, the MEP pathway was discovered only recently. 1-Deoxy-d-xylulose 5-Phosphate (DXP) synthase was the first protein identified, in 1997 (*Sprenger et al., 1997*). The MEP pathway begins with condensation of glyceraldehyde 3-phosphate (G3P) and pyruvate to produce DXP by DXP synthase (DXS) followed by the MEP synthase (DXR)-catalyzed rearrangement and reduction of DXP to generate 2-C-methyl-erythritol 4-phosphate (MEP) (*Kuzuyama et al., 1998; Lois et al., 1998*). MEP is converted to 2-C-methyl-D-erythritol 2,4-cyclodiphosphate (cMEDP) by the successive actions of 4-diphosphocytidyl-2-C-methyl-D-erythritol (CDP-ME) synthase (IspD), CDP-ME 2-phosphate (CDP-ME2P) synthase (IspE), and cMEDP synthase (IspF) (*Herz et al., 2000*). 1-Hydroxy 2-methyl-2-buten-4-yl diphosphate (HDMAPP) is formed by the IspG-catalyzed ring opening of cMEDP (*Rohdich et al., 2003*). IPP and DMAPP are ultimately formed in one step.

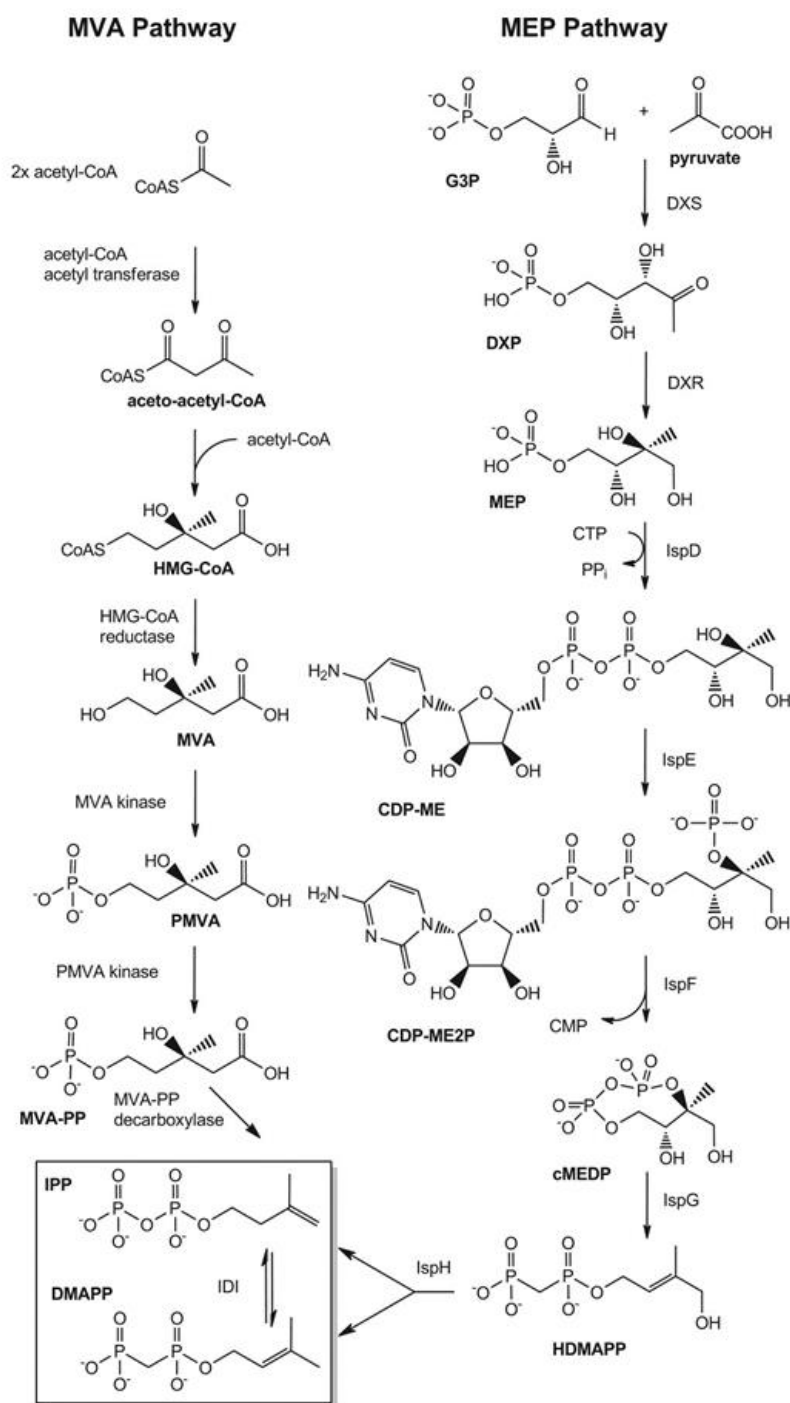


**Figure 5.1.** MEP and MVA pathways for isoprenoid biosynthesis. G3P, glyceraldehyde 3-phosphate; DXP, 1-Deoxy-d-xylulose 5-Phosphate; DXS, DXP synthase; DXR, MEP synthase; cMEDP, 2-C-methyl-D-erythritol 2,4-cyclodiphosphate; CDP-ME, 4-diphosphocytidyl-2-C-methyl-D-erythritol; IspD, CDP-ME synthase; IspE, CDP-ME 2-phosphate synthase; IspF, cMEDP synthase; HDMAPP, 1-Hydroxy 2-methyl-2-buten-4-yl diphosphate; IPP, Isopentenyl diphosphate; DMAPP, dimethylallyl diphosphate.

The condensation of IPP and DMAPP produces geranyl diphosphate (GPP), which forms farnesyl diphosphate (FPP) by head-tail reaction with another molecule of IPP. FPP is the substrate of squalene synthase, which initiates sterol biosynthesis. The squalene in eukaryotes is first epoxidized by squalene epoxidase (SQE) before cyclization by an oxidosqualene cyclase (OSC) (Figure 5.2). The cyclization of 2,3-epoxysqualene to lanosterol in animals and fungi, and cycloartenol in plants and green algae is catalysed by distinct OSCs. The next conserved reaction is catalysed by a cytochrome P450 (P450), sterol-14-demethylase (CYP51), which removes a methyl group from lanosterol in animals and fungi, and from obtusifoliol, a product of cycloartenol conversions, in the green lineage. After this reaction, the synthesis of sterols becomes more specific and varies depending on the phylogeny.

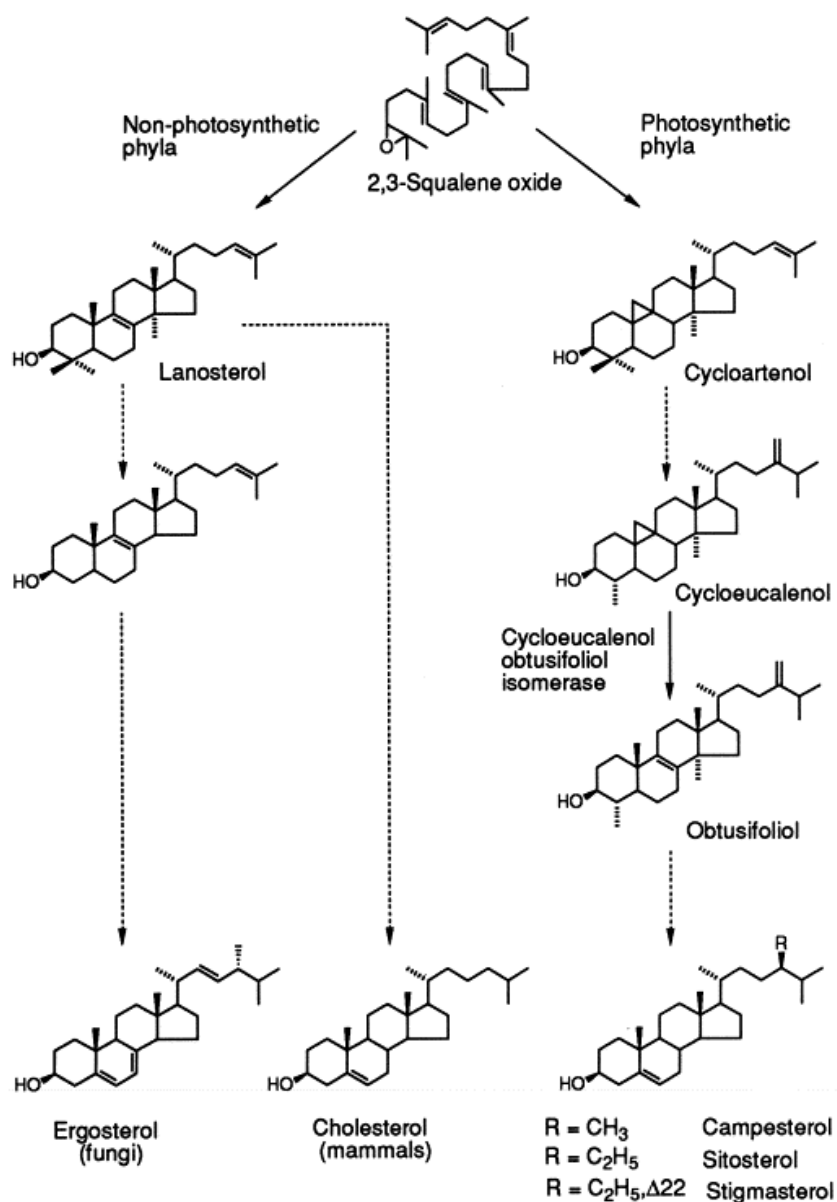


**Figure 5.2.** Oxidosqualene cyclase (OSC) pre-fold oxidosqualene into a chair-boat-chair conformation. There are distinct OSCs in animal and fungi and in photosynthetic organisms (plants and green algae): in the first case 2,3-epoxysqualene cyclization take to lanosterol and in the second case to cycloartenol. A last key step involves a P450 enzyme (CYP51) which uses lanosterol in animals and fungi, and obtusifoliol in plants as substrates to form the different cluster of sterols: ergosterol in funghi, cholesterol in mammals and campesterol, sitosterol, stigmasterol in plants. (Figure from *Hartmann M.*, 1998)

Contrary to the well understood biochemistry of sterols in animals, plants and fungi, our knowledge of this process in other organisms, and in particular in many groups of unicellular eukaryotes, remains fragmentary. Although efforts to chemically characterize the sterol composition of several diatom species have revealed a marked diversity in products (*Volkman, 2003; Rampen et al., 2010; Giner & Wikfors, 2011*), the few studies carried out so far on the biosynthetic pathways (*Fabris et al., 2014; Massé et al., 2004*) have left unresolved the origin of these compounds in the lineage. Some diatom sterols seem to derive from cycloartenol, like phytosterols, whereas others originate from lanosterol, making the collocation of the pathway difficult (*Rampen et al., 2010*). Diatoms belong to the same kingdom as the oomycetes, one of the rare eukaryotic groups that have lost the ability to synthesize sterols during their evolution (*Gaulin et al., 2010*). Therefore, the study of sterol biosynthesis in diatoms is fascinating, from both evolutionary and ecological perspectives.

Given the results that have led to the identification of sterol sulfates as possible cellular mediators in diatoms and in consideration of the modulation of steroid levels in *C. criptica* and *S. marinoi*, this part of the thesis addresses the characterization of the biosynthetic pathway of sterols by the incorporation of a labeled organic substrate. To this aim, it has been specifically designed conditions to grow diatoms upon  $^{13}\text{C}$ -labeled glucose as sole carbon and energy sources (*Chen, 2006*). Establishment of heterotrophic conditions depend on strain and culture parameters, whereas consumption of the carbon source depends on the transport or diffusion of the carbon source across the membrane, and on the enzymatic processes required for its incorporation into the central carbon metabolism (*Mojtaba et al., 2011*). Active transport appears to be the primary means by which algae acquire organic carbon substrates from the environment. Active transport of carbon sources has been documented in several species of diatoms (*Hellebust & Lewin, 1977*), and is likely the most common mechanism for sequestering these

compounds. *C. cryptica* was identified as model species in this study that is capable of heterotrophic growth (Hellebust, 1971; Pahl et al, 2010) and traced the biosynthetic pathway of sterols in this diatom.

## 5. 2. Results and discussion

### 5.2.1. Heterotrophic growth of *C. cryptica*

*C. cryptica* grow heterotrophically under different conditions (Hellebust, 1971; Pahl et al, 2010). According to the protocol of Rohmer for studying terpene biosynthesis (Schwender et al., 1996), the sugar was supplemented to established cultures of the diatom in the dark. Hellebust (1970) and White (1974) have independently reported 2 g L<sup>-1</sup> as optimal concentration to sustain heterotrophic growth of *C. cryptica*. Lower concentrations were reported to inhibit diatom growth, whereas higher concentrations did not increase substrate incorporation. Figure 5.3 reports the resulting curve of *C. cryptica* on 2 g L<sup>-1</sup> glucose in comparison with growth under standard photoautotrophic conditions. The cells remained dark brown in color and no contamination was observed under the heterotrophic conditions. According to Hellebust (1970 and 1971), the initial rate of growth was limited by glucose assimilation due to development of the transport system necessary to the transport across cell membrane (Hellebust, 1970; Hellebust, 1971). After this lag time, cell growth recovered and cultures entered in stationary phase. Under microscope, diatom cells appeared smaller but more numerous than under standard phototrophic conditions. The cultures were harvested on day 15 at the first point of declining phase when glucose consumption was 0.4 ± 0.1 g L<sup>-1</sup>. No significant differences between heterotrophic and photoautotrophic cultures were observed in the consumption of silicates and phosphates,

whereas nitrates showed a different trend with a quicker consumption under dark conditions (data not shown).

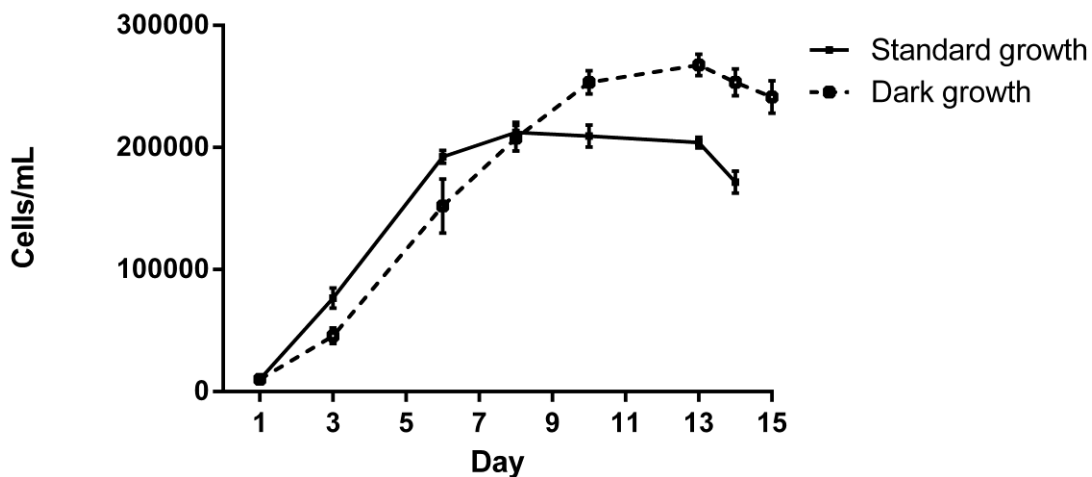


**Figure 5.3.** Growth curves of *C. cryptica* (Cells/mL): growth in standard conditions and growth in the dark on glucose.

To estimate incorporation of glucose, *C. cryptica* was incubated with 2 g/L [ $^{13}\text{C}_6$ ]-glucose under the same conditions. After 15 days cells were recovered and extracted as described in 8.10 and fatty acid composition was determined as methyl esters by GC-MS as described in 8.14.

The MS spectrum of the major species revealed high incorporation of labeled glucose (Figure 5.4). In particular, the molecular mass of the main species, namely  $\text{C}_{16:1}$  (Figure 5.4 a, b) and  $\text{C}_{16:0}$  (Figure 5.4 c, d), showed a clear increase of 16 uma which was consistent with incorporation of  $^{13}\text{C}$  atoms in all positions of the alkyl chain.

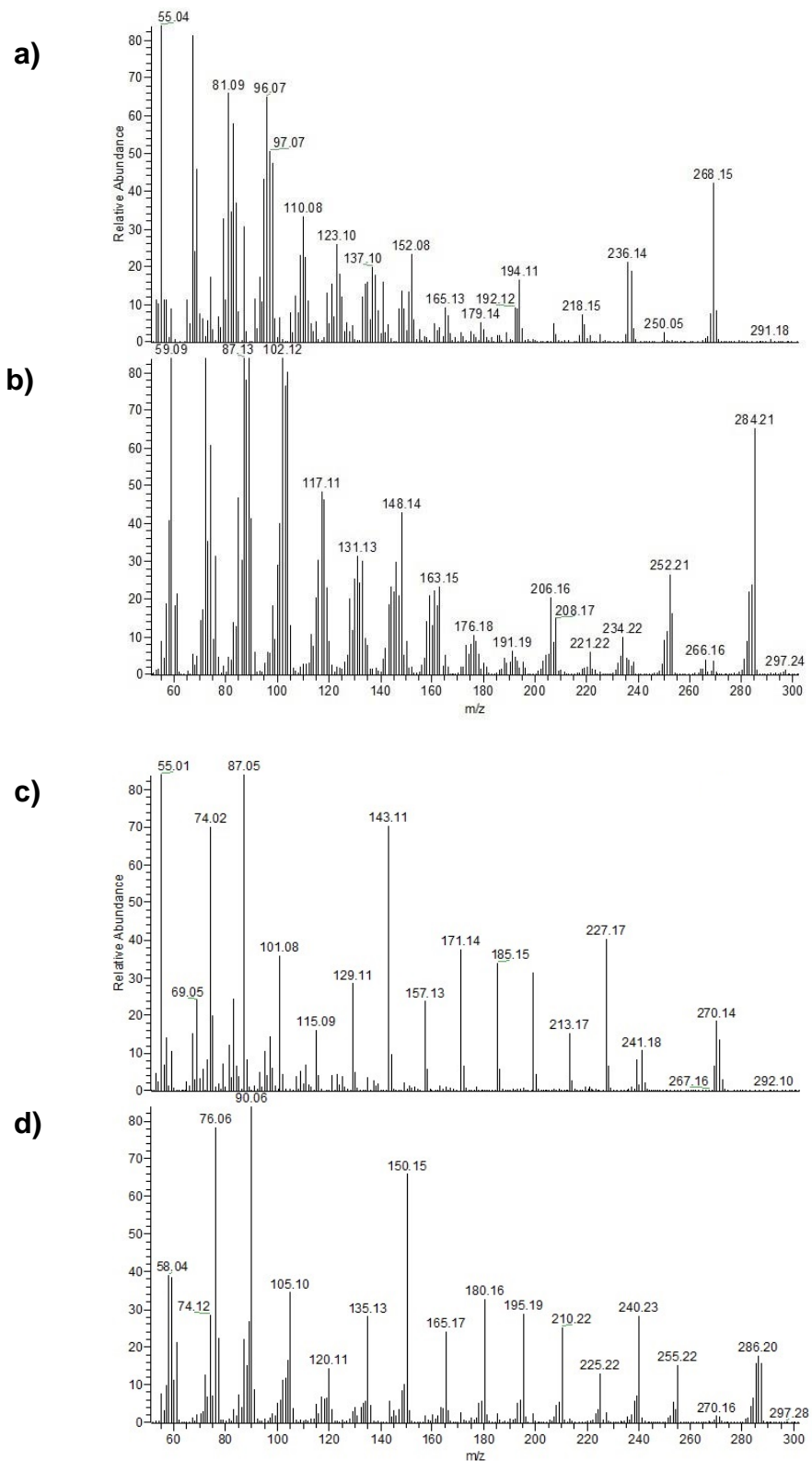


**Figure 5.4.** GC-MS fragmentation of methyl ester of  $C_{16:1}$  (**a, b**) and  $C_{16:0}$  (**c, d**) in the extract from *C. cryptica* cultures on unlabeled glucose (**a, c**) and on  $^{13}C_6$  glucose (**b, d**). It's evident as the label pattern of molecular ion (m/z 268 and 270 respectively) in the organic extracts of cells growth on  $^{13}C_6$  glucose shift to more 16 (m/z 284 and 286).

### 5.3.2. Characterization of sterols biosynthetic pathway

The biosynthetic experiment was performed by using [1-<sup>13</sup>C]-glucose as precursor, in order to discriminate the contribution of MVA and MEP pathway to the biosynthesis of sterols according to a different labelling of isoprene unit (Figure 5.5).

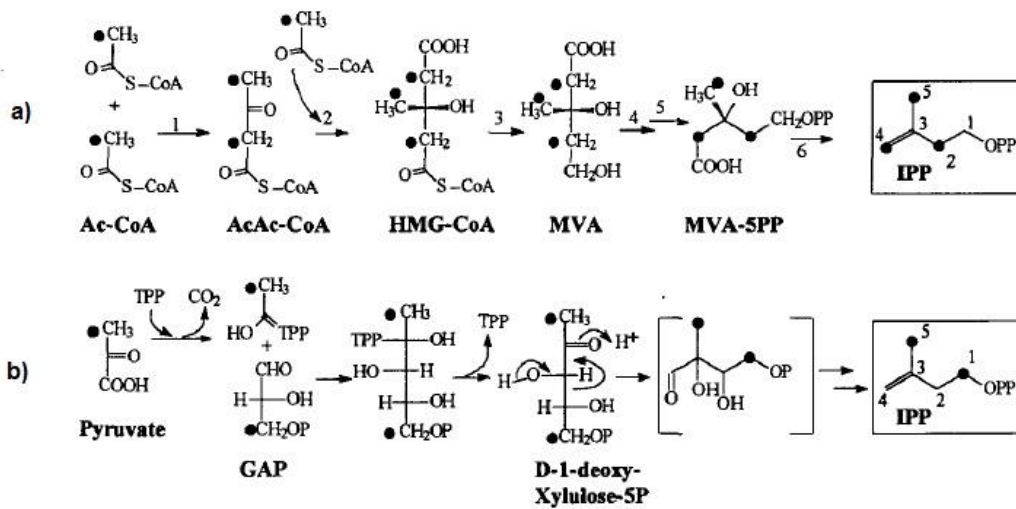


**Figure 5.5.** Formation of isopentenyl diphosphate (IPP) via MVA pathway (a) and MEP pathway (b). <sup>13</sup>C-label, which arises from feeding of [1-<sup>13</sup>C]-glucose to cell cultures (Rohmer *et al.*, 1993).

Sterols from organic extracts of heterotrophic cultures were purified by silica gel column with a gradient of ethyl ether: petroleum ether as illustrated in section 8.11 (Figure 5.6).

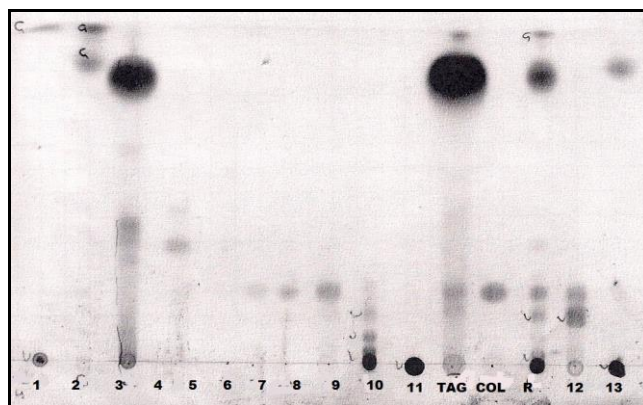


**Figure 5.6.** TLC analyses of a purification of *C. cryptica* extract (R) purification eluted in petroleum ether: ethyl ether (6:4; v/v). Spots were detected by Ce(SO<sub>4</sub>)<sub>2</sub> and cholesterol (col) and triglycerides

from fish oil (TAG) were used as reference. Pure fractions of sterol mixtures (fractions 7-8) were obtained in petroleum ether: ethylic ether 85:15 (v/v).

Purification by HPLC of the sterol fraction (Figure 5.7) gave dihydrobrassicasterol and 24-methylene cholesterol together with two other unidentified products.

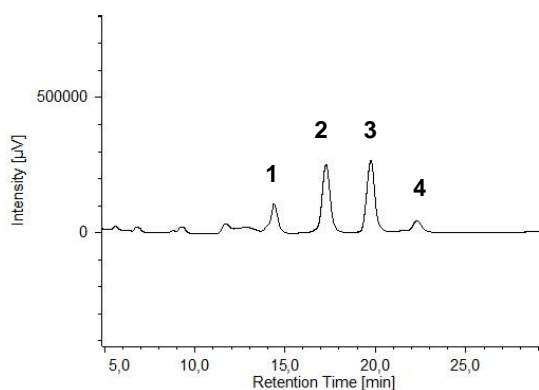


**Figure 5.7.** HPLC profile sterols silica gel fraction. UV profile was monitored at wavelength of 210 nm and the 4 main peaks were collected. The main compounds in the mixture correspond to 24- methylene cholesterol (peak 2), and to dihydrobrassicasterol (peak 3).

After acetylation, these fractions were also analyzed by GC-MS. Presence of cluster peak centered at  $m/z$  ratio higher than in natural isotopomers demonstrated the enrichment of  $^{13}\text{C}$ -labeling in the sterol nuclei of both compounds (Figure 5.8 and 5.9). In particular, molecular ion and fragmentation pattern of dihydrobrassicasterol acetate suggested average an incorporation of 5 labeled carbon atoms in the terpene molecule (Figure 5.8, b), whereas the MS spectra of 24-methylene cholesterol acetate showed mass shift of the main fragments consistent with average incorporation of 4 labeled carbon atoms (Figure 5.9).

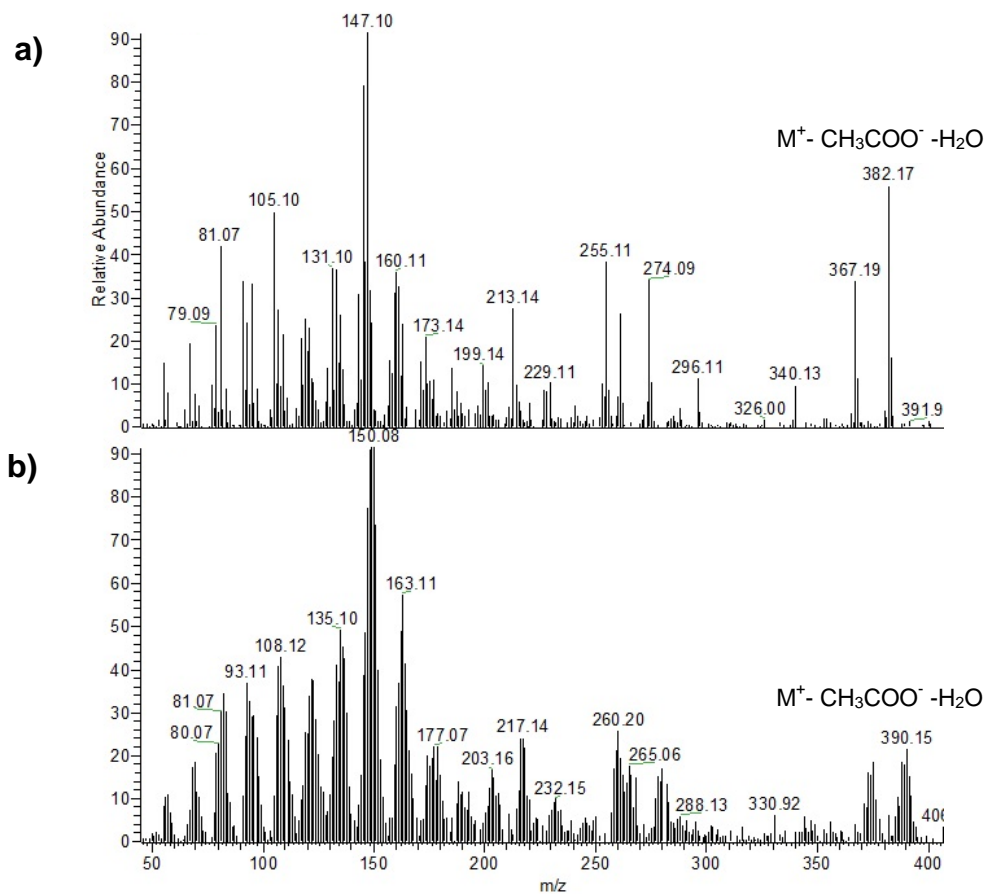


**Figure 5.8.** GC-MS fragmentation of dihydrobrassicasterol acetate in the extract from *C. cryptica* cultures on unlabeled glucose (**a**) and on  $[1-^{13}C]$ -glucose (**b**). The molecular ion is characterized by loss of acetate group and loss of a  $H_2O$  molecule ( $M^+ - CH_3COO^- - H_2O$ ) ( $m/z$  382 for natural compound and  $m/z$  390 for labeled compound).

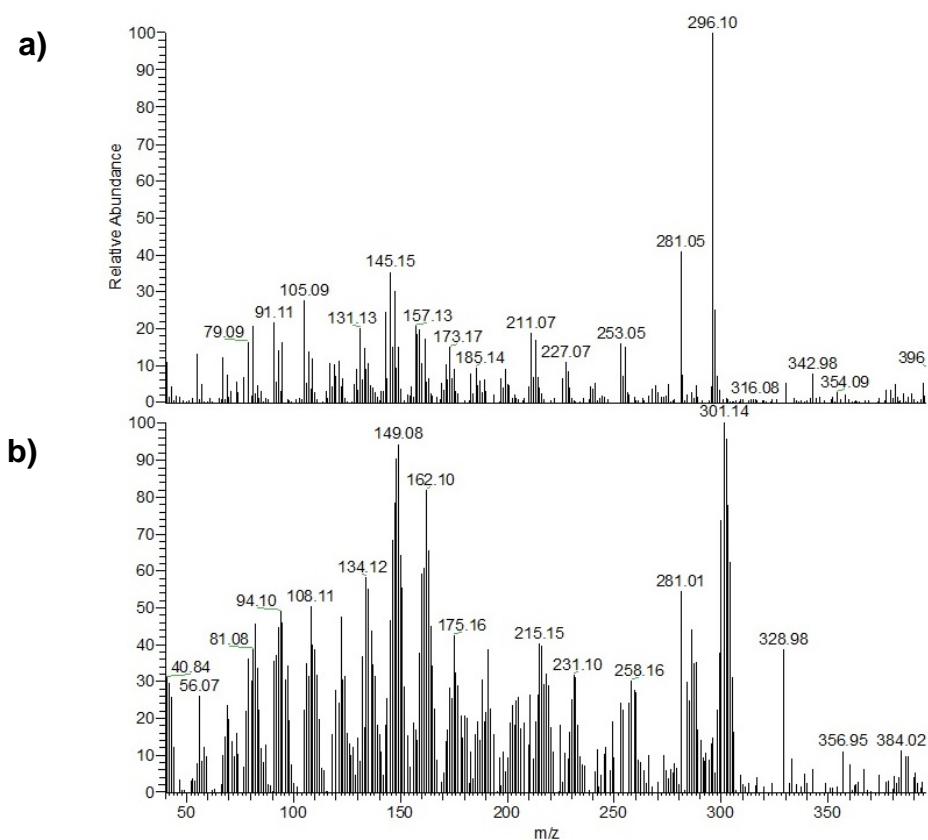


**Figure 5.9.** GC-MS fragmentation of 24-methylene cholesterol acetate in the extract from *C. cryptica* cultures on unlabeled glucose (a) and on [1-<sup>13</sup>C]-glucose (b).

<sup>13</sup>C NMR spectrum of purified dihydrobrassicasterol is reported in Figure 5.10. Comparison with average abundance of carbons in natural dihydrobrassicasterol clearly revealed selective incorporation in specific position of sterol skeleton (Popják et al, 1976). In particular, the data established enrichment at C-1, C-3, C-5, C-7, C-9, C-13, C-15, C-17, C-18, C-19, C-21, C-22, C-24, C-26, C-27 and C-28 (Figure 5.11). This latter carbon does not belong to the terpene skeleton and, according to Djerassi proposal (Djerassi, 1981), arises from methylation by S-adenosyl methionine (SAM).

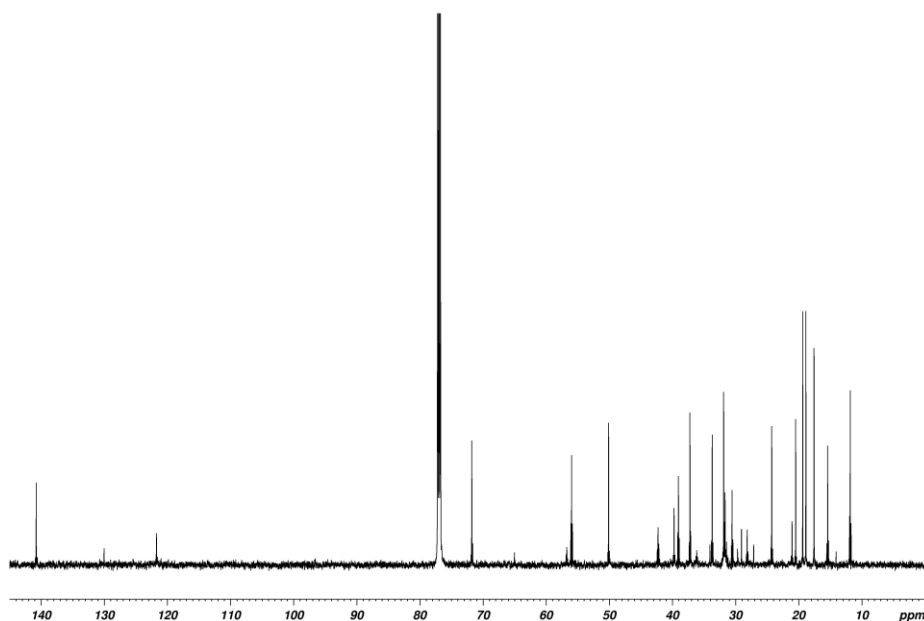


**Figure 5.10.**  $^{13}\text{C}$  NMR spectrum of dihydrobrassicasterol in  $\text{CDCl}_3$  (spectrum of compounds from sterol mixture of cells grown on labeled glucose).

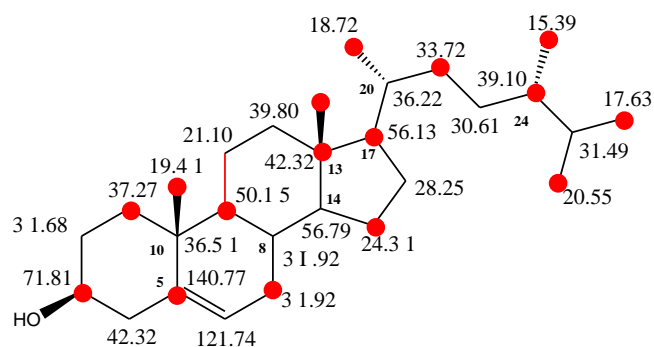


**Figure 5.11.**  $^{13}\text{C}$  chemical shift assignments in dihydrobrassicasterol expressed in ppm ( $\delta$ ), recorded at 600 MHz in  $\text{CDCl}_3$ . Red circles showed the labeled positions corresponding to C-1, C-3, C-5, C-7, C-9, C-13, C-15, C-17, C-18, C-19, C-21, C-22, C-24, C-26, C-27 and C-28.

As reported in Figure 5.12, a few positions such as C-6 (121.74 ppm) and C-16 (28.25 ppm) were clearly not labeled. Other carbon atoms resulted highly labeled, as C-1 (37.27 ppm), C-19 (19.41 ppm), C-18 (11.88 ppm) and C-7 (31.92 ppm). The labeling

at C-8 (31.92 ppm) could not be determined due to the overlapping with the signal of C-7 (31.92) ppm.

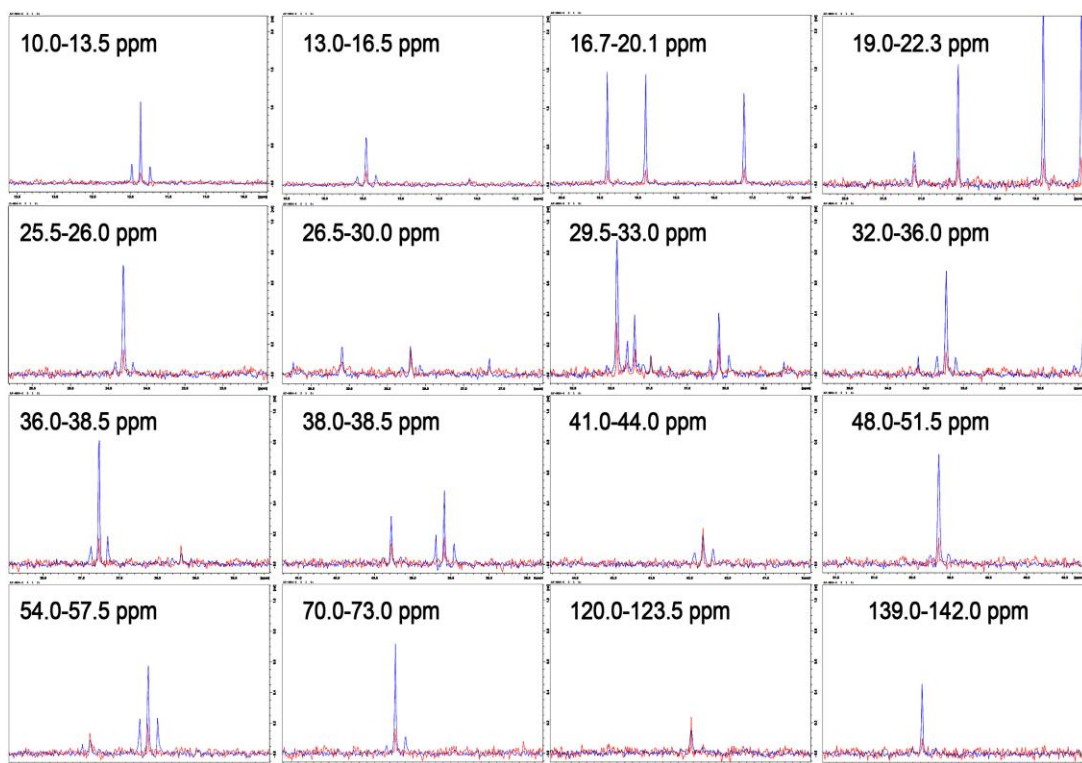


**Figure 5.12.** Enlargements of some regions of the  $^{13}\text{C}$  NMR spectra (10-140 ppm) in  $\text{CDCl}_3$  of dihydrobrassicasterol from *C. cryptica* cells growth on unlabeled glucose (red peaks) and on  $[1-^{13}\text{C}]$ -glucose (blue peaks). All signals are normalized on C14 (56.79 ppm).

Mapping of these positions permitted to conclude that labeling was specifically present at C-2, C-4 and C-5 of the six isoprene units that form the rearranged terpene skeleton of dihydrobrassicasterol (Figure 5.13). On the contrary, very low or no labeling were observed at carbon positions derived from C-1 of the building isoprene units.

According to Rohmer scheme (Rohmer et al, 1993), this enrichment proved unambiguously synthesis of dihydrobrassicasterol by mevalonate pathway (Figure 5.5).

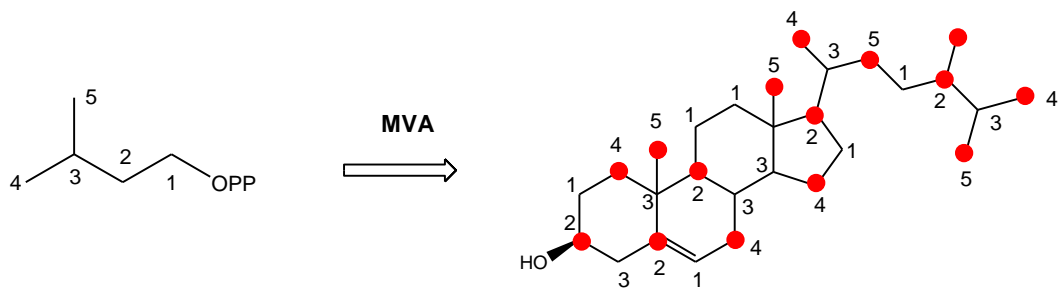


**Figure 5.13.** Labeling pattern of dihydrobrassicasterol found after heterotrophic growth of *C. cryptica* growth on [1-<sup>13</sup>C]-glucose with indication of correspondent carbon atoms of the isoprenic skeleton represented by isopentenyl diphosphate (IPP) (on the left). Red circles illustrate the labeled carbon atoms that correspond to positions 2, 4, 5 of IPP in according to mevalonate (MVA) biosynthetic pathway.

Labelling at C-2, C-4 and C-5 of the isoprene unit also indicated transformation of [1-<sup>13</sup>C]-glucose to [2-<sup>13</sup>C]-acetate, thus providing the first direct evidence of Embden-Meyerhof glycolysis in marine diatoms (Figure 5.14) Annotation of the diatom genome (*Phaeodactylum tricornutum*) revealed occurrence of Entner- Doudoroff pathway and a putative phosphoketolase pathway in addition to the conventional Embden-Meyerhof process. Both additional pathways are uncommon in eukaryotes (Fabris et al, 2014; Zheng et al, 2013), even if further experiments with labeled substrates will be necessary to exclude their presence in *C. cryptica*.

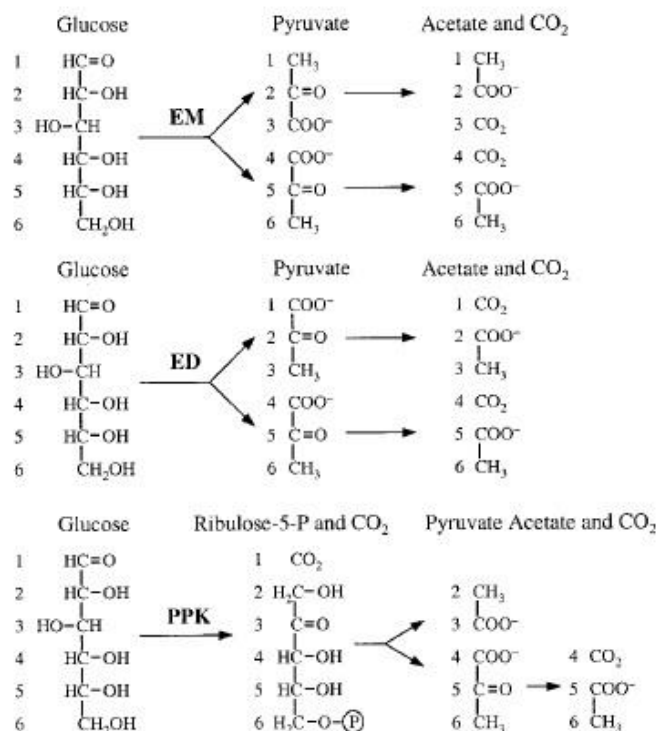


**Figure 5.14.** Expected labeling pattern of acetate and CO<sub>2</sub> from selectively labeled glucose via EM (Embden-Meyerhof, ED (Entner- Doudoroff), and PPK (phosphoketolase) pathways. The numbers show the fate of each carbon from glucose.

Interestingly many signals showed flanking doublets due to incorporation in the vicinal carbons in the same molecules (Figure 5.12). The intensity of the doublets was stronger in those signals whose proximity is in agreement with the biosynthetic sterol pathway (Figure 5.2). This was particularly evident with the pairs C-13/C-18 and C-24/C-28. Unfortunately these experiments did not allow us to determine whether cycloartenol or lanosterol was the precursors of dihydrobrassicasterol, but the incorporation and the co-occurrence of 24-methylene cholesterol are consistent with the biosynthetic pathway reported in Figure 5.15.

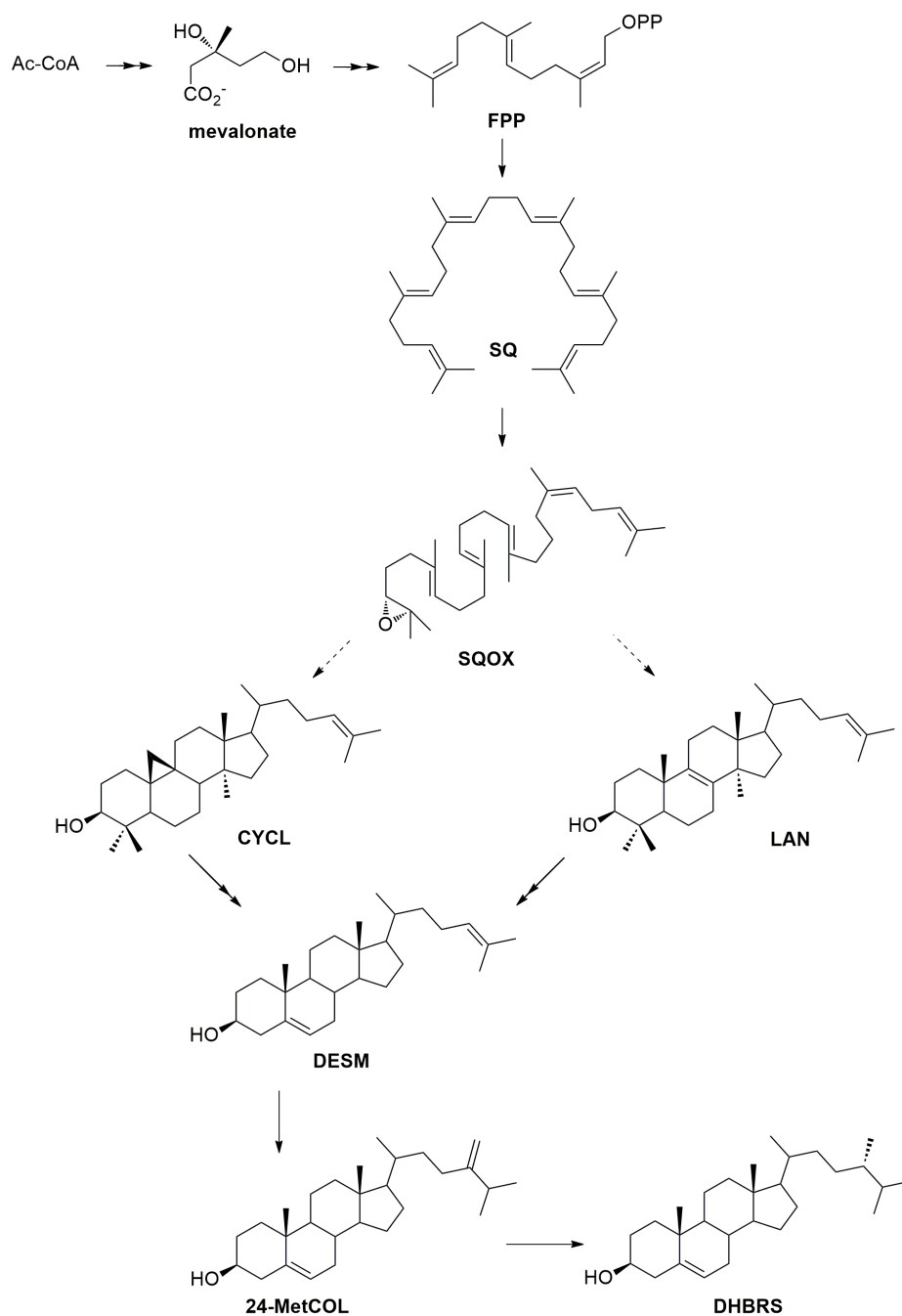


**Figure 5.15.** Proposed biosynthesis of sterols in the diatom *C. cryptica*. Acetyl-CoA (Ac-CoA) is converted to mevalonate by three-step reaction. Squalene synthase (SQS) catalyze two-step reaction in which two identical molecules of farnesyl pyrophosphate (FPP) are converted into squalene (SQ). Squalene is oxidized to oxidosqualene (SQOX) that is the substrate of various oxidosqualene cyclases, which produces lanosterol (LAN) or cycloartenol (CYCL). This biosynthetic step is not yet clear, but our results suggest that the following sterols precursor is desmosterol (DESM) from which 24-methylene cholesterol (24-MetCOL) and then dihydrobrassicasterol (DHBRs) are formed.

## 6. Inhibition of sterols sulfotransferase

### 6.1. Introduction

Sulfotransferases (SULTs) catalyze the transfer of a sulfonyl group ( $\text{SO}_3$ ) from the universal donor 3'-phosphoadenosine 5'-phosphosulfate (PAPS) to a hydroxyl group of various substrates in a process called the sulfonation reaction (Figure 6.1). These enzymes share highly conserved sequence regions across all kingdoms; however, their substrates and physiological function are predicted to be very diverse (*Hernández-Sebastiá et al., 2008*).

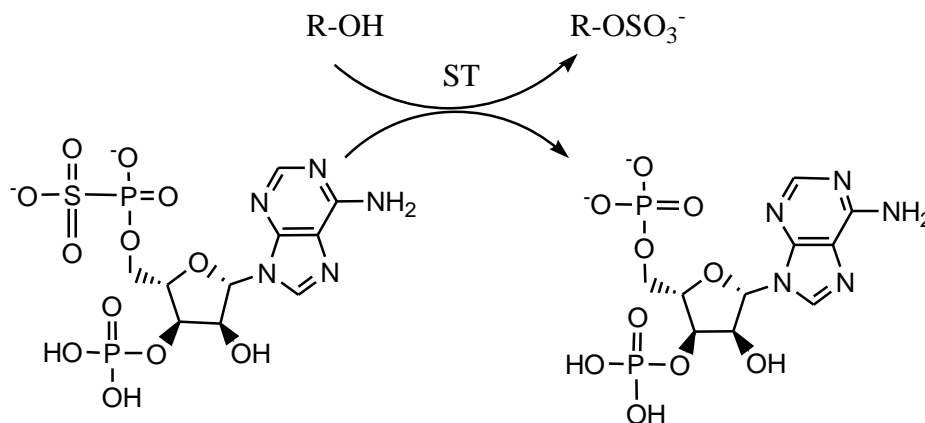


**Figure 6.1.** Enzymatic reaction catalyzed by sulfotransferases.

SULTs are classified as cytosolic and membrane-associated enzymes. Cytosolic SULTs perform the reaction of sulfonation of small organic molecules such as steroids, flavonoids, glucosinolates and hydroxyjasmonates. Membrane-associated SULTs show preference for larger biomolecules such as complex carbohydrates, peptides and proteins. In animals, including mammals, addition of sulfonate group is suggested to play a regulatory role and affect biological properties of substrates. Initially, the cytosolic SULTs were thought to be primarily involved in detoxification of endogenous

and exogenous metabolites. They were considered as part of the detoxification arsenal, which includes hydroxylases and glucuronidases. It is now clear that this is not their only function. For example, the sulfonation of steroids in mammals modulated the biological activity of this class of terpenes (*Clarke et al., 1982*). The roles of sulfated compounds in bacteria and plants are less clear and nothing has been hitherto reported about the function, expression or structure of SULTs in diatoms.

The enzyme that produces cholesterol sulfate was identified as a member of the cytosolic SULT superfamily (*Javitt et al., 2001*). The SULT superfamily is divided into five families, one of which (SULT2) is primarily engaged in the sulfoconjugation of sterols (*Nagata & Yamazoe, 2000*). The human SULT2 family is further divided into two subfamilies, i.e., SULT2A1 and SULT2B1; furthermore, the SULT2B1 subfamily consists of two isoforms designated SULT2B1a and SULT2B1b (*Her et al., 1998*). SULT2B1b sulfonates cholesterol and is more than an order of magnitude more active than the other SULT2 isozymes (*Fuda et al., 2002*).

To date, efforts to develop inhibitors for the SULTs have focused on targeting the sulfate transfer. Molecules such as environmental toxins, natural products and bisubstrate-based compounds (compounds that incorporate elements from the substrate and the cofactor PAPS) have been tested mostly on cytosolic SULTs (*Armstrong et al., 2001*). Polychlorinated biphenols and compounds that mimic the end products of sulfate transfer have been identified as inhibitors of estrogen, phenol and cholesterol SULTs (*Rath et al., 2004; Wang & James, 2006*).

The last part of my thesis was focused on the characterization of the regulatory mechanism of the sulfotransferase reaction involved in synthesis of sterol sulfates in the marine diatoms. To this aim, the effect of inhibitors of SULTs was evaluated in *S. marinoi* and *C. cryptica*, as well as we carried out a first Real-Time PCR analysis of putative sulfotransferase gene in *S. marinoi*.

## 6. 2. Results and discussion

### 6.2.1. Preliminary sulfotransferase inhibitors assay

Seven established inhibitors (Figure 6.2) of mammalian SULTs were screened for cell proliferation activity on *S. marinoi* in 24 multiwell plates. Effects on viability and diatom growth were determined by cell number and by extrapolation of chlorophyll *a* fluorescence.

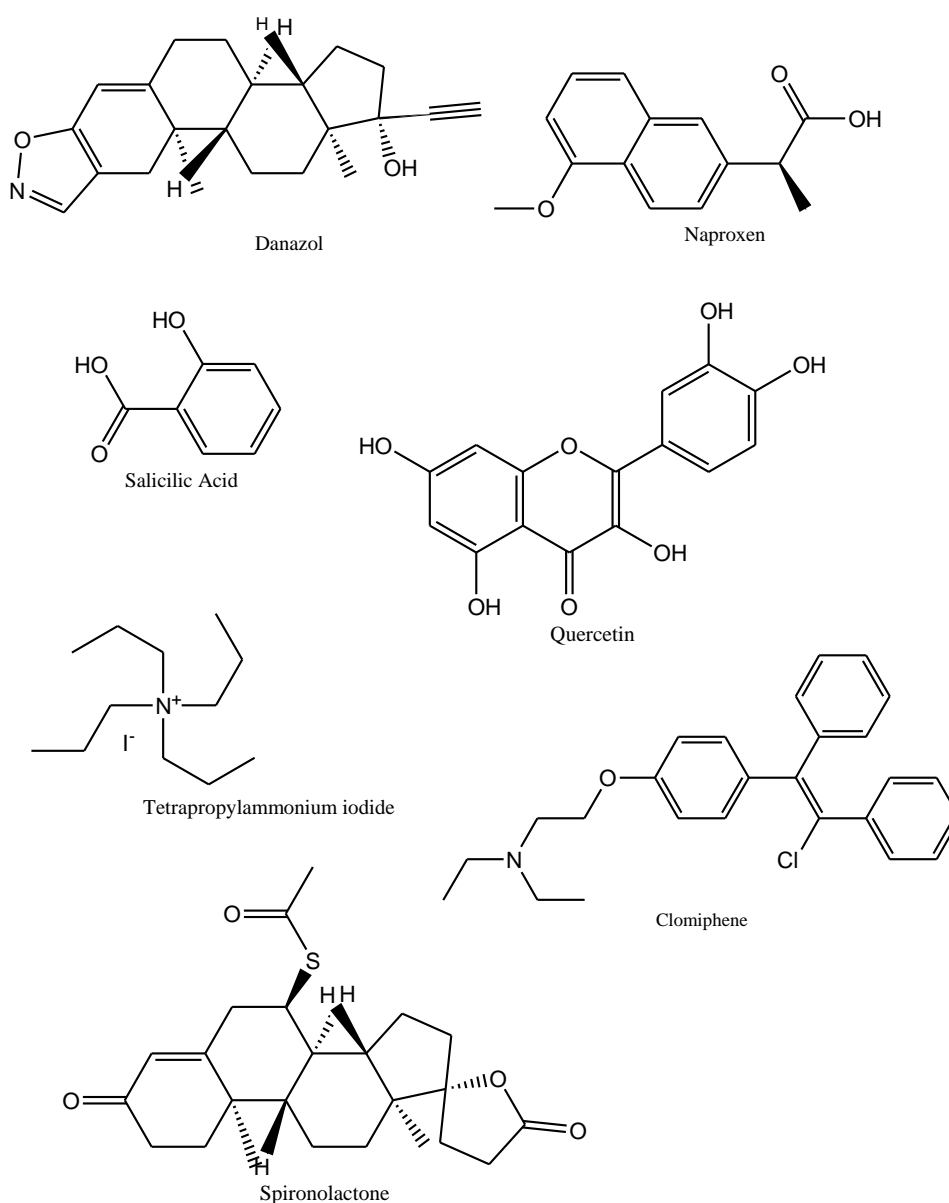


**Figure 6.2.** Structures of sulfotransferase inhibitors tested on diatoms cells.

Among the tested compounds, only quercetin gave good results (Figure 6.4). At the highest dose (40  $\mu\text{M}$ ) the flavonol blocked reversibly cell growth, whereas at concentrations between 10 and 20  $\mu\text{M}$  the molecule induced significant cell proliferation. No effect was found at lower concentrations. In addition to increase of cell number, quercetin determined duration of the growth curve until day 9 whereas the untreated cells were in declining phase already at day 8. Furthermore, unlike control cultures that showed irregular shape and little chains, *S. marinoi* cells treated with quercetin formed long and numerous chains with regularly-shaped cells (Figure 6.5). The mechanism seemed to be structure-dependent since the other molecules were all toxic or ineffective. In fact, cells treated with salicylic acid, naproxen and tetrapropylammonium iodide showed growth rate and morphology very close to control over 7 day period. On the contrary clomiphene was toxic in the whole concentration range tested (0.25- 40  $\mu\text{M}$ ) with the 100% of cell mortality already in 24 hours (not shown), danazol revealed cytotoxic effects from 5 to 40  $\mu\text{M}$  with a mortality rate of 100% only at the highest concentrations and inhibition at lower concentration, and spironolactone was cytotoxic only in the range between 20 and 40  $\mu\text{M}$ .

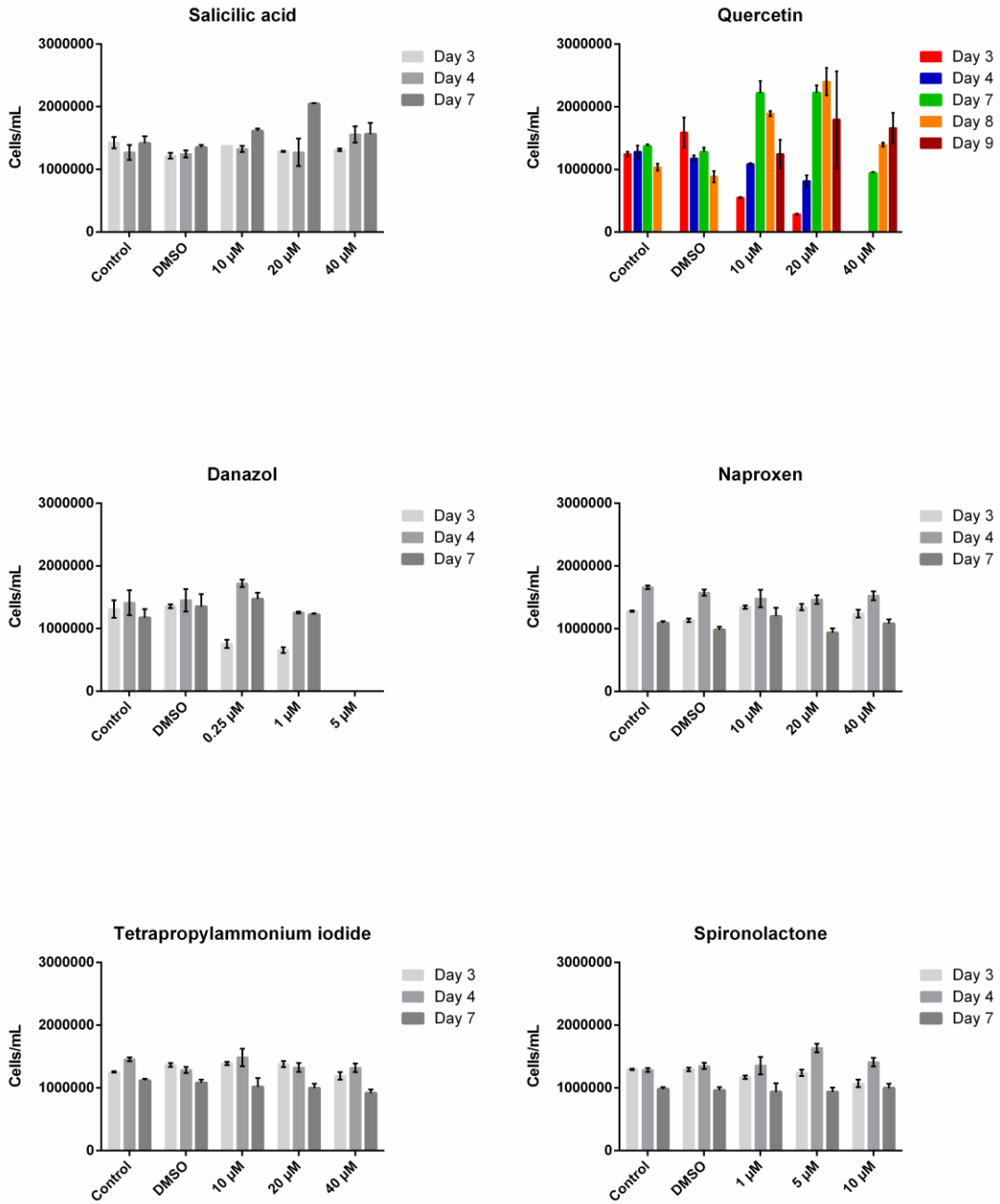


**Figure 6.4.** Test results of sulfotransferase inhibitors assayed on *S. marinoi* cells. Data are expressed as cellular concentration (Cells/mL) at day 3, 4 and 7 at different concentrations of compound tested, compared to cells growth under standard conditions (control) and cells growth with 10  $\mu$ L of DMSO (solvent used to dissolve the test compounds). While the other tested compounds have a toxic effect or none effect on *S. marinoi* growth, quercetin showed a proliferative effect in the concentration range 10-20  $\mu$ M.

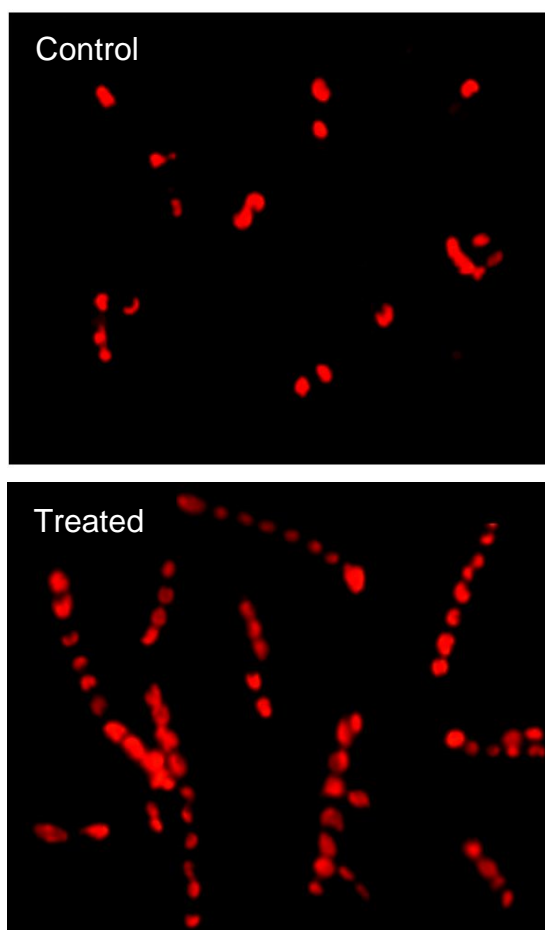


**Figure 6.5.** Enlargement of photo by fluorescence microscopy at 20 x magnification (530/30 BP emission filter for red fluorescence emission of chl) after 7 days of control cells and *S. marinoi* cells incubated with quercetin 20  $\mu$ M (Treated). Cells grown with quercetin are more numerous and form longer chains.

Quercetin is one of the most common natural flavonoid, one of the most widespread classes of secondary metabolite that play different physiological functions including floral pigmentation, UV filtration, radical scavenging and cell cycle inhibitors. Flavonoids compounds are sensitive to light exposure in water and the products are dependent on pH of the aqueous solutions. In particular, UVA and UVB radiations induce degradation of quercetin to give a single product deriving from oxidation and addition to the 2,3 double bond (*Dall'Acqua et al, 2012*). In neutral or basic media, the reaction leads to the addition of water with formation of a stable 2-hydroxy derivative (Figure 6. 6, compound 2).

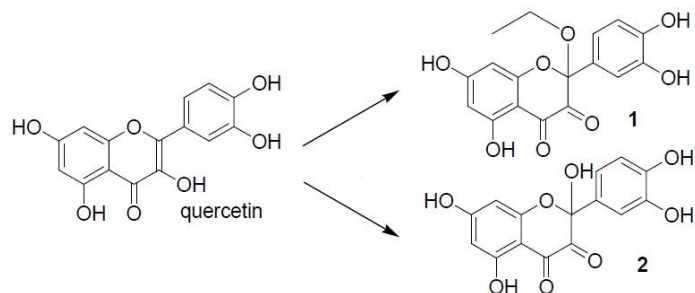


**Figure 6.6.** Structures of quercetin products obtained by either UVA or UVB irradiation (1) or in alkaline solution (2).

Because this inherent reactivity of the molecule, we evaluated the stability of quercetin in f/2 medium prior to start testing the substance on diatom cells on larger volumes. Maximum UV absorption of the flavonol in organic solvent (acetonitrile) was at 375 nm but it gradually shifted toward blue wavelengths (295 nm) in water under the conditions used to grow diatoms. The presence of at least two isosbestic points at 275 and 325 nm suggested that at least one or more photoproducts were formed under these conditions. After only one hour of light exposure in f/2 medium, main absorption peak was at 325 nm. No UV activity was evident after three days, thus suggesting that the hemi-life of the compound in diatom cultures could be no longer than 36 hours (Figure 6.7).

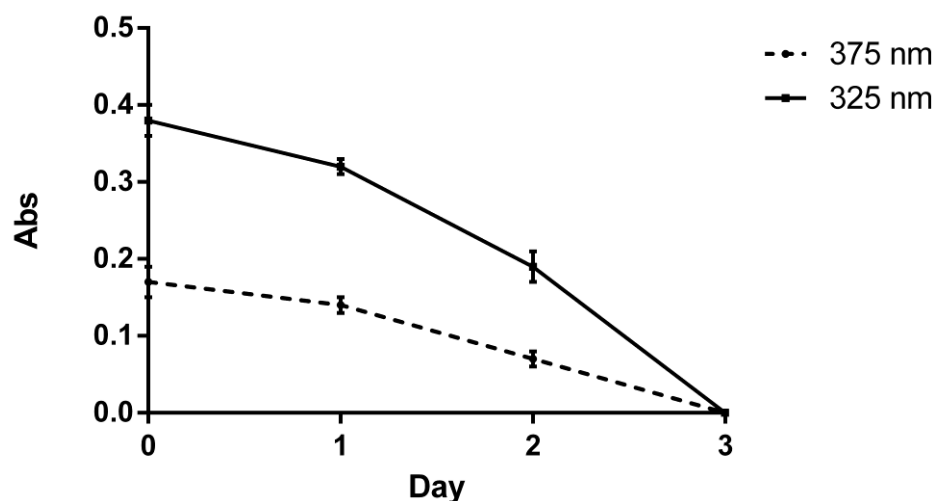


**Figure 6.7.** UV absorption (Abs) of quercetin and its degradation products at 325 and 375 nm in *S. marinoi* cultures.

#### 6.2.2. Effect of quercetin on *S. marinoi*

To examine in depth the physiological role of quercetin on diatom cells, 20  $\mu\text{M}$  (6  $\mu\text{g mL}^{-1}$ ) solution of the flavonol in DMSO was administered to *S. marinoi* in 2-L carboy. Because macronutrients, namely phosphate and silicate, were consumed completely within 4 days under standard conditions (data not shown), nutrients were supplemented by two regimes corresponding to one single administration at day one or two administrations at day 1 and 4.

Under both experimental conditions, addition of quercetin to f/2 medium triggered regular reduction in the level of the sulfated sterols in comparison with control cultures (Figure 6.8). As already discussed in Section 4, levels of these lipids increased regularly along the growth curve but the rate was retarded in cells treated with the flavonol. In cultures with gradual nutrient depletion (Figure 6.8a), concentration of sulfated sterols never increased above 0.5 pg/cell, whereas it was higher than 1.3 pg/cell during declining phase in untreated diatoms. It is worth noting that these values are both lower

than the cytotoxic level estimated by external addition of cholesterol sulfate (37 pg/cell), but it has also to be considered that most of this latter compound is presumably lost after addition to the cultures due to the low solubility in water.

The effect of quercetin on inhibition of sulfated sterol synthesis was even more marked under the second experimental set-up (Figure 6.8b). In fact, whereas the addition of nutrient at day 4 did not produce significant change in level of these lipids in standard cultures, quercetin maintained the cellular concentration of sulfated sterols below 0.5 pg during more than 10 days. The consequence of this process was an apparently higher responsiveness of *S. marinoi* to repletion of nutrients that caused a net increase of the number of cells and an extended duration of the stationary phase, which is consistent with the hypothesis that sulfated sterols mediate cell death in diatoms.

In collaboration with Dr. Mariella Ferrante of Stazione Zoologica A. Dohrn in Naples, we have identified four genes (*SmSulf1*, *SmSulf2*, *SmSulf3*, *SmSulf4*) coding for putative sulfotransferases in *S. marinoi*. The comparative expression of these genes from treated and untreated diatom sampled along the growth curves reported in Figure 6.8a showed that only *SmSulf1* was down-regulated at day 6 and up-regulated at day 7 (personal communication of Dr. Valeria Sabatino), which is in well agreement with the difference in concentration of sulfated sterols between day 6 and day 7. The correlation of molecular and biochemical data seem to support the role of *SmSulf1* in the biosynthesis of sulfated sterols in *S. marinoi*, as well as they are consistent with direct regulation of quercetin on the reaction of sulfonation in this diatom.

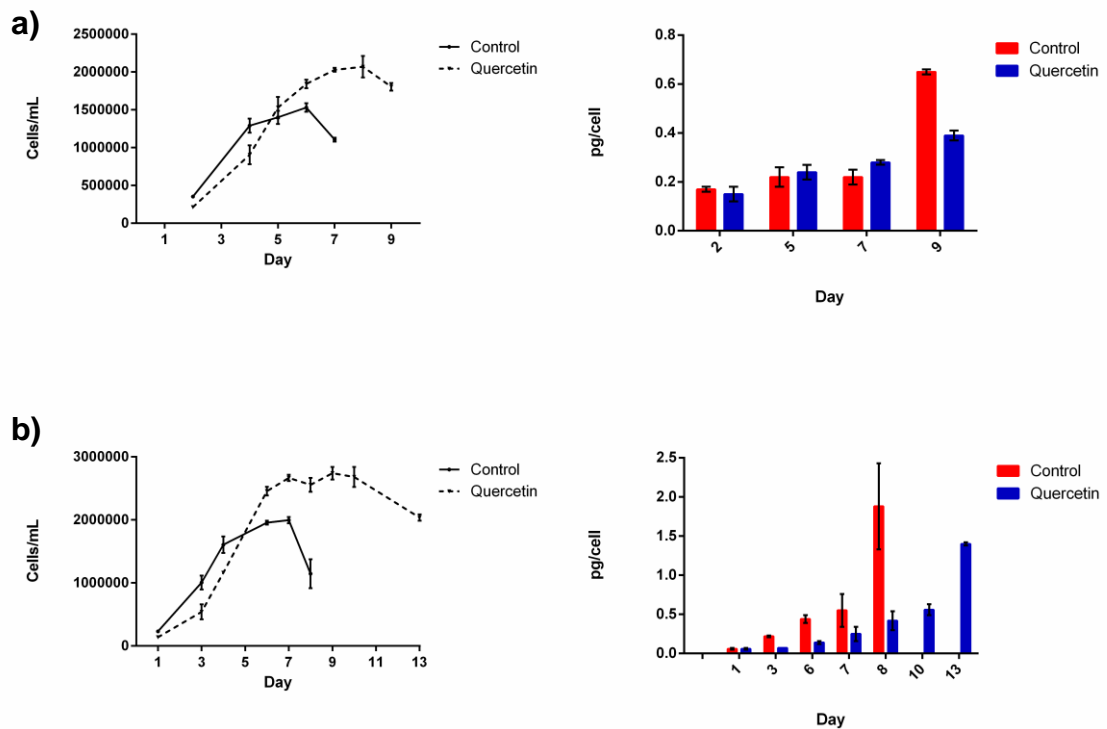


**Figure 6.8.** *S. marinoi* growth curves in standard conditions (Control) and supplemented with quercetin 20  $\mu$ M (Quercetin) with gradual nutrient depletion (a) and the addition of nutrient at day 4 (b). On the right side is reported the correspondent quantitative analysis of sterol sulfates along both of growth curves. Under both experimental conditions, addition of quercetin triggered regular reduction in the level of the sulfated sterols in comparison with control cultures and induced a transient lag in the progression of algal growth increasing the cells number.

Although the effect of quercetin on cellular levels of sulfated sterol is direct and likely mediated by inhibition of *SmSulf1*, the result on diatom growth is unquestionably due to a more complex process that probably involves physiological adaptation of the diatom. In fact, addition of the flavonoid to the culture of *S. marinoi* induced a transient lag in the progression of algal growth. Only after a few days the number of the treated cells rose above that of control cultures (Figure 6.8). Although the final cell concentration was independent of quercetin, diatoms supplemented with nutrient only at day 1 (Figure 6.8a) were delayed during the exponential phase but showed a longer stationary phase

with consequent expansion of the whole growth curve until day 10. Repletion of nutrients at day 4 (Figure 6.8b) produced a significant increase of *S. marinoi* growth with the cell concentration (about  $2.4 \cdot 10^5$  cells mL<sup>-1</sup>) that doubled the number of cells of controls (about  $1.3 \cdot 10^5$  cells mL<sup>-1</sup>).

In addition to confirm the *anti-age* effect of quercetin on *S. marinoi*, these experiments put forward a possible use of this compound to improve the culture yield of the diatom. As matter of fact, the addition of the flavonoid led to net increase in biomass and lipid content (Table 6.1) without affecting significantly the percentages of the major lipid pools (Figure 6.10). We only noticed a limited remodeling (less than 15%) of the glycolipids (GLs), namely monogalactosyldiacylglycerols (MGDG) and sulfoquinovosyldiacylglycerols (SQDG), to the detriment of phospholipids (PLs).

**Table 6.1.** Biomass amount (wet weight) and lipid content of *S. marinoi* cultures in standard conditions (Control) and treated with quercetin (Quercetin) at day 9.

	<b>Biomass</b> (g/L)	<b>Lipid content</b> (mg/L)
<b>Control</b>	1.9 ± 0.2	41.04 ± 1.1
<b>Quercetin</b>	2.8 ± 0.1	61.40 ± 11.4

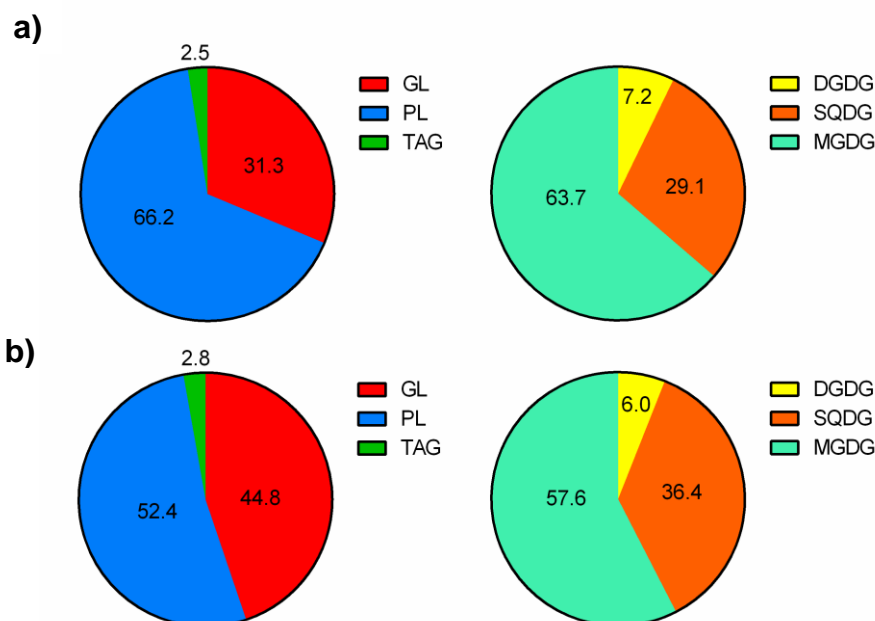


**Figure 6.10.** *S. marinoi* lipid composition obtained by ERETIC <sup>1</sup>H-NMR analysis as described in 8.10 in control (a) and treated with quercetin (b). TAG= triglycerides; PL= phospholipids; GL= glycolipids; MGDG= monogalactosyldiacylglycerols; DGDG= digalactosyldiacylglyceroltriacylglycerols; SQDG= sulfoquinovosyldiacylglycerols Data are expressed as percentage.

### 6.2.3. Effect of quercetin on *C. cryptica*

In consideration of the effect on *S. marinoi*, we decided to test quercetin on cultures of *C. cryptica* that has attracted attention as species of biotechnological interest. As reported in Figure 6.11, this diatom showed a cellular response similar to that of *S. marinoi*. In fact, the flavonoid was inactive at concentration below 5  $\mu$ M and toxic above 40  $\mu$ M. A concentration between 10 and 40  $\mu$ M, the flavonoid showed a reversible inhibitory effect that after day 4 led to recovery of growth progression. As also observed with *S. marinoi*, whereas control cells of *C. cryptica* showed a round and irregular shape, cells treated with 10 and 20  $\mu$ M quercetin had mostly rectangular shape.

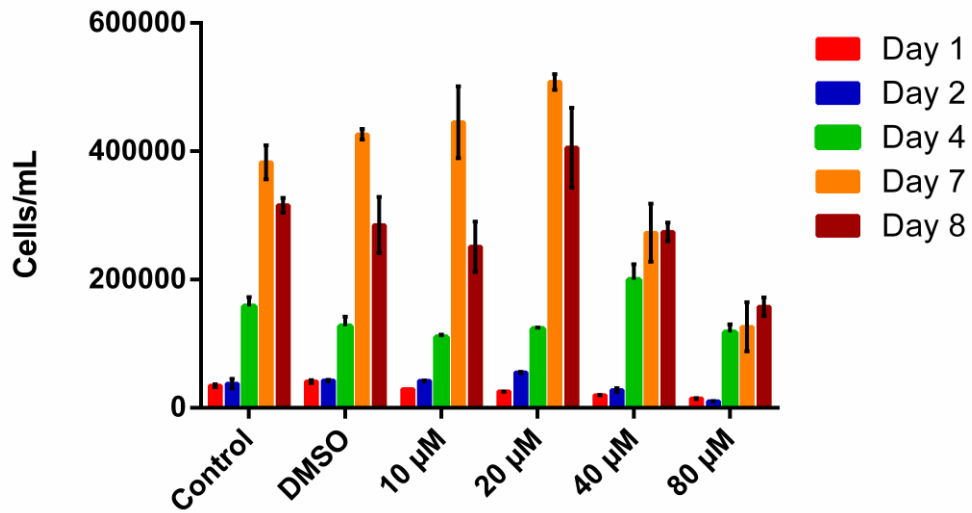


**Figure 6.11.** Test results of quercetin assayed on *C. cryptica* cells. Data are expressed as cellular concentration (Cells/mL) at day 1, 2, 4, 7 and 8 at different concentrations of compound quercetin, compared to cells growth under standard conditions (Control) and cells growth with 10 μL of DMSO (solvent used to dissolve the test compounds).

As shown in Figure 6.12, *C. cryptica* was more sensitive to addition of quercetin in comparison to *S. marinoi* and increase of cell number could be achieved without nutrients repletion.

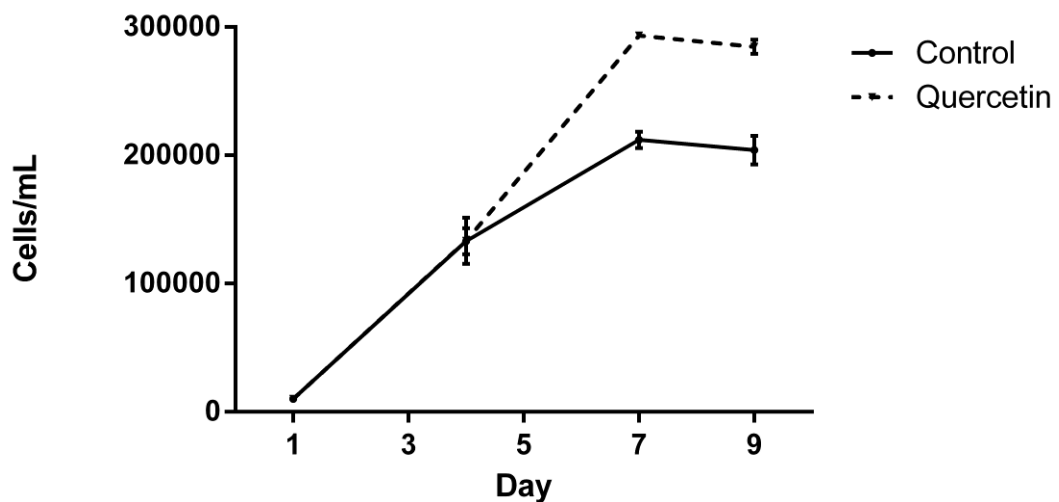


**Figure 6.12.** Growth curves of *C. cryptica* cultures (cells/mL) in standard conditions and with 20 μM quercetin. In the stationary phase (day 7-9) resulted a significant increase of cells number in the cultures treated with the flavonoid.

In fact, the shape and duration of the growth curve was the same until day 7 under both experimental conditions. After that point, cultures treated with the flavonoid experienced a significant increase of cell number that almost double that of controls ( $3.2 \cdot 10^5$  cells  $\text{mL}^{-1}$  vs  $2.0 \pm 0.1 \cdot 10^5$  cells  $\text{mL}^{-1}$ , respectively) with a consequent increase in biomass (dry weight) ( $147.2 \pm 1.0$  mg  $\text{L}^{-1}$  vs  $119.7 \pm 5.4$  mg  $\text{L}^{-1}$ , respectively). Carbohydrates percentage decreased to  $8.1 \pm 2$  % of dry weight and protein content increased to  $30.6 \pm 5.9$  %, while lipids percentage increased to  $29.6 \pm 6.8$  % (compared to  $24.4 \pm 2$  % in untreated cultures) (Figure 6.13). The increase in cell density corresponds thus a slight increase in total biomass and a change in the biochemical composition. The most evident effect is the reduction of the component of carbohydrates with a relative increase in the fraction of protein and lipid.

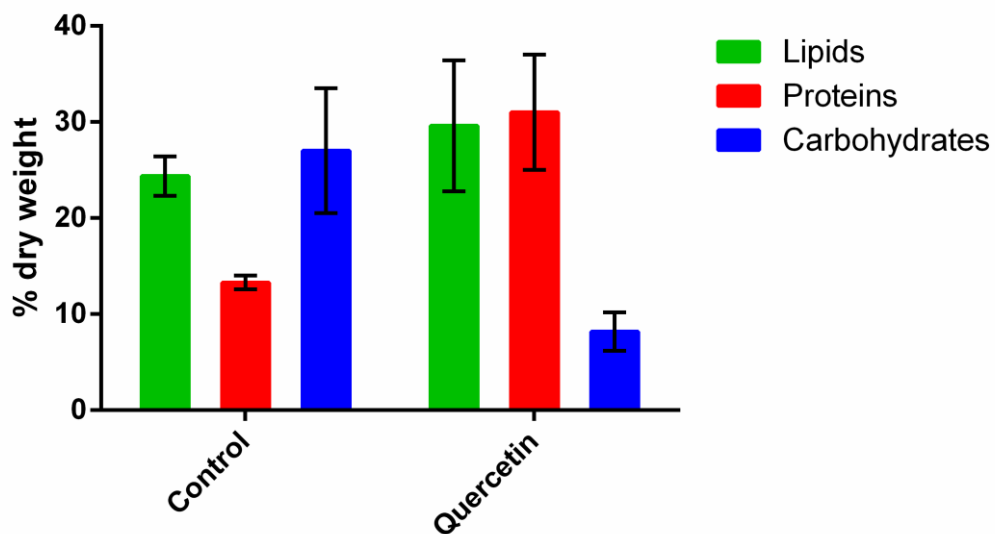


**Figure 6.13.** Biochemical composition of *C. cryptica* biomass growth in standard condition (Control) and supplemented with quercetin 20  $\mu\text{M}$  (Quercetin). Data referred to the last point of growth curve.

In the lipid composition the proportion of triglycerides increased reaching a percentage of about 86% (Figure 6.14) compared to about 70% in control cultures. The

phospholipids percentage is reduced by half, while the percentage of glycolipids remains almost unchanged. Among these there is a slight decrease of DGDG and SQDG and an increase of 10% in the MGDG percentage.

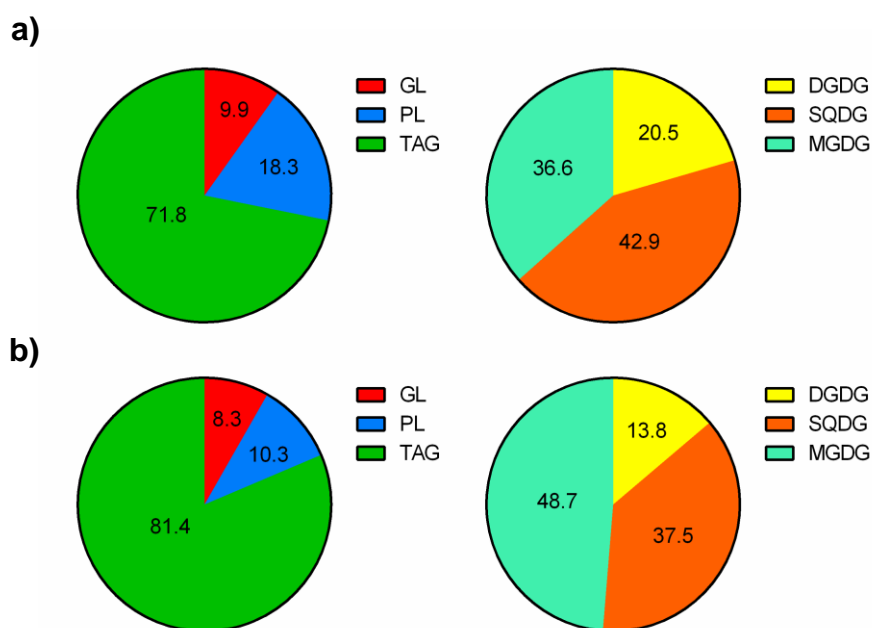


**Figure 6.14.** *C. cryptica* lipid composition obtained by ERETIC  $^1\text{H}$ - NMR analysis as described in 8.10 in standard conditions (a) and growth supplemented with quercetin (b). TAG= tryglicerides; GL= glycolipids; PL= phospholipids. MGDG= monogalactosyldiacylglycerols; DGDG= digalactosyldiacylglycerolstriacylglycerols; SQDG= sulfoquinovosyldiacylglycerols. Data are expressed as percentage.

Quercetin has therefore on *C. cryptica* cells an effect comparable to that found in *S. marinoi*: an increase in cell density, with the relative increase of biomass and reduced production of sterol sulfates. In *C. cryptica* there is also an evident change in the biochemical composition.

## 7. Conclusions

Prokaryotes and eukaryotes produce a wide range of organic compounds, most of which have species-specific distribution and, sometimes, those vary at level of strain or clone. These substances, traditionally known as “secondary metabolites” or “natural products”, are the results of highly-regulated pathways often occurring among limited taxonomic groups. Usually these compounds possess specific function in the adaptive protection against predators and microbial infections, or in inter- or intra-specific signals, such as attractants for pollinating insects. Within marine planktic communities, an important topic is the potential role of secondary metabolites as defensive or allelopathic agents (allelochemicals affect competition between plant species) in controlling species successions during bloom development, species competition and defense against zooplanktic grazers, mainly copepods (*Ianora et al.*, 2006). Chemical interactions are very well known and studied in terrestrial ecosystems (*Inderjit & Duke*, 2003), but studies in aquatic systems have been biased by technical difficulties, mainly arising from dilution in the water medium and physical constraints such as viscosity or shear forces (*Wolfe*, 2000). In aquatic systems there is a broader diversity of species and chemical compounds than in terrestrial ecosystems (*McClintock et al.*, 2001).

This Doctoral thesis was focused on production of secondary metabolites in diatoms, a lineage that is responsible for almost 20% of primary marine productivity and is thus crucial to sustain life on the planet. In the natural environment, diatoms (*Bacillariophyceae*) often outcompete other classes of algae for nutrients and growth and are among the most productive and environmentally-flexible eukaryotic microorganisms on Earth (*Hildebrand et al.*, 2012). They are also identified as the best candidate organisms for lipid-based biofuels production (*Sheehan et al.*, 1998).

Bioassay-guided fractionation led to the isolation and characterization of four sulfated sterols, namely cholesterol sulfate (1), dihydrobrassicasterol sulfate (2),  $\beta$ -sitosterol sulfate (3) and 24-methylen-cholesterol sulfate (4), as responsible of cytotoxic effect on cells of *S. marinoi*, a diatom species that is, responsible for the wintry maximum annual phytoplankton biomass in the Adriatic Sea.

Following identification of sulfated sterols in other species of diatoms (e.g. *Pseudonitzchia multistriata*, *Pseudonitzchia arenysensis*, *Phaeodactylum tricornutum*, *Thalassiosira weissflogii*, *Cyclotella cryptica*) strongly suggest that this class of molecules is commonly present in the lineage. Nevertheless, like the distribution of oxylipins previously reported in diatoms (*Fontana et al.*, 2007; *Lamari et al.*, 2013; *Gerecht et al.*, 2011), their qualitative and quantitative occurrence seems to vary from species to species (Table 7.1).

**Table 7.1.** Occurrence of sulfated sterols across diatom lineage: cholesterol sulfate (1), dihydrobrassicasterol sulfate (2),  $\beta$ -sitosterol sulfate (3) and 24-methylen-cholesterol sulfate (4)

Diatom sp.	Sulfated sterols
<i>Skeletonema marinoi</i>	1, 2, 3, 4
<i>Pseudonitzchia multistriata</i>	1
<i>Pseudonitzchia arenysensis</i>	4
<i>Phaeodactylum tricornutum</i>	4
<i>Thalassiosira weissflogii</i>	2, 4
<i>Cyclotella cryptica</i>	2, 4

Although the sulfoconjugation of steroids was first described in the late 1930s and early 1940s, the sulfoconjugation of sterols, in particular of cholesterol, was not appreciated until much later, when the isolation of cholesterol sulfate from a natural source appeared in 1964 (*Drayer et al.*, 1964). While the initial report (*Siiteri*, 1970) described

the isolation of cholesterol sulfate from the bovine adrenal gland, it was subsequently isolated from diverse human sources and tissues. The discovery of the existence of cholesterol sulfate was followed by a concerted effort to discern its biologic importance. Of particular interest was the finding that cholesterol sulfate can function as a regulatory molecule (*Ikuta et al.*, 1994; *Denning et al.*, 1995). Sterol sulfates have been detected occasionally in lower life forms, such as sponges (*Gunasekera, et al.*, 1994, *Patil et al.*, 1996), echinoderms (*Goodfellow & Goao*, 1983, *Shubina et al.*, 1998) and ophiuroids (*McKee et al.*, 1994). In literature sulfated sterols are reported to have antiviral, antitumor effects (*McKee et al.*, 1994; *Roccatagliata et al.*, 1996; *Roccatagliata et al.*, 1998) and were in the last years described as ligand of a nuclear receptor, conveyed outside the cells by a polar transporter (*Charles et al.*, 2003; *Kallen et al.*, 2004; *Sepe et al.*, 2011). On the other hand, there are few reports of sterol sulfates in diatoms (*Kates et al.*, 1977; *Anderson et al.*, 1978; *Kazufumi & Masami*, 2002), but physiological and ecological function, mechanism of action and biosynthesis were unknown in plankton communities.

This study proved that toxicity of sulfated sterols **1-4** on *S. marinoi* cells was mediated by an increase of NO and hROS. Both products have been previously reported as stress cellular signals related to the programmed cell death (PCD) activation (*Mittler et al.*, 2004; *Kwak et al.*, 2006; *Vardi*, 2006). Use of Annexin V-FITC and TUNEL seems to confirm the role to trigger PCD also in *S. marinoi* by a caspase-like mechanism, even if these results need further confirmation by molecular studies. Cellular production of sulfated sterols occurred under physiological conditions and increased gradually along the growth curve up to toxic concentration on the verge of the declining phase when the estimated amount per liter of (0.8 mg L<sup>-1</sup>) is comparable to EC<sub>50</sub> established by addition of exogenous cholesterol sulfate (2.2 mg L<sup>-1</sup> at 48 h). Sterol sulfates can passively cross cell membranes and may target specific intracellular receptors triggering PCD.

In order to understand the key factors that affect this process, part of the Thesis has been committed to fully elucidate the biosynthesis of sulfated sterols in diatoms. Firstly, qualitative and quantitative composition of sulfated sterols perfectly matched that of sterols in different species, thus proving that there were no preferential sulfonation of specific sterols. This also suggested that regulation of the process may occur during terpene assembly during synthesis of isopentenyl/dimethylallyl pyrophosphate, production of squalene or cyclization and functionalization of the sterol nucleus.

Sterols are vital components of all eukaryotic cells. They are precursors for many signaling molecules that regulate growth and development in plants and animals, in higher plants, sterols play a structural role in cell viability and modulation of activity and distribution of membrane-bound proteins such as enzymes and receptors. Sterols belong to a class of isoprenoids derived from isopentenyl pyrophosphate (IPP), a universal precursor of isoprenoids. In animals and fungi, the cytoplasmic mevalonic acid (MVA) pathway is the only route for biosynthesis of IPP, the building block for lanosterol, which is then metabolized into cholesterol in animals and ergosterol in fungi. In higher plants, IPP can be derived via either the MVA pathway or the plastidial 1-deoxyxylulose 5-phosphate or methylerythritol phosphate (MEP) pathway (*Rohmer, 1999*), despite the former being the main contributor to sterol biosynthesis. Distribution of MVA and MEP pathways within taxonomic order has been so far addressed by incorporation of  $^{13}\text{C}$ - or  $^2\text{H}$ - labeled precursors (*Rohmer, 1999*), use of highly specific inhibitors of MVA and MEP pathways (*Bach & Lichtenthaler, 1982; Zeidler et al., 1998*), or measuring the distribution of the genes of both pathways (*Boucher & Doolittle, 2000*). Based on these approaches, it has been established that archaea, certain bacteria, yeasts, fungi, and some protozoa and animals use only MVA pathway, whereas many bacteria, green algae, and some protists rely on MEP pathway. On the other hand, both routes have been reported in few species of algae, streptomycetes,

mosses, liverworts, higher plants and two diatoms (Cvejic & Rohmer, 2000). Recently, the biosynthetic pathway from acetyl-coenzyme A to sterols has been suggested on the basis of molecular considerations in *Phaeodactylum tricorutum* (Fabris et al., 2014). In analogy with the concomitant results in *Nannochloropsis oceanica* (Lu et al., 2014), the inferred biosynthetic pathway has features of both higher plants and mammals, but to date there was no biochemical confirmation.

During the Thesis full biosynthesis of sterol and sulfated sterols was achieved by incorporation of  $^{13}\text{C}$ -labelled glucose according to Rohmer protocols (Schwender et al., 1996). To this aim, *C. cryptica* was grown under heterotrophic condition by use of glucose as sole source of carbon and energy (Chen, 2006; Hellebust, 1971; Pahl et al., 2010). The study proved that glucose was metabolized to acetyl-CoA mostly by Embden-Meyerhof pathway and synthesis of IPP and DMAPP occurred by MVA pathway. Incorporation rate of labeled glucose in *C. cryptica* and analysis of the sterol composition in the other diatoms also allow us to put forward the biosynthetic scheme depicted in Figure 7.1. Although the present results do not allow to make conclusion about the key intermediate of cyclization, thus both routes through cycloartenol (plant route) or lanosterol (animal and fungal route) cannot be established, sterol biosynthesis of diatoms are to involve sequential transformation of desmosterol (DESM) to cholesterol (COL) or 24-methylene cholesterol (24-MetCOL). This latter product is the suggested precursor of  $\beta$ -sitosterol ( $\beta$ -SITO) and dihydrobrassicasterol (DHBR).

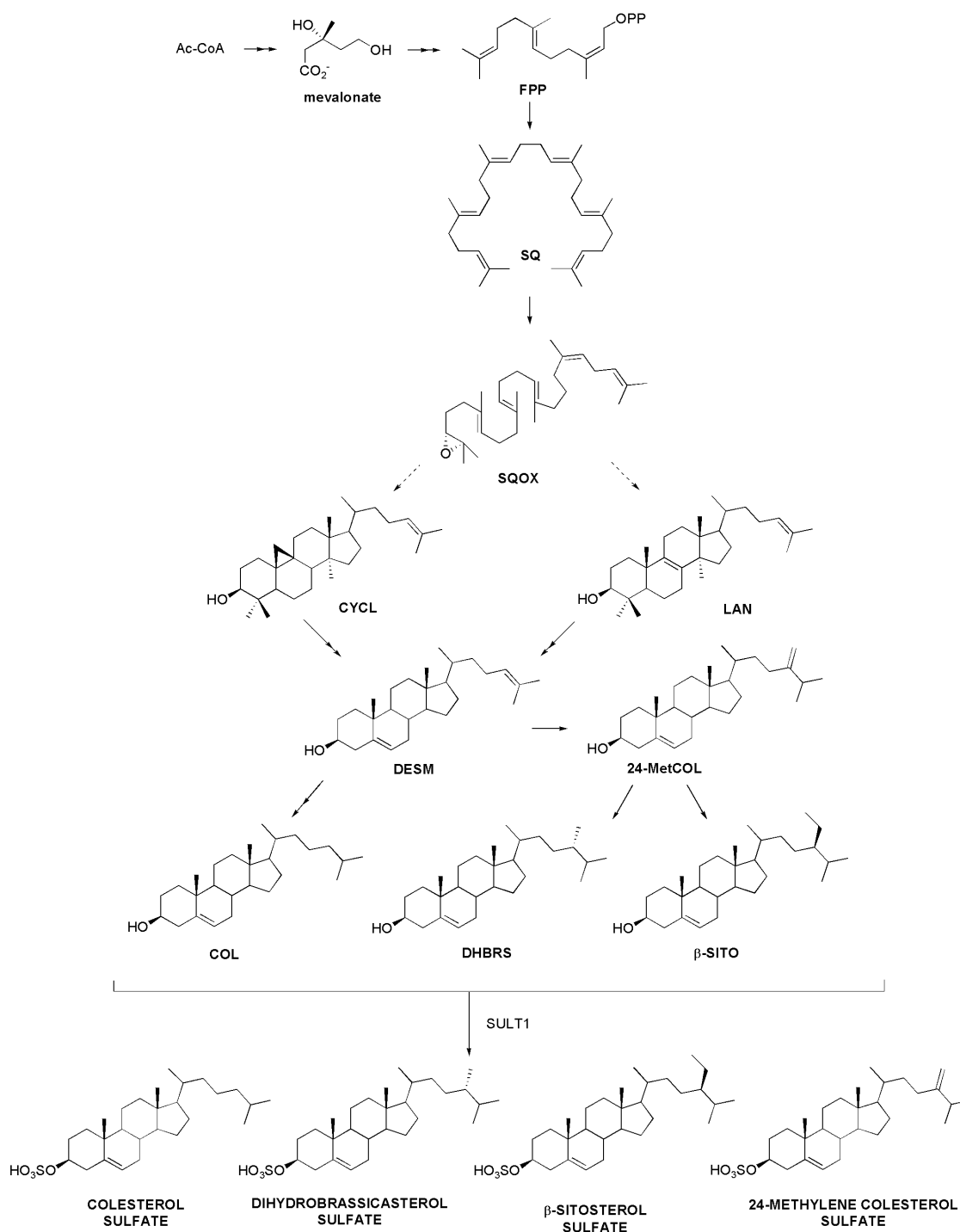


**Figure 7.1.** Proposed biosynthesis of sulfated sterols across diatom lineage. Acetyl-CoA (Ac-CoA) is converted to farnesyl pyrophosphate (FPP) by mevalonate pathway. FPP is converted into squalene (SQ). Squalene is oxidized to oxidosqualene (SQOX) that is the substrate of various oxidosqualene cyclases, which produces lanosterol (LAN) or cycloartenol (CYCL). This biosynthetic step is not yet clear, but our results suggest that the following sterols precursor is desmosterol (DESM) from what cholesterol (COL) and 24-methylene cholesterol are synthesized (24-MetCOL). 24-MetCOL is the precursor of dihydrobrassicasterol (DHBRs) and  $\beta$ -sitosterol ( $\beta$ -SITO). The last biosynthetic step is catalyzed by a sulfotransferase (SULT 1) that converts sterols in their sulfated derivatives.

Last biosynthetic step to sulfated sterols is sulfonation, that was studied by biochemical and molecular approaches. The enzyme that catalyzes the sulfoconjugation of sterols is part of a superfamily of cytosolic sulfotransferases (SULTs). Specific inhibitors of diatoms SULTs are not reported, thus different classes of human sulfotransferase inhibitors were tested on *S. marinoi* and *C. cryptica* cells. Among the seven different compound types, only quercetin reduced levels of sulfated sterols in both diatoms. According to the role of signal in PCD, biochemical inhibition of this class of molecules affected positively diatom growth and induced increase of cell density, extension of the stationary phase and morphological improvement of diatom cells. Furthermore, analysis of DNA expression of the major SULTs in the transcripts of *S. marinoi* identified *SmSulf1* gene as key gene for the sulfonation reaction in this species.

In conclusion, this thesis has identified for the first time the role of secondary metabolites, namely sulfated sterols, with pro apoptotic effects in diatoms. In addition to the different tools that have been developed to carry out this study, the major outcome of this work concern the first establishment of a cellular mechanism to control Programmed Cell Death in the lineage and the first direct elucidation of the biosynthesis in these organisms.

## 7.1. Further developments

In the latest years, algae cultivation has attracted enormous interest of the scientific and industrial communities for the potential application of these organisms as CO<sub>2</sub> mitigation system and as source of fuels and products. In algaculture the goal is to trigger and sustain the initial proliferative growth for as long as possible – the notion of ‘bloom sustainability’. However, due to the ‘open’ nature of artificial systems, cultivated microalgae are still faced with typical cellular cycle, availability of light and nutrients, grazing and viral infection. Artificial cultures of microalgae therefore must be viewed as an intensified yet managed mesocosm representative of open sea conditions - essentially a miniature ocean sharing common processes and problems. This work of Thesis has concerned the role of sulfated sterols as cellular signals involved in the physiological control of growth and development of diatoms cells. Yet, in view of the parallelism of the ecological parameters that rule natural and artificial systems, this activity has a potential use as tool to intensify massive cultivation of algae and/or induce higher yield of biomass or promote accumulation of specific products (e.g. triglycerides). Thus, the chemical signaling that is mediated by sulfated sterols is no longer only of ecological relevance but it also becomes central for biotechnological application. According to this presupposition, the effect of quercetin on biomass production and lipid accumulation in *C. cryptica*, as reported in Section 6, are extremely encouraging.

This centric diatom has been already considered as a potential model organism for biofuel production because of the capacity to grow quickly and to accumulate large amount of triglycerides (Roessler, 1988), with consistent productivity levels of 20 g·m<sup>-2</sup> d<sup>-1</sup> in outdoor ponds (Huesemann et al., 2009). Recently, *C. cryptica* has been selected as candidate species for biofuel production on large scale because of an oil

concentration (above 70 % of organic extract) that was much higher of 31 other species of diatoms and green microalgae (*d'Ippolito et al, 2015*). Furthermore, *C. cryptica* can grow heterotrophically, which offers a further biotechnological advantage. Figure 9.2 summarizes the lipid composition of *C. cryptica* from dark cultures on glucose as organic source. Analyses were carried out according to *Nuzzo et al. (2014)*.

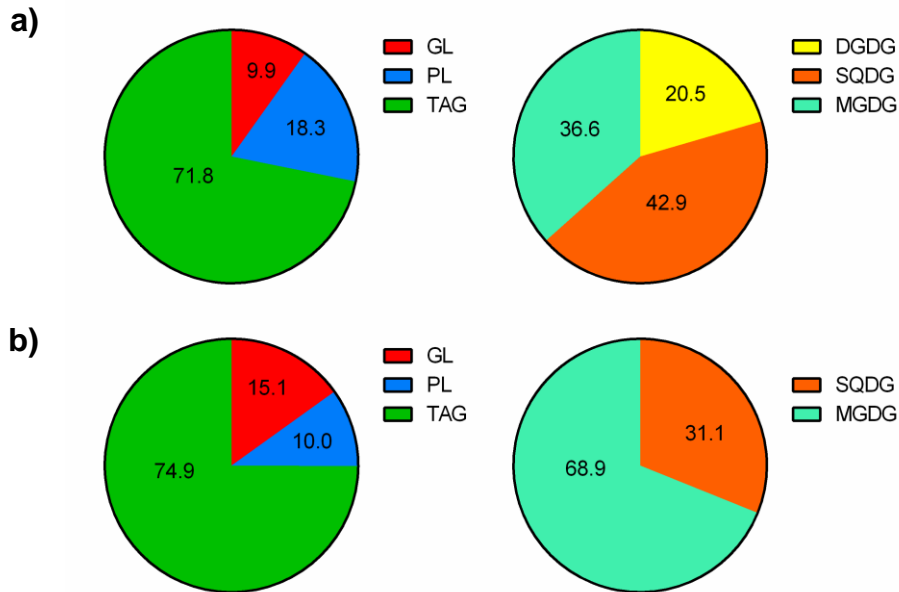


**Figure 7.1.** *C. cryptica* lipid composition obtained by NMR-ERETIC analysis according to *Nuzzo et al. (2014)* in photoautotrophic conditions (a) and dark growth on glucose as organic source (b). TAG= tryglicerides; GL= glycolipids; PL= phospholipids. MGDG= monogalactosyldiacylglycerols; DGDG= digalactosyldiacylglycerolstriacylglycerols; SQDG= sulfoquinovosyldiacylglycerols. Data are expressed as percentage.

The data showed that heterotrophic conditions stimulate glycolipids and triglycerides to detriment of phospholipids. In particular, MGDG almost doubled, while decreased the levels of SQDG and disappeared the component of DGDG. Galactolipids are the predominant lipids in thylakoid membranes and indispensable for photosynthesis. The accumulation of MGDG and the absence of DGDG are probably related to the reduction of the photosynthesis under heterotrophic growth. Finally, in comparison with standard

photoautotrophic conditions, the fatty acid fraction of *C. cryptica* was enriched in palmitic acid (C<sub>16:0</sub>), palmitoleic acid (C<sub>16:1</sub>) and eicosapentenoic acid (C<sub>20:5</sub>) (Table 9.2). Together with the increase in biomass reported in Section 5 and 6, this change in lipid profile under heterotrophic cultures is very promising in view of biotechnological applications and, for the first time, give concrete support to the possibility to manipulate microalgal growth by chemical methods.

**Table 9.2** Fatty acids distribution (%) in the lipid classes in *C. cryptica* extracts growth in standard conditions (Control) and growth on heterotrophic conditions (Dark): total extract (EXT), glycolipids (GL), triglycerides (TAG) and phospholipids (PL). The results are expressed as mean percentage of a triplicate with standard deviation  $\leq 1$  %.

%	EXT		GL		TAG		PL	
	<i>Control</i>	<i>Dark</i>	<i>Control</i>	<i>Dark</i>	<i>Control</i>	<i>Dark</i>	<i>Control</i>	<i>Dark</i>
C14:0	10,6	0,49	3,2	0	10,1	1,48	1,4	0
C16:3	4,6	0,72	8,9	0	3,8	2,16	4,2	0
C16:1	28,3	65,31	43,2	84,39	36,6	44,19	33,8	67,35
C16:0	31,4	18,39	25	15,61	27,1	25,74	32	13,81
C18:3	3,8	0	2,4	0	4	0	2,3	0
C18:2	1,5	0	0,5	0	1,2	0	1,4	0
C18:1	1,6	0,96	2,7	0	1,2	2,87	8,2	0
C18:0	0,8	0,24	0,4	0	0,3	0,72	1,1	0
C20:5	16,4	13,89	13,8	0	15,4	22,83	15,7	18,84

## 8. Experimental section

### 8.1.1 Microalgae cultures

Stock cultures of the diatom *Skeletonema marinoi* (CCMP 2092), *Pseudonitzschia multistriata* (VF235), *Pseudonitzschia arenysensis* (B758), *Thalassiosira weissflogii* (P09), *Cyclotella criptica* (CCMP 331) and *Phaeodactylum tricornutum* purchased from Bigelow Laboratories, were maintained in f/2 medium (Guillard & Ryther, 1962) in batch culture using a week transfer cycle. In particular the medium consists of sea water supplemented with 1 mL L<sup>-1</sup> of following stock solutions (g L<sup>-1</sup>): Na<sub>2</sub>SiO<sub>3</sub> • 9H<sub>2</sub>O 30.0, NaNO<sub>3</sub> 75.0, NaH<sub>2</sub>PO<sub>4</sub> • H<sub>2</sub>O 5.0. Then are added 1 mL L<sup>-1</sup> of a vitamin solution containing biotin (0.5 mg L<sup>-1</sup>), B12 vitamin (0.5 mg L<sup>-1</sup>) and tiamin-HCl (100 mg L<sup>-1</sup>), and 1 mL L<sup>-1</sup> of a trace metal solution containing (g L<sup>-1</sup>): Na<sub>2</sub>EDTA 4.36, FeCl<sub>3</sub> • 6H<sub>2</sub>O 3.15, MnCl<sub>2</sub> • 4H<sub>2</sub>O 0.18, CuSO<sub>4</sub> • 5H<sub>2</sub>O 0.01, ZnSO<sub>4</sub> • 7H<sub>2</sub>O 0.022, CoCl<sub>2</sub> • 6H<sub>2</sub>O 0.01, NaMoO<sub>4</sub> • 2H<sub>2</sub>O 0.006.

For experiments, diatoms were grown in 10 L-sterile carboy in prefiltered sterile (0.22 µm) f/2 medium at an initial concentration of 1·10<sup>4</sup> cells mL<sup>-1</sup>. The cultures were maintained in a growth chamber at 20 ± 2°C on a 14:10 light:dark cycle under a photon flux density of 100 µmol quanta m<sup>-2</sup> sec<sup>-1</sup>. After the experiment was repeated in triplicates, to accumulate a large quantity of microalgal biomass, *S. marinoi* was cultivated (n = 4) under fed-batch condition in a 40 L-photobioreactor with an inoculum 5% (v/v) and f/2 algae culture medium. The cultures (initial concentration of 6· 10<sup>4</sup> cells mL<sup>-1</sup>) were carried out over a period of 7 days under a photon flux density of 350-400 µmol quanta m<sup>-2</sup> sec<sup>-1</sup> on a 14:10 h light: dark cycle in a room with temperature control maintained at 20 ± 3 °C. The culture was bubbled with CO<sub>2</sub> 0.04% in air (v/v). The nutrients of f/2 culture medium were added every day. The pH of medium was first automatically adjusted in the range of 7.5–8.5 by feeding of Mops 50 mM, then

bubbling with CO<sub>2</sub> 5% in air (v/v) for 8 hours per day. The cells were counted and monitored every day by microscopic observation (AxioVertA1; Carl Zeiss; magnification of 20 and 40 x), counting by using a Bürker chamber. This chamber consists of nine squares delimited by three adjacent lines and has a total volume of 0.1 mm<sup>3</sup> (10<sup>-4</sup> cm<sup>3</sup> = 1 mL); the concentration of cells per milliliter (cells / mL) was determined by the following calculation:

$$\text{Cells/ mL} = \text{average count per square} \cdot \text{dilution factor} \cdot 10^4$$

Cells were harvested by centrifugation at 3600 rpm for 10 minutes at 12 °C using a swing-out rotor (Allegra X12R - Beckman Coulter). For all sterol sulfates qualitative analysis culture in 1-L carboy were performed for all species in the same conditions. All pellets for quantitative analysis were then frozen in liquid nitrogen and stored at -80° C until analysis.

#### *8.1.2. C. cryptica cultures for biosynthesis experiment*

Culture medium was supplemented with antibiotics to obtain axenic cultures according to published protocols (Kobayashi et al. 2003; Bruckner & Kroth 2009). In particular we supplemented liquid culture medium with 1.5 mg mL<sup>-1</sup> penicillin, 1.0 mg mL<sup>-1</sup> streptomycin, 1.0 mg mL<sup>-1</sup> ampicillin and 0.5 mg mL<sup>-1</sup> kanamycin.

For experiments, diatoms were grown in 1 L-sterile culture flasks (TPP25-300 cm<sup>2</sup>) in prefiltered sterile (0.22 µm) f/2 medium supplemented with antibiotics and 2 g L<sup>-1</sup> of glucose or 1-<sup>13</sup>C-glucose (Sigma Aldrich) (in the first experiment we used <sup>13</sup>C<sub>6</sub> glucose) at an initial concentration of 1·10<sup>4</sup> cells mL<sup>-1</sup>. The culture flasks were ventilated with filter screw caps. Diatoms were incubated in the dark in a growth chamber at 20 ± 2°C in constant gentle agitation. Cells were harvested by centrifugation at 3750 rpm for 10

minutes at 12 °C using a swing-out rotor. All pellets were frozen in liquid nitrogen and stored at -80° C until analysis.

### 8.1.3. *S. marinoi* and *C. cryptica* cultures for experiment with sulfotransferase inhibitor

Cultures in 2-L carboy in triplicates were set up as described in section 8.1.1 or supplemented with 20 µM quercetin (Sigma Aldrich). For quantitation of sterol sulfates and RNA analysis in each analysis point pellets from 0.2 L of each culture were recovered by centrifugation at 3750 rpm for 10 minutes at 12°C using a swing-out rotor. All pellets were frozen in liquid nitrogen and stored at -80° C until analysis.

### 8.2. *Extraction and fractionation of S. marinoi* biomass

The cell pellets were collected in 50 mL Falcon tubes and immediately extracted in boiling methanol (Jüttner, 2001; Cutignano et al., 2006). The resulting suspension was centrifuged at 3750 rpm for 5 minutes at 5° C. After removing the methanol extract the residual pellet was successively extracted two more times with methanol. The combined methanol extracts were evaporated under reduced pressure with a rotary evaporator (Buchi, Rotavapor R-200).

The extracts were then fractionated according to the protocol reported in table 8.1 using a solid phase extraction method based on polystyrene–divinyl benzene columns (CHROMABOND® HR-X), a reversed stationary phase with a higher capacity for polar compounds than C18 because of its higher carbon percentage used for desalting and adsorption–elution of natural products from aqueous extracts (Dittmar et al., 2008). About 15.3 ±5 mg of each extract (60 ±10 mg of extracts/g of resin) were suspended in 1 mL of distilled water and sonicated for few seconds in an ultrasonic bath working at 104 MHz before loading them on a CHROMABOND® HR-X column (column

volume=3 mL; resin=200 mg). According to the manufacturers' guidelines, the cartridge was rinsed with 1 cartridge filling of methanol and 1 cartridge filling of water immediately before use. After the sample loading, salts were immediately eluted with 3 mL of distilled water. Polar compounds and then the increasingly apolar compounds were eluted with 12 mL of water, 9 mL of methanol: water (1:1, v/v), 9 mL of acetonitrile: water (7:3, v/v), 6 mL of acetonitrile and 6 mL of dichloromethane: methanol (9:1, v/v), respectively.

**Table 8.1.** Protocol scheme of fractionation of organic extracts on HR-X resin. The volumes are referred to a column volume of 3 mL and 200 mg of HR-X resin

<b>I. Sample preparation:</b>	<b>II. Column equilibration:</b>	<b>III. Elution solvents:</b>
Add 1 mL of distilled H <sub>2</sub> O	3 mL CH <sub>3</sub> OH	12 mL H <sub>2</sub> O
Sonicate	3 mL H <sub>2</sub> O	9 mL CH <sub>3</sub> OH:H <sub>2</sub> O (1:1 v/v)
		9 mL CH <sub>3</sub> CN:H <sub>2</sub> O (7:3 v/v)
		6 mL CH <sub>3</sub> CN
		6 mL CH <sub>2</sub> Cl <sub>2</sub> :CH <sub>3</sub> OH (9:1 v/v)

The resulting fractions were monitored by thin layer chromatography (TLC) on 0.2-mm silica-gel-coated sheets (Merck, Germany) developed with petroleum ether: ethylic ether (6:4, v/v), chloroform: methanol (95:5, v/v) and chloroform: methanol: water (65:25:4, v/v/v). Spots were detected by cerium sulfate (Ce (SO<sub>4</sub>)<sub>2</sub>), a general stain for TLC, or Dittmer reagent for determination of phospholipid (this reagent would give a blue spot to indicate the presence of phosphate) and  $\alpha$ - naphthol reagent for glycolipid or carbohydrates determination (this reagent would give a red- or purple-colored spot to indicate the presence of carbohydrate). Cholesterol is used as reference. Each fraction was also analyzed by NMR and LC-MS.

### 8.3. Purification and characterization of sterol sulfates

The bioactive fraction was purified by HPLC (Jasco LC-2000) on a reversed phase semipreparative column (Phenomenex, C-18 Luna 10 x 250 mm, 100 Å) using a linear CH<sub>3</sub>OH/H<sub>2</sub>O gradient (Table 8.2) with a column flow of 3 mL min<sup>-1</sup>. The only active fraction obtained was finally obtained as pure compound on analytical reversed phase column (Phenomenex, C-18 Luna 4.6 x 250 mm, 100 Å) by using a linear CH<sub>3</sub>OH/H<sub>2</sub>O gradient (Table 8.3) with 1 mL min<sup>-1</sup> flow. One-fifth of the column flow was channeled by a post-column split to the Evaporative Light Scattering Detector (evaporation temperature 45°C; nebulization temperature 60°C, N<sub>2</sub> flow 1.4 mL min<sup>-1</sup>). All HPLC analyses were performed on a JASCO system (PU-2089 Plus-Quaternary gradient pump equipped with a Jasco MD-2018 Plus photodiode array detector).

**Table 8.2.** Solvent system and standard gradient employed for HPLC fractionation

<i>Time</i> (min)	<i>Methanol</i> (%)	<i>Water</i> (%)
0	80	20
20	80	20
30	100	0
40	100	0

**Table 8.3.** Solvent system and standard gradient employed for analytical HPLC

<i>Time</i> (min)	<i>Methanol</i> (%)	<i>Water</i> (%)
0	85	15
10	85	15
40	90	10
50	100	0
60	100	0

Once individuate the class of molecules responsible for the bioactivity, to accumulate larger amounts for the characterization of minor compounds, the first step of fractionation by HPLC was replaced by preparative, centrifugally accelerated, radial, thin-layer chromatography (Harrison Research Chromatrotron, model 7924T) (Figure 8.1).  $100 \pm 10$  mg of HR-X fractions were diluted in  $\text{CHCl}_3$  and loaded on Chromatroton and elution was carried out by increasing gradient of MeOH in  $\text{CHCl}_3$ . The resulting fractions were monitored by TLC on 0.2-mm aluminum-coated sheets (Merck, Germany) developed with  $\text{CHCl}_3:\text{CH}_3\text{OH}:\text{H}_2\text{O}$  (65:25:4; v/v/v).

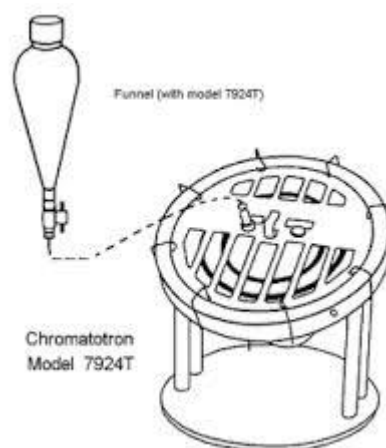


**Figure 8.1.** Schematization of a Chromatrotron Model 7924T

Pure compounds were analyzed by NMR and MS analysis. For NMR experiments samples were dissolved in 700  $\mu\text{L}$   $\text{CD}_3\text{OD}$  and analysis were performed on a DRX 600 Bruker spectrometer, using an inverse TCI CryoProbe fitted with a gradient along the Z-axis. A dual probe ( $^1\text{H}/^{13}\text{C}$ ) was used. LC-MS analysis was performed on a micro-Quadrupole time-of-flight (micro-QToF) Mass spectrometer (Water Spa, Milan, Italy) equipped with elettrospray ionization (ESI) source (negative mode) and coupled with a Waters Alliance HPLC system. For ESI-QToF-MS/MS experiments, argon was used as collision gas at a pressure of 22 mbar.

#### 8.4.1. *Biological assay*

Methanolic extracts and fractions obtained as described above were tested in 24 well plates at different concentrations of *S. marinoi* cells (from  $6 \cdot 10^4$  to  $8 \cdot 10^5$  cells mL<sup>-1</sup>) and products. All the tests were performed in duplicate twice. In two wells the extract was not inoculated and in two wells were inoculated only 10  $\mu$ L of methanol to exclude that the observed activity was due to the solvent in which the samples were diluted or to a non-optimal physiological state of cells used for the assays. The cells were counted and monitored at 24 and 48 hours by microscopic observation (AxioVertA1; Carl Zeiss; magnification of 20 and 40 x), counting by using a Bürker chamber.

#### 8.4.2. *Chlorophyll a fluorescence measurement*

Cellular growth was also monitored by chlorophyll *a* fluorescence intensity that increases proportionally to cellular density (*Veldhuis & Kraay, 2000*). Chlorophyll *a* fluorescence was detected using a fluorometer (Jasco FP-8300) equipped with a microplate reader with a 451/5 nm excitation wavelength and a 679/5 nm emission wavelength.

#### 8.4.3. *Cells vitality measurement*

Cells vitality was monitored by using fluorescein diacetate [3',6'-diacetylfluorescein (FDA)] fluorescence according to the staining procedure of *Lage et al. (2001)*. Optimal concentration and time of incubation were assessed experimentally. Briefly, a stock solution of fluorescein diacetate (FDA, Sigma Aldrich) (5 mg mL<sup>-1</sup> in DMSO) was prepared and stored at 4°C. Just before use, each aliquot of the stock solution was diluted 40-fold into cold 3.2% NaCl, pH 7.9, kept on ice in the dark, and 25  $\mu$ L were subsequently injected in 1 mL of cell culture (FDA final concentration 7.5  $\mu$ M).

Samples were incubated in the dark for 10 min and analyzed with an AxioVertA1 (Carl Zeiss) epifluorescence microscopy (magnification of 40 and 100 x). The green cells were positive. The FDA fluorescence was also estimated using the fluorometer (Jasco FP-8300) with a 472/10 nm excitation wavelength and a 512/10 nm emission wavelength.

#### 8.4.4. Sulfotransferase inhibitor assay

Different molecules already known as *in vivo* and *in vitro* inhibitors of human SULTs (Figure 6.4) were tested with 1 mL of the exponentially growing *S. marinoi* ( $6 \cdot 10^4$  cells  $\text{mL}^{-1}$ ) in 24 well plates. Experiments with *C. cryptica* cells were performed at concentration of  $1 \cdot 10^4$  cells  $\text{mL}^{-1}$ . Each compound was assessed between 0.25 and 40  $\mu\text{M}$  in 10  $\mu\text{L}$  of DMSO. All the tests were performed in duplicate twice. DMSO was used as control (10  $\mu\text{L}$ ). Plates were incubated under the previously mentioned conditions (section 8.4.1). The cells were counted and monitored for 7 days by microscopic observation (AxioVertA1; Carl Zeiss; magnification of 20 and 40 x). Cells were counted by a Bürker chamber and chlorophyll *a* fluorescence was measured as described above (section 8.1.1 and 8.4.2).

#### 8.5. hROS detection

*S. marinoi* cells from 100 mL of culture were harvested at 3600 rpm at 12°C for 10 min. The cells were suspended in 10 mL of f/2 and divided in ten aliquots: one aliquot was used as control whereas the others were loaded with HPF /H<sub>2</sub>O (sea water) 1:8 (30  $\mu\text{L}$ ). After 30 min of dark incubation, the samples were centrifuged and washed two times with f/2. Two aliquots are then incubated with 200  $\mu\text{M}$  of H<sub>2</sub>O<sub>2</sub> as positive control to verify the reliability of HPF as a probe for hROS detection in *Skeletonema* cells; two aliquots are untreated and the others were incubate with f/2 containing 50, 100 and 200

$\mu\text{g mL}^{-1}$  of cholesterol sulfate. All tests were carried out in 24-wells plates. To quantify hROS accumulation, fluorescence was measured by a Jasco (FP-8300) Fluorescence Microplate Reader (excitation 488/2.5 nm, emission 515/2.5 nm) (Setsukinai et al., 2003) at 1, 3, 4 hours; as blank we considered the  $t_0$  value. The fluorescence was also monitored microscopically by using a 530/30 BP emission filter with an AxioVertA1 (Carl Zeiss) epifluorescence microscopy (magnification of 40 and 100 x).

#### 8.6. NO measurements

For NO measurements, *S. marinoi* cells derived from 100 mL of culture (about  $6 \cdot 10^5$  cell  $\text{mL}^{-1}$ ) were harvested via centrifugation, were suspended in 10 mL f/2 and divided in ten aliquots in a 24-wells plate. NO generation was measured by fluorometry using the NO-sensitive dye 4-amino-5-methylamino- 2',7'- difluorescein diacetate (DAF-FM; Sigma Aldrich). Cells were incubated in the dark with 10  $\mu\text{M}$  DAF-FM (Itoh et al., 2000) for 60 min followed by two washing steps (incubation for 30 min after the first wash to remove the excess of probe). Two aliquots were then used as controls whereas 4 aliquots were loaded with two NO donors (0.5 mM), diethylamine nitric oxide (DEANO) and sodium nitroprusside (SNP), as positive controls to verify the reliability of DAF-FM as a probe for NO detection in *S. marinoi* cells. The others aliquots were incubated in f/2 containing 50 e 100  $\mu\text{g mL}^{-1}$  of cholesteryl sulfate (this compound has been used in high concentration in order to detect a short time effect). To quantify NO accumulation, DAF-FM fluorescence was measured by a Jasco (FP-8300) Fluorescence Microplate Reader (excitation 485/30 nm, emission 530/30 nm) at 1, 3, 4 hours; as blank we considered the  $t_0$  value. The fluorescence was also monitored microscopically by using a 530/30 BP emission filter with an AxioVertA1 (Carl Zeiss) epifluorescence microscopy (magnification of 40 and 100 x).

### 8.7. Annexin V-FITC assay

*S. marinoi* cells ( $1 \cdot 10^6$  cell mL<sup>-1</sup>) were harvested via centrifugation after 2 hours of incubation with 5  $\mu$ M cholesterol sulfate, suspended in 100  $\mu$ L of 1x Annexin binding buffer and stained with 10  $\mu$ L of Annexin V-FITC (Sigma Aldrich; Italy) for 20 minutes at room temperature in the dark. After being stained, cells were pelleted via centrifugation, washed twice with 500  $\mu$ L of PBS and suspended in 200  $\mu$ L of sea water with 2% of formaldehyde. Stained cell were visualized and photographed by epifluorescence microscopy (Carl Zeiss, magnification of 100 x) using a 515/565 BP emission filter and a coupled-device camera interfaced with Axio Vision acquisition/image analysis software (version 4.8). An unstained control was used for each sample. All assays were repeated in triplicate.

### 8.8. TUNEL assay

*S. marinoi* cells were washed once in PBS, fixed in 2% formaldehyde for 20 minutes and permeabilized with 3% Triton X-100 (Sigma Aldrich) for 15 minutes in ice. The free 3'-OH of DNA strand breaks produced during the process of apoptosis were labeled with green- fluorescing fluorescein labels incorporated in modified nucleotide polymers in an enzymatic reaction.

The complete protocol consists of three phases that can be described as follows:

1) Fixation of cells: 10 mL of *S. marinoi* cultures at a concentration of about  $1 \cdot 10^6$  cells mL<sup>-1</sup> for each sample were centrifuged and resuspended in 1 mL of filtered sea water with 4% formalin. The cells were left at 4 ° C 30 minutes as reported for *Thalassiosira weissflogii* (Casotti et al., 2005).

2) Permeabilization of external cell membranes: cells are centrifuged (each sample now has the concentration of  $1 \cdot 10^7$  cell mL<sup>-1</sup> as determined in the different protocols

reported) and washed with PBS at pH 7.5 containing 5 mM MgCl<sub>2</sub>, which corresponds to the concentration required for maximum activity of Tdt enzyme and DNase enzyme used as a positive control. Then each sample is suspended in 200 µL of permeabilizing solution: 3% Triton X-100 in 0.1% sodium citrate on ice 15 minutes. Cells were again washed with PBS and two samples are used as positive control: these are incubated 10 minutes with 500 µL of a solution of DNase 2000 U / mL (Roche) in PBS containing 1 mg mL<sup>-1</sup> of BSA at room temperature. For the negative control sample, we assay cells from culture that were not incubated with cholesterol sulfate. Subsequently cells were pelleted and washed with PBS.

3) Incubation with the reaction mix (enzyme + labeled nucleotides in reaction buffer): cells were labeled according to the manufacturer's instructions (Roche Diagnostics GmbH), analyzed by epifluorescence microscopy (Carl Zeiss) using a 515/565 BP (for only green fluorescence), a 525/50 BP (for green and red fluorescence) and a LP615 (for only red fluorescence) emission filter and a coupled-device camera interfaced with Axio Vision acquisition/image analysis software (version 4.8). All assays were repeated in triplicate.

#### *8.9. Extraction procedure for quantitative analysis of sterol sulfates*

All samples were extracted with methanol (5 mL g<sup>-1</sup> of wet weight) and homogenized. The resulting suspension was centrifuged at 3750 rpm for 5 minutes at 5° C. After removing the methanol extract the residual pellet was successively extracted with methanol and two times with chloroform: methanol (2:1, v/v; 5 mL g<sup>-1</sup> of wet weight). Centrifugation and shaking was repeated after each extraction step. The combined organic extracts were evaporated under reduced pressure with a rotary evaporator (Buchi, Rotavapor R-200).

### *8.10. Extraction procedure for lipid analysis*

Frozen pellets were lyophilized in a Savan Micro Modulyo freeze dryer (Thermo Scientific, Austin, TX, USA). Microalgal extracts were prepared according to the modified Folch method (1957) according to the following protocol (solvent volumes are referred to 50 mg of dry weight):

1. Cover dry sample with 1 mL methanol and kept at 4 °C for 1 min.
2. Add 2 mL chloroform.
3. Homogenized and incubate with shaking for 5 min.
4. Centrifuge (3750 rpm) for 5 min at room temperature.
5. Transfer supernatant to a fresh tube.
6. Suspend solid residue in 2 mL chloroform: methanol (2:1 v/v) and incubate with shaking for 2 min.
7. Repeat steps 4 and 5.
8. To combined supernatants from steps 5 and 7, add 1 mL deionized water.
9. Vortex, centrifuge and discard the upper phase.
10. Recover lower phase (organic extract) with a Pasteur pipette and transfer to a glass rotary evaporator flask.
11. Remove solvent and dry sample under vacuum at room temperature.

For qualitative and quantitative analysis of lipid composition 20 µg ( $24.4 \cdot 10^{-3}$  µmol) internal standard [(4-chlorophenyl)-trihexadecylsilane] for each mg of dry sample was added during the extraction procedure. The organic extracts were dissolved in 700 µL

CDCl<sub>3</sub>/CD<sub>3</sub>OD 1:1 (v/v) and transferred to the 5-mm NMR tube for <sup>1</sup>H NMR analysis. Chemical shift was referred to CHD<sub>2</sub>OD signal at δ 3.34. Quantitative assessment was established by the ERETIC method in agreement with *Akoka et al. (1999)* by using a new method developed by us for analysis of lipid composition of microalgal extracts (*Nuzzo et al. 2013*). The ERETIC signal was calibrated on the doublet signal at δ 7.40 of 4-chlorophenyl-trihexadecylsilane (2.20 μmol in 700 μL CDCl<sub>3</sub>/CD<sub>3</sub>OD 1:1). Peak integration, ERETIC measurements and spectrum calibration were obtained by the specific subroutines of Bruker Top-Spin 3.1 program. Spectra were acquired with 14 ppm of spectral width (8417.5 Hz), 32 K of time domain data points, 90° pulse, 32 K spectrum size, and processed with 0.6 Hz of line broadening for the exponential decay function.

#### *8.11. Isolation and analysis of sterols from S. marinoi and C. cryptica*

The organic extracts were methylated with diazomethane in diethyl ether (0.4 mL *per* 10 mg extract) for 1 h at room temperature to convert free fatty acids in methyl esters. After removing the organic solvent under N<sub>2</sub>, the resulting methylated extract was used for a first step of sterols purification by silica gel column. The methylated extracts (40 ± 10 mg) were diluted in the minimal volume of dichloromethane and loaded on silica gel column (100 mg silica gel/ mg fraction). Elution was achieved by an increasing gradient of diethyl ether in petroleum ether. Purification (Figure 5.6) starts with petroleum ether as eluent (fraction 1) to increasing volume ratio of ethylic ether: petroleum ether: ethylic ether (95:5; v/v) (fractions 2), petroleum ether: ethylic ether (9:1; v/v) (fractions 3-6), petroleum ether: ethylic ether (85:15; v/v) (fractions 7-8), petroleum ether: ethylic ether (80:20; v/v) (fraction 12), and chloroform (fraction 9), acetone: methanol (9:1; v/v) (fraction 10), chloroform: methanol (2:1; v/v) (fraction 11), methanol (fraction 13). Pure fractions of sterol mixtures (fractions 7-8) were obtained in petroleum ether: ethylic

ether 85:15 (v/v). Fractions 3 are enriched of triglycerides. Product elution was monitored by SiO<sub>2</sub>-TLC on 0.2-mm aluminum-coated sheets (Merck, Germany) developed with petroleum ether: ethylic ether (1:1; v/v). Sterols fractions were acetylated with Ac<sub>2</sub>O (100 μL/ 0.5 mg fraction) in dry pyridine (500 μL/0.5 mg fraction) under magnetic stirring overnight at room temperature. After removal of the organic solvent under nitrogen stream, sterols analyses were carried out using GC-MS with an ion-trap MS instrument in EI mode (70 eV) connected with a GC system (Thermo Focus GC Polaris Q), by using a 5% diphenyl- polysiloxane column (OV-5 column) and helium as gas carrier. Elution of acetylated sterols required an isocratic temperature method at 300°C for 20 min. Samples dissolved in methanol with a drop of THF were directly injected (2 μL) in split mode (1:10), with a blank window of 3 minutes, inlet temperature of 300° C, transfer line set at 310° C and ion source temperature of 300° C (*Laakso, 2005*). We identified the mass spectra of sterols in according to literature (*Rampen et al., 2010; Nusaibah et al., 2011*). [25,26,26,26,27,27,27-D<sub>7</sub>]-Cholesterol- (C/D/N Isotopes) was used as internal standard.

For NMR analysis sterols fraction were dissolved in 700 μL CDCl<sub>3</sub> and transferred to the 5-mm NMR tube. <sup>1</sup>H and <sup>13</sup>C NMR spectra were recorded on Bruker DRX 600 spectrometer equipped with an inverse TCI CryoProbe.

Each sterol was then purified by an RP-HPLC column (C18-Luna, Phenomenex, 5 μm 100A 250 × 10 mm) by an isocratic gradient of methanol: acetonitrile: water: isopropanol: acetone with a column flow of 1 mL min<sup>-1</sup> monitoring UV absorbance at 210 nm. HPLC analyses have been performed on a Jasco system (PU-2089 Plus-Quaternary gradient pump equipped with a Jasco MD-2018 Plus photodiode array detector). Pure compounds were dissolved in 700 μL CDCl<sub>3</sub> and transferred to the 5-

mm NMR tube for  $^1\text{H}$  and  $^{13}\text{C}$  NMR analysis. All  $^{13}\text{C}$  NMR analyses were recorded with a relaxation delay of 6 seconds for a nearly complete longitudinal relaxation.

#### 8.12. Sterol sulfates quantitation

The distribution and the amount of the three StS (**1-3**) was estimated in the pellets along a growth curve of *S. marinoi* and *C. cryptica* [25,26,26,26,27,27,27-D<sub>7</sub>]-Cholesterol-sulfate (C/D/N Isotopes) was used as standard for LC-MS calibration curve. All calibration consisted of blank and standard samples in triplicates at concentrations ranging from 1 to 20  $\mu\text{g mL}^{-1}$ . Each concentration point was prepared by successive dilution of a bulk MeOH solution containing 20  $\mu\text{g mL}^{-1}$  of standard. The bulk samples were stored at  $-20^\circ\text{C}$ . The calibration curve was constructed by plotting peak areas of standard against concentrations (Figure 8.2). The standard and sterol sulfates quantifications were carried out by Waters QUANLINK software according to the manufacturer's instructions.

The extracts were dissolved in methanol to a final concentration of  $1\mu\text{g }\mu\text{L}^{-1}$  and directly analyzed by LC-MS. The MS method was based on a micro-QToF instrument equipped with an ESI source in negative ion mode (scan range 150- 600  $m/z$ ). For ESI-QToF-MS/MS experiments, argon was used as collision gas at a pressure of 22 mbar. Chromatographic analysis was carried out on a reverse phase column (Phenomenex, C-8 Kromasil 4.6 x 250 mm, 100 Å) using a linear MeOH: H<sub>2</sub>O gradient (Table 8.4) with a column flow of  $1\text{ mL min}^{-1}$ . One-tenth of the column flow was channelled by a post-column split to the ESI (Q-ToF). Measurements were in triplicate.

**Table 8.4.** Solvent system and standard gradient employed for analytical LC-MS

<i>Time</i> (min)	<i>Methanol</i> (%)	<i>Water</i> (%)
0	81	19
15	81	19
28	90	10
35	100	0
50	100	0

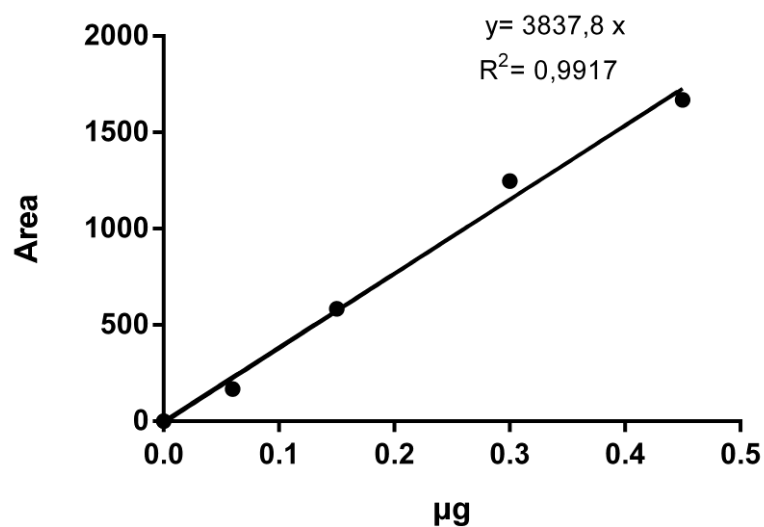


**Figure 8.2.** LC-MS calibration curve of cholesterol-25,26,26,26,27,27,27-D7 sulfate in the range 0-0.5 µg injected in 20 µL of methanol.

The above method was optimized for quantification of sterol sulfates along *the* growth curve of *C. cryptica*. Analysis were performed by QExactive Hybrid Quadrupole-Orbitrap mass spectrometer (Thermo Scientific) (coupling a quadrupole as a front-end mass filter to an Orbitrap™ mass analyzer) with an ESI source in negative ion mode (scan range 500- 600 *m/z*) coupled with a HPLC Infinity 1290 apparatus (Agilent

Technologies) getting high-resolution mass spectra. Chromatographic analysis was carried out on a reverse phase column (Phenomenex, C-8 Luna 4.6 x 250 mm, 100 Å) using the same linear MeOH: H<sub>2</sub>O gradient reported in Table 8.4 and a column flow of 1 mL min<sup>-1</sup>. Calibration curves of the deuterated standard consisted of blank and standard samples in triplicates at concentrations ranging from 0.01 to 0.2 µg mL<sup>-1</sup> (Figure 8.3). Diatom extracts were dissolved in methanol at a final concentration of 10 µg mL<sup>-1</sup> and directly analyzed by LC-MS. The quantifications were carried out by Excalibur software according to the manufacturer's instructions.

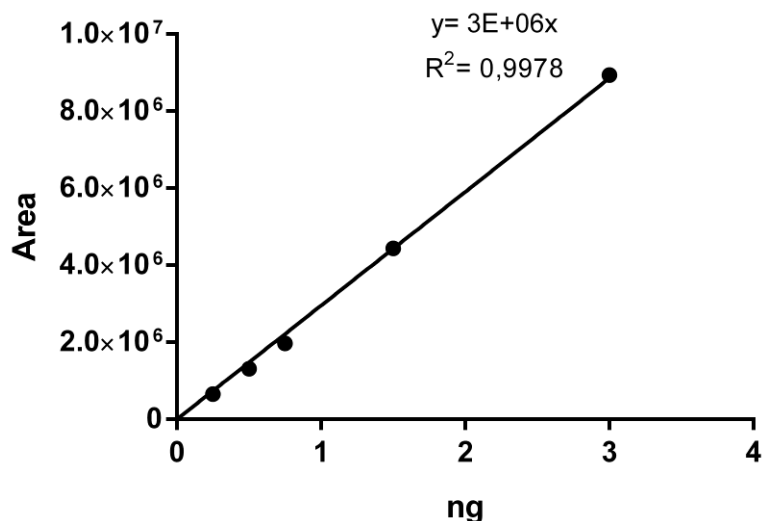


**Figure 8.3.** LC-MS calibration curve of cholesterol-25,26,26,26,27,27,27-D<sub>7</sub> sulfate in the range 0-3.5 ng injected in 5 µL of methanol.

### 8.13. Estimation of glucose consumption in *C. cryptica* heterotrophic cultures

*C. cryptica* culture (10 mL) were centrifuged at 3750 rpm for 10 minutes at 12 °C and glucose consumption was estimated by dinitrosalicylic acid (DNS) assay (Miller, 1959). The aldehyde group of glucose converts 3,5-dinitrosalicylic acid (DNS) to 3-amino-5-nitrosalicylic acid, which is the reduced form of DNS. The formation of 3-amino-5-

nitrosalicylic acid results in a change in the amount of light absorbed, at wavelength 546 nm. The absorbance measured using a spectrophotometer (Jasco V-650) is directly proportional to the amount of reducing sugar. The DNS reagent (100 mL) is prepared dissolving 1g of 3, 5- dinitrosalicylic acid in 20mL 2M NaOH by stirring at room temperature. Then 30 g sodium potassium tartrate is added slowly and the solution is diluted to a final volume of 100 mL using distilled water. An aliquot of the sample (10-20  $\mu$ L) to a final volume of 250  $\mu$ L with distilled water is pipetted in duplicate in a test tube with 0.25 mL of DNS reagent. The mixture is incubated in a boiling water bath for 5 minutes. After cooling to room temperature, 0.5 mL of distilled water was added and the absorbance of the samples was measured at 546 nm. A calibration curve is performed with a glucose stock solution at concentration of 1 mg mL<sup>-1</sup>.

#### *8.14. Fatty acid methyl esters analysis*

The total fatty acid composition of organic extracts and of lipid classes was determined by GC-MS on the corresponding fatty acid methyl esters (FAME) obtained after saponification of lipid extracts with Na<sub>2</sub>CO<sub>3</sub> in methanol at 42°C for 4 hours. FAME mixtures were dissolved in n-hexane (1  $\mu$ g mL<sup>-1</sup>) and analysed by GC-MS equipped with an ion-trap, on a 5% diphenyl column, in EI (70 eV) and negative mode analyzer. Elution of free fatty acid methyl esters required an increasing gradient of temperature according to the following method: 200° C for 2.5 min then 15° C min<sup>-1</sup> till 290° C, followed by 7 min at 290° C. 2  $\mu$ L samples were directly injected in split mode (1:10), with a blank window of 3 minutes (inlet temperature of 270° C, transfer line set at 280° C and ion source temperature of 250° C). FAMEs have been identified by retention time assigned after analysis of standard mixture FAME (Marine source, analytical standard, Sigma Aldrich).

#### *8. 15. Estimate of quercetin incorporation*

To monitor the uptake, 20  $\mu$ M quercetin was incubated in 1 mL of diatom culture. After centrifugation at 3750 rpm 10 minutes at 12°C, quercetin in the supernatant was assessed by UV at 325 and 375 nm (JASCO spectrophotometer V-650) (Dall'Acqua et al., 2012).

#### *8. 16. RNA extraction and cDNA preparation for sulfotransferase analysis*

Total RNA was extracted with TriPure (Roche) according to manufacturer's instructions with the following few modifications. After the addition of 1.5 mL of TriPure, the samples were incubated with 0.5 mg of glass beads (Sigma Aldrich) in a thermoshaker at 60°C for 10 minutes with maximum rpm (1400). The samples were centrifuged briefly for one minute and supernatants were transferred to 2 mL Eppendorf tubes. RNA was treated with DNase (Roche) to eliminate possible contaminations from genomic DNA according to the manufacturer's instructions. Clean up with RNeasy plant mini kit (Qiagen) and Reverse Transcription of cDNA with QuantiTect Reverse Transcription (Qiagen) were performed according to the manufacturers' instructions.

#### *8. 17. Real time PCR*

cDNA from treated and untreated diatom cells (control) were used in real time quantitative PCR (qPCR) for the gene expression analysis of SULT genes. Expression profiles were analyzed by using ACT, RPS and CDK as normalization genes. qPCR was performed using 1  $\mu$ L of cDNA (1:5 dilution), 4  $\mu$ L of the primers (final concentration 0.7  $\mu$ M of each primer) and 5  $\mu$ L of Fasta SYBR Green Master mix with Rox (Applied Biosystems) in a final volume of 10  $\mu$ L, using ViiA™ 7 Real-Time PCR System (Applied Biosystems). PCR conditions were as follows: 95°C for 20 s, 40 cycles at

95°C for 1 s and 60°C for 20 s, 95°C for 15 s, 60°C for 1 min, and a gradient from 60°C to 95°C for 15 min. The results were analyzed and collected in an Excel sheet using the ViiA™ 7 software. Gene expression analysis was performed on three biological replicates, and each of these was run in technical triplicates.

#### *8.18. Protein assay for biochemical analysis*

The protein content was determined by using the Lowry protein assay following the manufacturer's instructions (Bio-Rad) with BSA as standard. All measurements were performed in triplicates and data are presented as means  $\pm$  SD.

The pellet from 10 mL of culture was lyophilized and dissolved in 100  $\mu$ L of phosphate buffer 50 mM and 20  $\mu$ L of Triton 25%. Samples were then sonicated in ice 5 minutes in an ultrasonic bath at 100 MHz (UltraSONIK NDI) and incubated 15 minutes at room temperature. 380  $\mu$ L of phosphate buffer was added to each sample and they were centrifuged at 4°C 5 minutes at 10000 rpm (Thermo ALC PK131R). 10, 20 and 40  $\mu$ L of supernatant were assayed.

#### *8.19. Carbohydrates assay for biochemical analysis*

The determination of intracellular carbohydrates was performed by the phenol / sulfuric acid assay (Dubois et al, 1956) derived from a method of spectrophotometric analysis of total carbohydrates. Calibration curves were performed with D- glucose as standard. Cells from 50 mL of culture were dissolved in 400  $\mu$ L of distilled water and hydrolyzed in 1.6 mL of H<sub>2</sub>SO<sub>4</sub> (98%) for 20 hours. After diluting with distilled water (1:3; v/v) samples were centrifuged 4°C 5 minutes at 10000 rpm (Thermo ALC PK131R) and supernatants were assayed. In test tubes were added 100  $\mu$ L of sample, 400  $\mu$ L of distilled water, 250  $\mu$ L phenol 5% and 1.25 mL of H<sub>2</sub>SO<sub>4</sub> (98%). The samples were

shaken and incubated 30 minutes at room temperature. Absorbance readings were performed at  $\lambda = 490$  nm with a spectrophotometer Jasco (V-650).

## References

- Adolph S., Bach S., Blondel M., Cueff A., Moreau M., Pohnert G., Poulet S.A., Wichard T., Zuccaro A. (2004) Cytotoxicity of diatom-derived oxylipins in organisms belonging to different phyla. *The Journal of Experimental Biology*, 207: 2935–2946.
- Agranoff B.W., Eggerer H., Henning U., Lynen F. (1960) Biosynthesis of terpenes. VII. Isopentenyl pyrophosphate isomerase. *J. Biol. Chem.*, 235:326–332.
- Agrawal A.A. (2000) Mechanisms, ecological consequences and agricultural implications of tri-trophic interactions. *Current Opinion in Plant Biology*, 3: 329-335.
- Akoka S., Barantin L., Trierweiler M.(1999) Concentration Measurement by Proton NMR Using the ERETIC Method. *Anal. Chem.*, 71: 2554–2557.
- Amdur B.H., Rilling H., Bloch K. (1957) The enzymatic conversion of mevalonic acid to squalene. *J. Am. Chem. Soc.*, 79:2646–2647.
- Anderson R., Livermore B. P., Kates M., Volcani B.E. (1978)The lipid composition of the non-photosynthetic diatom *Nitzschia alba*. *Biochim Biophys Acta.*, 528(1): 77-88.
- Apel K., Hirt H. (2004) Reactive oxygen species: metabolism, oxidative stress, and signal transduction. *Annu Rev Plant Biol*, 55: 373–399.

- Armbrust E.V. (2009) The life of diatoms in the world's oceans. *Nature*, 459: 185-192.
- Armbrust E.V., Berges J.B., Bowler C., Green B.R., Martinez D., Putnam N.H., Zhou S., Allen A.E., Apt K.E., Bechner M., Brzezinski M.A., Chaal B.K., Chiovitti A., Davis A.K., Demarest M.S., Detter J.C., Glavina T., Goodstein D., Hadi M.Z., Hellsten U., Hildebrand M., Jenkins B.D., Jurka J., Kapitonov V.V., Kröger N., Lau V.V.Y., Lane T.W., Larimer F.W., Lippmeier J.C., Lucas S., Medina M., Montsant A., Obornik M., Schnitzler-Parker M., Palenik B., Pazour G.J., Richardson P.M., Rynearson T.A., Saito M.A., Schwartz D.C., Thamatrakoln K., Valentin K., Vardi A., Wilkerson F.P. and Rokhsar D.S. (2004). The genome of the diatom *Thalassiosira pseudonana*: ecology, evolution, and metabolism. *Science*, 306: 79-86.
- Armbrust E.V., Chisholm S.W. (1990) Role of light and the cell cycle on the induction of spermatogenesis in a centric diatom. *J. Phycol.*, 26: 470-478.
- Armstrong J.I., Ge X., Verdugo D.E., Winans K.A., Leary J.A., Bertozzi C.R. (2001) A library approach to the generation of bisubstrate analogue sulfotransferase inhibitors. *Org Lett.*, 3: 2657-2660.
- Bach T. J. and Lichtenthaler H. ut K.(1982) Mevinolin: A Highly Specific Inhibitor of Microsomal 3-Hydroxy-3-Methylglutaryl-Coenzyme A Reductase of Radish Plants. *Z. Naturforsch.*, 37: 46-50.
- Becker E.W. (1994) *Microalgae: Biotechnology and Microbiology*; Cambridge University Press: Cambridge, UK, p. 293.

- Bentley-Mowat J. A. (1982). Application of fluorescence microscopy to pollution studies on marine phytoplankton. *Bot. Mar.*, 25: 203–4.
- Benveniste P. (2004) Biosynthesis and accumulation of sterols. *Annual Review of Plant Biology*, 55: 429–457.
- Berges, J. A., and Falkowski P. G. (1998). Physiological stress and cell death in marine phytoplankton: induction of proteases in response to nitrogen or light limitation. *Limnol. Oceanogr.*, 43:129–135.
- Berman-Frank I., Bidle K.D., Haramaty L., Falkowski P.G. (2004) The demise of the marine cyanobacterium, *Trichodesmium* sp., via and autocatalysed cell death pathway. *Limnol. Oceanogr.*, 49: 997–1005.
- Bhattacharya D., Medlin L. (1995) The phylogeny of plastids: a review based on comparison of small subunit ribosomal coding region. *J. Phycol.*, 31: 489-498.
- Bidle K. D. and Bender S. J. (2008) Iron Starvation and Culture Age Activate Metacaspases and Programmed Cell Death in the Marine Diatom *Thalassiosira pseudonana*. *Eukaryot Cell*. February, 7(2): 223–236.
- Bidle K.D., and Falkowski P.G. (2004) Cell death in planktonic, photosynthetic microorganisms. *Nat. Rev. Microbiol.*, 8: 643–655.
- Boucher Y., Doolittle W.F. (2000) The role of lateral gene transfer in the evolution of isoprenoid biosynthesis pathways. *Mol Microbiol.*, 37(4): 703-16.
- Bowler C. (2008) Diatom signalling: deadly messages. *Curr. Biol.*, 18 (12): 518-519.

- Bratbak, G., Egge J. K. and Heldal M. (1993). Viral mortality of the marine alga *Emiliana huxleyi* (Haptophyceae) and termination of algal blooms. *Mar. Ecol. Prog. Ser.*, 93:39–48.
- Broers, S.T.J. (1994) Ph.D. Thesis, Eidgenössische Technische Hochschule, Zürich, Switzerland.
- Bruckner C. and Kroth P. G. (2009). Protocols for the removal of bacteria from freshwater benthic diatom cultures. *J. Phycol.*, 45: 981-986.
- Brussaard C. P. D., Noordeloos A. A. M., and Riegman R. (1997). Autolysis kinetics of the marine diatom *Ditylum brightwellii* (Bacillariophyceae) under nitrogen and phosphorus limitation and starvation. *J. Phycol.*, 33: 980–987.
- Burke R.W., Diamondstone B.I., Velapoldi R.A., Menis O. (1974) Mechanisms of the Liebermann-Burchard and Zak color reactions for cholesterol. *Clin. Chem.*, 20 (7): 794-81.
- Casotti R., Mazza S., Brunet C., Vantrepotte V., Ianora A., et al. (2005) Growth inhibition and toxicity of the diatom aldehyde 2-trans, 4-trans-decadienal on *Thalassiosira weissflogii* (Bacillariophyceae). *J Phycol*, 41: 7–20.
- Charles A.C., Mostovskaya N., Asas K., Evans C.J., Dankovich M.L., Hales T.G. (2003) Coexpression of  $\delta$ -opioid receptors with  $\mu$  receptors in GH3 cells changes the functional response to  $\mu$  agonists from inhibitory to excitatory. *Mol Pharmacol*, 63: 89–95.
- Chen G.Q., Chen F. (2006) Growing phototrophic cells without light. *Biotechnol Lett*, 28:607–616.
- Chisti Y. (2007) Biodiesel from microalgae. *Biotechnol. Adv.*, 25: 294–306.

- Chung C., Hwang S. P., and Chang J. (2005) Cooccurrence of ScDSP gene expression, cell death, and DNA fragmentation in a marine diatom, *Skeletonema costatum*. *Appl. Environ. Microbiol.*, 71:8744–8751.
- Chung C., Sheng-Ping L. Hwang, Chang J. (2008) Nitric Oxide as a Signaling Factor To Upregulate the Death-Specific Protein in a Marine Diatom, *Skeletonema costatum*, during Blockage of Electron Flow in Photosynthesis. *Appl Environ Microbiol.*, 74(21): 6521–6527.
- Clarke C., Thorburn P., McDonald D., Adams J. B. (1982) Enzymic synthesis of steroid sulphates. XV. Structural domains of oestrogen sulphotransferase. *Biochim Biophys Acta*, 707: 28–37.
- Connor W.E., Lin D.S., Wolf D.P., Alexander M. (1998) Uneven distribution of desmosterol and docosahexaenoic acid in the heads and tails of monkey sperm. *J. Lipid Res.*, 39: 1404-1411.
- Cutignano A., d’Ippolito G., Romano G., Cimino G., Febbraio F., Nucci R., Fontana A. (2006) Chloroplastic galactolipids fuel the aldehyde biosynthesis in the marine diatom *Thalassiosira rotula*. *ChemBioChem.*, 7 (3): 450-456.
- Cvejic J.H, Rohmer M. (2000) CO<sub>2</sub> as main carbon source for isoprenoid biosynthesis via the mevalonate-independent methylerythritol 4-phosphate route in the marine diatoms *Phaeodactylum tricornutum* and *Nitzschia ovalis*. *Phytochemistry*, 53: 21–28.
- d’Ippolito G., Romano G., Caruso T., Spinella A., Cimino G., Fontana A. (2003) Production of octadienal in the marine diatom *Skeletonema costatum*. *Org. Lett.*, 5: 885–887.

- d'Ippolito G., Cutignano A., Briante R., Febbraio F., Cimino G., Fontana A. (2005) New C16 fatty-acid-based oxylipin pathway in the marine diatom *Thalassiosira rotula*. *Organic and Biomolecular Chemistry*, 3: 4065-4070.
- d'Ippolito G., Cutignano A., Tucci S., Romano G., Cimino G., Fontana A. (2006) Biosynthetic intermediates and stereochemical aspects of aldehyde biosynthesis in the marine diatom *Thalassiosira rotula*. *Phytochemistry*, 67: 314-322.
- d'Ippolito G., Lamari N., Montresor M., Romano G., Cutignano A., Gerech A., Cimino C. and Fontana A. (2009) 15S-Lipoxygenase metabolism in the marine diatom *Pseudo-nitzschia delicatissima*, , *New Phytologist*, 183, 4: 1064–1071.
- d'Ippolito G., Sardo A., Paris D., Vella F.M., Adelfi M.G., Botte P., Gallo C. and Fontana A. (2015) Potential of lipid metabolism in marine diatoms for biofuel production. *Biotechnology for Biofuels*, 8:28.
- Dall'Acqua S., Miolo G., Innocenti G. and Caffieri S. (2012) The Photodegradation of Quercetin: Relation to Oxidation. *Molecules*, 17(8), 8898-8907.
- D'Auria M. V., Riccio R., Minale L., Barre S. L., Pusset J. (1987) Novel marine steroid sulfates from pacific ophiuroids. *J. Org. Chem.*, 52, 3947-3952.
- D'Auria M.V., Riccio R., Uriarte E., Minale L., Tanaka J., Higa T. (1989) Isolation and structure elucidation of seven new polyhydroxylated sulfated sterols from the ophiuroid *Ophiolepis superba*. *J. Org. Chem.*, 54: 234:239.
- D'Auria M. V., Giannini C., Zampella A., Minale L., Debitus C., Roussakis C. (1998) *J. Org. Chem.*, 63, 7382.

- de Pinto M.C., Tommasi F., De Gara L. (2002) Changes in the antioxidant systems as part of the signaling pathway responsible for the programmed cell death activated by nitric oxide and reactive oxygen species in tobacco Bright-Yellow 2 cells. *Plant Physiol*, 130: 698-708.
- Delledonne M., Zeier J., Marocco A., Lamb C. (2001) Signal interactions between nitric oxide and reactive oxygen intermediates in the plant hypersensitive disease resistance response. *Proceeding of the National Academy of Sciences, USA*, 98: 13454-13459.
- Denning M. F., Kazanietz M. G., Blumberg P. M., Yuspa S. H. (1995) Cholesterol sulfate activates multiple protein kinase C isozymes and induces granular cell differentiation in cultured murine keratinocytes. *Cell Growth Differ*, 6: 1619–1626.
- Desmond E., Gribaldo S. (2009). Phylogenomics of sterol synthesis: insights into the origin, evolution, and diversity of a key eukaryotic feature. *Genome Biology and Evolution*, 1: 364–381.
- Dhe-Paganon S., Magrath J., Abeles R.H. (1994) Mechanism of mevalonate pyrophosphate decarboxylase: evidence for a carbocationic transition state. *Biochemistry*, 33: 13355–13362.
- Dittmar T., Koch B., Hertkorn N., Kattner G. (2008) A simple and efficient method for the solid-phase extraction of dissolved organic matter (SPE-DOM) from seawater. *Limnol. Oceanogr. Methods*, 6: 230–235.
- Djerassi C. (1981) Recent studies in the marine sterol field. *Pure & Appl. Chem.*, 53: 873-890.

- Drayer N. M., Roberts K. D., Bandi L., Lieberman S. (1964) The isolation of cholesterol sulfate from bovine adrenals. *J. Biol. Chem.*, 239: 3112–3114.
- Dubois M., Gilles K.A., Hamilton J.K., Rebers P.A., Smith F. (1956) Colorimetric method for determination of sugars and related substances. *Analytical Chemistry*, 28: 350-356.
- Dufourc E.J. (2008) Sterols and membrane dynamics. *Journal of Chemical Biology*, 1: 63–77.
- Dunahay T. G., Jarvis E. E., Dais S. S., Roessler P. G. (1996) Manipulation of microalgal lipid production using genetic engineering. *Applied Biochemistry and Biotechnology*, 57-58(1): 223-231.
- Fabris M., Matthijs M., Carbonelle S., Moses T., Pollier J., Dasseville R., Baart G.J., Vyverman W., Goossens A. (2014) Tracking the sterol biosynthesis pathway of the diatom *Phaeodactylum tricornutum*. *New Phytol.* 2014, 204(3):521-35.
- Falciatore A., Bowler C. (2002) Revealing the molecular secrets of marine diatoms. *Annual Review of Plant Biology*, 53:109-130.
- Falkowski P.G., Barber R.T., Smetacek V. (1998) Biogeochemical controls and feedbacks on ocean primary production. *Science*, 281: 200-206.
- Field C.B., Behrenfeld M.J., Randerson J.T., Falkowski P. (1998) Primary production of the Biosphere: Integrating terrestrial and oceanic components. *Science*. 281: 237-240.

- Folch J., Lees M., Sloanne-Stanley G.H. (1957) A simple method for the isolation and purification of total lipids from animal tissues. *J. Biol. Chem.*, 226: 497-509.
- Fontana A., d'Ippolito G., Cutignano A., Miralto A., Ianora A., Romano G., Cimino G. (2007a) Chemistry of oxylipin pathways in marine diatoms. *Pure Appl. Chem.*, 79: 475–484.
- Fontana A., d'Ippolito G., Cutignano A., Romano G., Lamari N., Massa Gallucci A., Cimino G., Miralto A., Ianora A. (2007b) A metabolic mechanism for the detrimental effect of marine diatoms on zooplankton grazers. *ChemBioChem.*, 8: 1810–1818.
- Franklin D. J., Brussard C.P.D., Berges J.A. (2006) What is the role and nature of programmed cell death in microalgal ecology? *Eur. J. Phycol.*, 41: 1–41.
- Fuda H., Lee Y.C., Shimizu C., Javitt N.B., Strott C.A. (2002) Mutational analysis of human hydroxysteroid sulfotransferase SULT2B1 isoforms reveals that exon 1B of the SULT2B1 gene produces cholesterol sulfotransferase, whereas exon 1A yields pregnenolone sulfotransferase. *J Biol Chem*, 277:36161–36166.
- Galea A.M., Brown A.J. (2009) Special relationship between sterols and oxygen: were sterols an adaptation to aerobic life? *Free Radical Biology & Medicine*, 47: 880–889.
- Gaulin E., Bottin A., Dumas B. (2010) Sterol biosynthesis in oomycete pathogens. *Plant Signaling & Behavior*, 5: 258–260.

- Gavrieli Y., Sherman Y., and Ben-Sasson S. A. (1992) Identification of programmed cell death in situ via specific labeling of nuclear DNA fragmentation. *J. Cell. Biol.*, 119(3): 493-501.
- Gerecht A., Romano G., Ianora A., d'Ippolito G., Cutignano A., Fontana A. (2011) Plasticity of oxylipin metabolism among clones of the marine diatom *Skeletonema marinoi* (Bacillariophyceae). *J. Phycol.* 47, 1050–1056.
- Gerwick W.H., Moghaddam M.F., Hamberg M. (1991) Oxylipin metabolism in the red alga *Gracilariopsis lemaneiformis*: Mechanism of formation of vicinal dihydroxy fatty acids. *Archives of biochemistry and biophysics*, 290: 436-444.
- Giner J-L., Wikfors G.H. (2011) “Dinoflagellate Sterols” in marine diatoms. *Phytochemistry*, 72: 1896–1901.
- Goodfellow R.M. and Goao L.J. (1983) The steryl sulphate content of echinoderms and some other marine invertebrates. *Comp. Biochem. Physiol.*, 76(3): 575-578.
- Grizard G., Sion B., Jouanel P., Benoit P., Boucher D. (1995) Cholesterol, phospholipids and markers of the function of the accessory sex glands in the semen of men with hypercholesterolaemia. *Int. J. Androl.*, 18 (3): 151-156.
- Guillard R.R.L., Ryther J.H. (1962) Studies of marine planktic diatoms. I. *Cyclotella nana* Hustedt and *Detonula confervacea* Cleve *Can J Microbiol*, 8 pp. 229–239
- Gunasekera S.P., Sennett S.H., Kelly-Borges M. (1994) Ophirapstatyol trisulfate, a new biologically active steroid sulfate from the deep water marine

- sponge *Topsentia Ophzraphidites*. *Journal of Natural Products*, 57(12): 1751 - 1754.
- Hancock J.T., Desikan R., Neill S.J. (2001) Role of Reactive Oxygen Species in Cell Signaling Pathways. *Biochemical and Biomedical Aspects of Oxidative Modification*, 29(2): 345-350.
  - Hartmann M.A., 1998. Plant sterols and the membrane environment. *Trend in Plant Science*, 3: 170-175.
  - Harun R., Singh M., Forde G.M., Danquah M.K. (2010) Bioprocess engineering of microalgae to produce a variety of consumer products. *Renew. Sust. Energ. Rev.*, 14: 1037–1047.
  - Hay M.E. (1996) Marine chemical ecology: What's known and what's next? *Journal of Experimental Marine Biology and Ecology*, 200: 103-134.
  - Hay M.E., Fenical W. (1996) Chemical ecology and marine biodiversity: insights and products from the sea. *Oceanography*, 9: 10-20.
  - Hellebust J.A. (1971a) Kinetics of glucose transport and growth of *Cyclotella cryptica* Reimann, Lewin & Guillard. *J. Phycol.* 7: 1-4.
  - Hellebust, J. A. (1971b) Glucose uptake by *Cyclotella cryptica*: Dark induction and light inactivation of transport system. *Journal of Phycology*, 7: 345–349.
  - Hellebust, J. A. & Lewin J. (1977) Heterotrophic nutrition. In Werner, (ed.) *The Biology of Diatoms*. University of California Press, Berkeley, 169–197.
  - Her C., Wood T.C., Eichler E.E., Mohrenweiser H.W., Ramagli I.S., Siciliano M.J., Weinshilboum R.M. (1998) Human hydroxysteroid sulfotransferase

- SULT2B1: two enzymes encoded by a single chromosome 19 gene. *Genomics*, 53:284–295.
- Hernández-Sebastiá C., Varin L., Marsolais F. (2008) Sulfotransferases from Plants, Algae and Phototrophic Bacteria. *Advances in Photosynthesis and Respiration*, 27: 111-130.
  - Herth, W., and Zugenmaier P. (1977) Ultrastructure of the chitin fibrils of the centric diatom *Cyclotella cryptica*. *Journal of Ultrastructure Research*, 61(2): 230-239.
  - Herz S., et al. (2000) Biosynthesis of terpenoids: YgbB protein converts 4-diphosphocytidyl-2-C-methyl-D-erythritol 2-phosphate to 2-C-methyl-D-erythritol 2,4-cyclodiphosphate. *Proc. Natl. Acad. Sci. U. S. A.*, 97:2486–2490.
  - Hildebrand M., Davis A.K., Smith S.R., Traller J.C., Abbriano R. (2012) The place of diatoms in the biofuels industry. *Biofuels*, 3: 221–240.
  - Hu Q., Sommerfeld M., Jarvis E., Ghirardi M., Posewitz M., Seibert M., Darzins A. (2008) Microalgal triacylglycerols as feedstocks for biofuel production: perspectives and advances. *Plant J.*, 54: 621–639.
  - Huesemann M., Hausmann T., Bartha R. (2009) Biomass productivities in wild type and pigment mutant of *Cyclotella sp.* (diatom). *Applied Biochemistry*, 3: 507–526.
  - Ianora A., Boersma M., Casotti R., Fontana A., Harder J., Hoffman F., Pavia H., Potin P., Poulet S.A., and Toth G. (2006). New trends in marine chemical ecology. *Estuaries Coasts*, 29: 531–551.

- Ianora A., Miralto A., Poulet S.A., Carotenuto Y., Buttino I., Romano G., Casotti R., Pohnert G., Wichard T., Colocci D'Amato L., et al. (2004) Aldehyde suppression of copepod recruitment in blooms of a ubiquitous planktonic diatom. *Nature*, 429: 403–407.
- Ikuta T., Chida K., Tajima O., Matsuura Y., Iwamori M., Ueda Y., Mizuno K., Ohno S., Kuroki T. (1994) Cholesterol sulfate, a novel activator for the eta isoform of protein kinase C. *Cell Growth Differ.*, 5: 943–947.
- Inderjit, Duke S.O. (2003) Ecophysiological aspects of allelopathy. *Planta*, 217: 529–539.
- Itoh Y., Ma F.H., Hoshi H., Oka M., Noda K., et al. (2000) Determination and bioimaging method for nitric oxide in biological specimens by diamino fluorescein fluorometry. *Anal Biochem*, 287: 203–209.
- Javitt N.B., Lee Y.C., Shimizu C., Fuda H., Strott C.A. (2001) Cholesterol and hydroxycholesterol sulfotransferases: Identification, distinction from dehydroepiandrosterone sulfotransferase, and differential tissue expression. *Endocrinology*, 142:2978–2984.
- Jüttner F. (2001) Liberation of 5,8,11,14,17-eicosapentenoic acid and other polyunsaturated fatty acids from lipids as a grazer defense reaction in epilithic diatom biofilms. *J. Phycol.*, 37: 744–755.
- Kallen J., Schlaeppli J. M., Bitsch F., Delhon I., Fournier B. (2004) Crystal structure of the human RORalpha Ligand binding domain in complex with cholesterol sulfate at 2.2 Å. *J Biol Chem.*, 279:14033–14038.

- Kates M., Tremblay P., Anderson R. (1977) Identification of the Free and Conjugated Sterol in a Non-Photosynthetic Diatom, *Nitzschia alba*, as 24-Methylene Cholesterol. *Lipids*, 13: 34-41.
- Kazufumi T., and Masami I. (2002) 5 $\alpha$ ,8 $\alpha$ -Epidioxysterol sulfate from a diatom *Odontella aurita*. *Phytochemistry*, 61(4): 359-360.
- Khozin-Goldberg I., Cohen Z. (2011) Unraveling algal lipid metabolism: Recent advances in gene identification. *Biochimie*, 93: 91–100.
- Kobayashi K., Kobiyama A., Kotaki Y., and Kodama M. (2003) Possible occurrence of intracellular bacteria in *Pseudonitzschia multiseries*, a causative diatom of amnesic shellfish poisoning. *Fish. Sci.*, 69:974-978.
- Kuzuyama T., Shimizu T., Takahashi S., Seto H. (1998) Fosmidomycin, a specific inhibitor of 1-deoxy-D-xylulose 5-phosphate reductoisomerase in the nonmevalonate pathway for terpenoid biosynthesis. *Tetrahedron Lett.*, 39:7913–7916.
- Kwak J. M., Nguyen V., Schroeder J. I. (2006) The role of reactive oxygen species in hormonal responses. *Plant Physiol*, 141: 323–329.
- Laakso, P. (2005) Analysis of sterols from various food matrices. *Eur. J. Lipid Sci. Technol.*, 107: 402-410.
- Lage O. M., Sansonetty F., O'Connor J. E. and Parente A. M. (2001) Flow cytometric analysis of chronic and acute toxicity of copper(II) on the marine dinoflagellate *Amphidinium carterae*. *Cytometry*, 44:226–35.

- Laloi C., Apel K., Danon A. (2004) Reactive oxygen signalling: the latest news. *Curr Opin Plant Biol*, 7: 323–328.
- Lalumière G., Bleau G., Chapdelaine A., Roberts K.D. (1976) Cholesteryl sulfate and sterol sulfatase in the human reproductive tract. *Steroids*, 27: 247-260.
- Lamari N., Ruggiero M.V., d’Ippolito G., Kooistra W.H.C.F., Fontana A., Montresor M. (2013) Specificity of Lipoyxygenase Pathways Supports Species Delineation in the Marine Diatom Genus *Pseudo-nitzschia*. *PLoS One*, 8(8): 1-10.
- Landsberg J.H. (2002) The effects of harmful algal blooms on the aquatic organisms. *Reviews in Fisheries Science*, 10: 113-390.
- Langlais J., Zollinger M., Plante L., Chapdelaine A., Bleau G., Roberts K.D. (1981) Localization of cholesteryl sulfate in human spermatozoa in support of a hypothesis for the mechanism of capacitation. *Proc. Natl Acad. Sci.*, 78(12): 7266-7270.
- Leblanc C., Falciatore A., Bowler C. (1999) Semi-quantitative RT-PCR analysis of photoregulated gene expression in marine diatoms. *Plant Mol. Biol.*, 40: 1031-1044.
- Lee Y.K. (2001) Microalgal mass culture systems and methods: Their limitation and potential. *J. Appl. Phycol.*, 13: 307–315.
- Lerch M. L., Faulkner D. J. (2001) Unusual polyoxygenated sterols from a Philippine sponge *Xestospongia* sp. *Tetrahedron*, 57: 4091- 4094.

- Lewin J. C., Ralph A. (1960) Autotrophy and heterotrophy in marine littoral diatoms. *Canadian Journal of Microbiology*, 6(2): 127-134.
- Liu M.S., and J.A. Hellebust. (1976) Effects of salinity changes on growth and metabolism of the marine centric diatom *Cyclotella cryptica*. *Canadian Journal of Botany*, 54(9): 930-937.
- Liu W., Ming Y., Huang Z., Li P. (2012) Impacts of florfenicol on marine diatom *Skeletonema costatum* through photosynthesis inhibition and oxidative damages. *Plant Physiology and Biochemistry*, 60: 165-170.
- Lohr M., Schwender J., Polle J.E.W. (2012) Isoprenoid biosynthesis in eukaryotic phototrophs: a spotlight on algae. *Plant Science*, 185–186: 9–22.
- Lois L.M., et al. (1998) Cloning and characterization of a gene from *Escherichia coli* encoding a transketolase-like enzyme that catalyzes the synthesis of D-1-deoxyxylulose 5-phosphate, a common precursor for isoprenoid, thiamin, and pyridoxol biosynthesis. *Proc. Natl. Acad. Sci. U. S. A.*, 95:2105–2110.
- Long J. D., Smalley G. W., et al. (2007) "Chemical cues induce consumer-specific defenses in a bloom-forming marine phytoplankton." *Proceedings of the National Academy of Sciences of the United States of America*, 104(25): 10512-10517.
- Lu Y., Zhou W., Wei L., Li J., Jia J., Li F., Smith S.M. and Xu J. (2014) Regulation of the cholesterol biosynthetic pathway and its integration with fatty acid biosynthesis in the oleaginous microalga *Nannochloropsis oceanica*. *Biotechnology for Biofuels*, 7:81.

- Ma J., Lin F., Zhang R., Yu W., Lu N. (2004) Differential sensitivity of two green algae, *Scenedesmus quadricauda* and *Chlorella vulgaris*, to 14 pesticide adjuvants. *Ecotoxicol. Environ. Saf.*, 58: 61-67.
- Makarewicz J.C. (1987) Phytoplankton composition, abundance, and distribution: nearshore Lake Ontario and Oswego River and Harbor. *Journal of Great Lakes Research*, 13(1):56-64.
- Makarieva T.N., Gorshkov B.A., Gorshkova I.A., Kalinovsky A.I., Stonik V.A. (1986) Steroids in Porifera. VII. Obtaining of sokotrasterol and halistanol sulfate derivatives and structure–activity interrelation for these compounds. *Khim. Prirod. Soedin.*, 4: 441 – 445.
- Mann D.G. (1993) Patterns of sexual reproduction in diatoms. *Hydrobiologia*, 269/270: 11-20.
- Mann D.G. (1999). The species concept in diatoms. *Phycologia*, 38: 437-495.
- Massè G., Belt S.T., Rowland S.J., Rohmer M. (2004) Isoprenoid biosynthesis in the diatoms *Rhizosolenia setigera* (Brightwell) and *Haslea ostrearia* (Simonsen). *Proceedings of the National Academy of Sciences*, USA 101: 4413–4418.
- Mckee T. C., Cardellina J. H., Riccio R., D’Auria M. V., Iorizzi M., Minale L., Moran R. A., Gulakowski R. J., McMahon J. B., Buckheit R. W., Snader K. M., Boyd M. R. (1994) HIV- inhibitory natural products. 11. Comparative studies of sulfated sterols from marine invertebrates. *J. Med. Chem.*, 37, 793.
- McClintock J.B., Baker B.J. (2001). *Marine Chemical Ecology Series*.

- Miller G.L. (1959) Use of dinitrosalicylic acid reagent for determination of reducing sugar. *Analytical Chemistry*, 31: 426-428.
- Mills E.L., Leach J.H., Carlton J.T., Secor C.L. (1993) Exotic species in the Great Lakes: a history of biotic crises and anthropogenic introductions. *Journal of Great Lakes Research*, 19(1): 1-54.
- Miralto A., Barone G., Romano G., Poulet S.A., Ianora A., Russo G.L., Buttino I., Mazzarella G., Laabir M., Cabrini M., Giacobbe M.G. (1999) The insidious effect of diatoms on copepod reproduction. *Nature*, 402: 173-176.
- Mittler R., Vanderauwer S., Gollery M., van Breusegem F. (2004) Reactive oxygen gene network of plants. *Trends Plant Sci*, 9: 490–498.
- Mizioroko H. M., Lane M.D. (1977) 3-Hydroxy-3-methylglutaryl-CoA synthase. Participation of acetyl-S-enzyme and enzyme-S-hydroxymethylglutaryl-SCoA intermediates in the reaction. *J. Biol. Chem.*, 252:1414–1420.
- Mojtaba A., Mohd S., Rosfarizan M., Raha A., Arbakariya B. (2011) Improvement of medium composition for heterotrophic cultivation of green microalgae, *Tetraselmis suecica*, using response surface methodology. *Biochem Eng J*, 53:187–195.
- Mortainbertrand A., Descolasgros C., & Jupin H. (1988) Growth, photosynthesis and carbon metabolism in the temperate marine diatom *Skeletonema costatum* adapted to low temperature and low photon flux density. *Marine Biology*, 100: 135–141.
- Nagata K., Yamazoe Y. (2000) Pharmacogenetics of sulfotransferase. *Annu Rev Pharmacol Toxicol*, 40:159–176.

- NES W.R., Krevitz K., Behzadan S. (1976) Configuration at C-24 of 24-Methyl and 24-Ethylcholesterol in *Tracheophytes*. *Lipids*, 11(2):118-126.
- Norton T.A., Melkionian M., Andersen R.A. (1996) Algal biodiversity. *Phycologia*, 35: 308-326.
- Nusaibah, S. A., Siti Nor Akmar A., Mohamad Pauzi Z., Idris A. S. and Sariah M. (2011) Detection of phytosterols in *Ganoderma boninense*-infected oil palm seedlings through GC-MS analysis. *Journal of Oil Palm Research*, 23: 1069-1077.
- Nuzzo G., Gallo C., d'Ippolito G., Cutignano A., Sardo A., and Fontana A. (2013) Composition and Quantitation of Microalgal Lipids by ERETIC <sup>1</sup>H NMR Method. *Mar Drugs*, 11(10): 3742–3753.
- Orrenius S., Zhivotovsky B., Nicotera P. (2003) Regulation of cell death: the calcium–apoptosis link. *Nature Reviews Molecular Cell Biology*, 4: 552-565.
- Otake Y., Nolan A. L., Walle U. K., Walle T. (2000) Quercetin and resveratrol potently reduce estrogen sulfotransferase activity in normal human mammary epithelial cells. *Journal of Steroid Biochemistry & Molecular Biology*, 73: 265–270.
- Paffenhöfer G.A., Ianora A., Miralto A., Turner J.T., Kleppel G.S., Ribera d'Alcala M., Casotti R., Caldwell G.S., Pohnert G., Fontana A., Müller-Navarra D., Jonasdottir S., Armbrust V., Båmstedt U., Ban S., Bentley M.G., Boersma M., Bundy M., Buttino I., Calbet A., Carlotti F., Carotenuto Y., d'Ippolito G., Frost B., Guisande C., Lampert W., Lee R.F., Mazza S., Mazzocchi M.G., Nejstgaard J.C., Poulet S.A., Romano G., Smetacek V., Uye S., Wakeham S.,

- Watson S., Wichard T. (2005) Colloquium on Diatom-Copepod interactions. *Marine Ecology Progress Series*, 286: 293-305.
- Pahl S.L., Lewis D.M., Chen F., King K.D. (2010) Heterotrophic growth and nutritional aspects of the diatom *Cyclotella cryptica* (Bacillariophyceae): Effect of some environmental factors. *J Biosci Bioeng.*,109(3):235-239.
  - Pan Y., Bates S.S., Cemballa A.D. (1998). Environmental stress and domoic acid production by *Pseudo-nitzschia*: a physiological perspective. *Natural Toxins*, 6: 127-135.
  - Patil A. D., Freyer A.J., Breen A., Carte B., and Johnson R.K. (1996) Halistanol Disulfate B, a Novel Sulfated Sterol from the Sponge *Pachastrella* sp.: Inhibitor of Endothelin Converting Enzyme. *J. Nat. Prod.*, 59: 606-608.
  - Pickett-Heaps J.D., Schmid A.-M. & Edgar L.A. (1990) The cell biology of diatom valve formation. Biopress, Bristol.
  - Pohnert G. (2000) Wound-Activated Chemical Defense in Unicellular Planktonic Algae. *Angewandte Chemie International Edition*, 39(23): 4352–4354.
  - Pohnert G., Boland W. (2002). The oxylipin chemistry of attraction and defense in brown algae and diatoms. *Natural Product Reports*, 19: 108–122.
  - Popjåk G., Edmond J., Anet F.A.L., Easton N.R. (1976) Carbon-13 NMR Studies on cholesterol biosynthesized from (<sup>13</sup>C) mevalonates. *Journal of the American Chemical Society*, 99: 931-935.

- Pratt D.M. (1966) Competition between *Skelatonema costatum* and *Olisthodiscus luteus* in Narragansett Bay and in culture. *Limnology and Oceanography*, 11: 447-455.
- Pulz O., Gross W. (2004) Valuable products from biotechnology of microalgae. *Appl. Microbiol. Biotechnol.*, 65: 635–648.
- Puskaric, S., & Mortain-Bertrand, A. (2003). Physiology of diatom *Skeletonema costatum* (Grev.) Cleve photosynthetic extracellular release: Evidence for a novel coupling between marine bacteria and phytoplankton. *Journal of Plankton Research*, 25: 1227–1235.
- Rampen S.W., Abbas B.A., Schouten S., and Sinninghe Damste J.S. (2010) A comprehensive study of sterols in marine diatoms (Bacillariophyta): Implications for their use as tracers for diatom productivity. *Limnol. Oceanogr.*, 55(1): 91–105.
- Rath V. L., Verdugo D., Hemmerich S. (2004) Sulfotransferase structural biology and inhibitor discovery. *Drug Discov Today*, 9(23):1003-1011.
- Riccio R., Iorizzi M., Squillace Greco O., Minale L., Debray M., Menou J. L. (1985) Starfish saponins. Part 22. Asterosaponins from the starfish *Halityle regularis*: a novel 22,23- epoxysteroidal glycoside sulphate. *J. Nat. Prod.*, 48: 756-765.
- Roccatagliata A.J., Maier M.S., Seldes A.M., Pujol C.A., Damonte E.B. (1996) Antiviral sulfated steroids from the ophiuroid *Ophioplocus januarii*. *J. Nat. Prod.*, 59: 887-889.

- Roccatagliata A. J., Maier M. S., Seldes A.M. (1998) New Sulfated Polyhydroxysteroids from the Antarctic *Ophiuroid Astrotoma agassizii*. *J. Nat. Prod.*, 61: 370-374.
- Roessler P. (1988) Effects of silicon deficiency on lipid composition and metabolism in the diatom *Cyclotella cryptica*. *Journal of Phycology*, 24: 394–400.
- Rohdich F., et al. (2003) The deoxyxylulose phosphate pathway of isoprenoid biosynthesis: studies on the mechanisms of the reactions catalyzed by IspG and IspH protein. *Proc. Natl. Acad. Sci. U. S. A.*, 100:1586–1591.
- Rohmer M., Knani T. M., Simonin P., Sutter B. and Sahn H. (1993) Isoprenoid biosynthesis in bacteria: a novel pathway for the early steps leading to isopentenyl diphosphate. *Biochem. J.*, 295: 517-552.
- Rohmer M. (1999) The discovery of a mevalonate-independent pathway for isoprenoid biosynthesis in bacteria, algae and higher plants. *Nat Prod Rep*, 16 (5): 565–574.
- Round F.E., Crawford R.M. & Mann D.G. (1990) The diatoms. Biology and morphology of the genera. Cambridge University Press, Cambridge.
- Sarno D., Kooistra W.C.H.F., Medlin L.K., Percopo I., Zingone, A. (2005) Diversity in the genus *Skeletonema* (Bacillariophyceae). II. An assessment of the taxonomy of *S. costatum*-like species, with the description of four new species. *Journal of Phycology*, 41: 151-176.

- Schenk P.M., Thomas-Hall S.R., Stephens E., Marx U.C., Mussgnug J.H., Posten, C., Kruse O., Hankamer B. (2008) Second generation biofuels: High-efficiency microalgae for biodiesel production. *Bioenerg. Res.*, 1: 20–43.
- Sebaugh J. L. (2011) Guidelines for accurate EC<sub>50</sub>/IC<sub>50</sub> estimation. *Pharmaceutical Statistics*, 10(2): 128–134.
- Segovia M., Haramaty L., Berges J .A. and Falkowski P.G. (2003) Cell death in the unicellular chlorophyte *Dunaliella tertiolecta*. A hypothesis on the evolution of apoptosis in higher plants and metazoans. *Plant Physiol.*, 132: 99–105.
- Sepe V., Bifulco G., Renga B., D’Amore C., Fiorucci S., Zampella A. (2011) Discovery of Sulfated Sterols from Marine Invertebrates as a New Class of Marine Natural Antagonists of Farnesoid-X-Receptor. *J. Med. Chem.*, 54: 1314–1320.
- Setsukinai K., Urano Y., Kakinuma K., Majima H. J., Nagano T. (2003) Development of novel fluorescence probes that can reliably detect reactive oxygen species and distinguish specific species. *J Biol Chem.*, 31;278(5):3170-5. Epub 2002 Nov 4.
- Shackleton C. H., Reid S. (1989) Diagnosis of recessive X-linked ichthyosis: quantitative HPLC/mass spectrometric analysis of plasma for cholesterol sulfate. *Clin Chem.*, 35(9):1906-1910.
- Sheehan J., Dunahay T., Benemann J., Roessler P.(1998) Look Back at the U.S. Department of Energy’s Aquatic Species Program: Biodiesel from Algae; Close-Out Report; NREL/TP-580-24190.

- Shubina L.K., Fedorov S.N., Levina E.V., Andriyaschenko P.V., Kalinovskiy A.I., Stonik V.A., Smirnov I.S. (1998) Comparative study on polyhydroxylated steroids from echinoderms. *Comparative Biochemistry and Physiology Part B*, 119: 505–511.
- Siaut M., Heijde M., Mangonga M., Montsant A., Coesel S., Allen A., Falciatore A., Bowler C. (2007) Molecular toolbox for studying diatom biology in *Phaeodactylum tricornutum*. *Gene*, 406 (1-2): 23-35.
- Siiteri, P. K. (1970) The isolation of steroid conjugates. In *Chemical and Biological Aspects of Steroid Conjugation*. S. Bernstein and S. Solomon, editors. *Springer-Verlag*, New York. 182–218.
- Smetacek V. (2001) A watery arms race. *Nature*, 411: 745.
- Spolaore P., Joannis-Cassan C., Duran E., Isambert A. (2006) Commercial applications of microalgae. *J. Biosci. Bioeng.*, 101: 87–96.
- Sprenger G.A., et al. (1997) Identification of a thiamin-dependent synthase in *Escherichia coli* required for the formation of the 1-deoxy-D-xylulose 5-phosphate precursor to isoprenoids, thiamin, and pyridoxol. *Proc. Natl. Acad. Sci. U. S. A.*, 94:12857–12862.
- Steinke M., Malin G., Gibb S.W., Burkill P.H. (2002) Vertical and temporal variability of DMSP lyase activity in a coccolithophorid bloom in the northern North Sea. *Deep Sea Research Part II: Topical Studies in Oceanography*, 49: 3001-3016.

- Stoermer E.F., and J.J. Yang. (1969) Plankton diatom assemblages in Lake Michigan. Great Lakes Research Division, University of Michigan, Special Report No. 47.
- Stoermer E.F., and T.B. Ladewski. (1976) Apparent optimal temperatures for the occurrence of some common phytoplankton species in southern Lake Michigan. Great Lakes Research Division, University of Michigan, Publication No. 18.
- Subba Rao D.V., Pan Y., Smith S.J. (1995) Allelopathy between *Rhizosolenia alata* (Brightwell) and the toxigenic *Pseudonitzschia pungens* f. *multiseries* (Halse). In Lassus P., Arzul G., Erard E., Gentien P., Marcaillou C. (eds.). Harmful marine algal blooms. *Lavoisier Intercept. Ltd.*, pp. 681-686.
- Schwender J., Seemann M., Lichtenthaler H.K., Rohmer M. (1996) Biosynthesis of isoprenoids (carotenoids, sterols, prenyl side-chains of chlorophylls and plastoquinone) via a novel pyruvate/glyceraldehyde 3-phosphate non-mevalonate pathway in the green alga *Scenedesmus obliquus*. *Biochem. J.*, 316: 73-80.
- Thornberry N. A. and Lazebnik Y. (1998) Caspases: enemies within. *Science*, 281:1312–1316.
- Tomazic M.L., Najle S.R., Nusblat A.D., Uttaro A.D., Nudel C.B. (2011) A novel sterol desaturase-like protein promoting dealkylation of phytosterols in *Tetrahymena thermophila*. *Eukaryotic Cell*, 10: 423–434.
- Uren A. G., O'Rourke K, Pisabarro M. T., Seshagiri S., Koonin E. V., and Dixit V. M. (2000) Identification of paracaspases and metacaspases: two ancient

families of caspase-like proteins, one of which plays a key role in MALT lymphoma. *Mol. Cell*, 6:961–967.

- Valiela I. (1995). Marine ecological processes. *Springer-Verlag*, New York, NY.
- Van Den Hoek C., Mann D.G., Jahns H.M. (1997) Algae. An Introduction to Phycology. Cambridge University Press.
- Vardi A., Berman-Frank I., Rozenberg T., Hadas O., Kaplan A., Levine A. (1999) Programmed cell death of the dinoflagellate *Peridinium gatunense* is mediated by CO<sub>2</sub> limitation and oxidative stress. *Current Biology*, 9: 1061–1064.
- Vardi A. (2008) Cell signaling in marine diatoms. *Communicative & Integrative Biology* 1:2, 134-136; ©2008 Landes Bioscience.
- Vardi, A., Formiggini F., Casotti R., deMartino A., Ribalet F., Miralto A., and Bowler C. (2006) A stress surveillance system based on calcium and nitric oxide in marine diatoms. *PLoS Biol.*, 4:e60.
- Vasconcelos M. T. S. D., Almeida C. M. R. and Lage O. M. (2000) Influence of zwitterionic pH buffers on the bioavailability and toxicity of copper to the alga *Amphidinium carterae*. *Environ. Toxicol. Chem.*, 19:2542–50.
- Veldhuis M.J.W. and Kraay G.W.(2000) Application of flow cytometry in marine phytoplankton research: current applications and future perspectives. *SCI MAR*, 64(2): 121-134.

- Vinci G., Xia X., Veitia R.A. (2008) Preservation of genes involved in sterol metabolism in cholesterol auxotrophs: facts and hypotheses. *PLoS ONE* 3: e2883.
- Volkman J.K. (2003) Sterols in microorganisms. *Applied Microbiology and Biotechnology*, 60: 495–506.
- Vos M., Vet L.E.M., Wackers F.L., Middelburg J.J., Van der Putten W.H., Mooij W.M., Heip C.H.R., Van Donk E. (2006) Infochemicals structure marine, terrestrial and freshwater food webs: Implications for ecological informatics. *Ecological Informatics*, 1: 23-32.
- Wang L.Q., James M.O. (2006) Inhibition of sulfotransferases by xenobiotics. *Curr Drug Metab.*, 7(1):83-104.
- Weller M.G. (2012) A Unifying Review of Bioassay-Guided Fractionation, Effect-Directed Analysis and Related Techniques. *Sensors*, 12: 9181-9209.
- White A.W. (1974a) Growth of two facultatively heterotrophic marine centric diatoms. *J. Phycol.*, 10: 292-300.
- White A.W. (1974b) Uptake of organic compound by two facultatively heterotrophic marine centric diatoms. *J. Phycol.*, 10: 433-438.
- Wilkins K. A., Bancroft J., Bosch M., Ings J., Smirnov N., and Franklin-Tong V. E. (2011) Reactive Oxygen Species and Nitric Oxide Mediate Actin Reorganization and Programmed Cell Death in the Self-Incompatibility Response of Papaver. *Plant Physiology*, Vol. 156: 404–416.

- Wolfe G.V. (2000) The chemical defense ecology of marine unicellular plankton constraints, mechanisms, and impacts. *The Biological Bulletin (Woods Hole)*, 198: 225-244.
- Wright J.L.C., McInnes A.G., Shimizu S., Smith D.G., Walter J.A., Idler D., Khalil W. (1978) Identification of C-24 alkyl epimers of marine sterols by <sup>13</sup>C nuclear magnetic resonance spectroscopy. *Can. J. Chem.*, 56: 1898-1903.
- Wyllie S. G., Djerassi C. (1968) Mass spectrometry in structural and stereochemical problems. CXLVI. Mass spectrometric fragmentations typical of sterols with unsaturated side chains. *J. Org. Chem.*, 33: 305-313.
- Wyllie S. G., Amos B. A., Tökés L. (1977) Electron impact induced fragmentation of cholesterol and related C-5 unsaturated steroids. *J Org Chem.*, 42 (4):725-732.
- Yamasaki Y., Nagasoe S., Matsubara T., Shikata T., Shimasaki Y., Oshima Y., et al. (2007) Allelopathic interactions between the bacillariophyte *Skeletonema costatum* and the raphidophyte *Heterosigma akashiwo*. *Marine Ecology Progress Series*, 339: 83–92.
- Zeidler, J., Schwender J., Müller C., Wiesner J., Weidemeyer C., Beck E., Jomaa H., Lichtenthaler H.K.(1998) Inhibition of the non-mevalonate 1-deoxy-d-xylulose-5-phosphate pathway of plant isoprenoid biosynthesis by fosmidomycin. *Z. Naturforsch. Sect. C*, 53: 980-986.
- Zheng Y., Quinn A.H., Sriram G. (2013) Experimental evidence and isotopomer analysis of mixotrophic glucose metabolism in the marine diatom *Phaeodactylum tricornutum*. *Microb Cell Fact*, 14: 12-109.

- Zvyagintseva T.N., Makarieva T.N., Stonik V.A., Elyakova L.A. (1986)  
Sulfated steroids from sponges of family *Halichondriidae*—natural inhibitors of  
1,3- $\beta$ -, d-glucanases. *Khim. Prirod. Soedin.*,1: 71 – 77.